

**The PD-1/B7-H1 Pathway in a Transgenic Mouse Model for
Spontaneous Autoimmune Neuroinflammation:
Immunological Studies on Devic B7-H1^{-/-} Mice**

Dissertation zur Erlangung des
naturwissenschaftlichen Doktorgrades
der Julius-Maximilians-Universität Würzburg



Vorgelegt von
Angela Dreykluft
aus Würzburg

Würzburg, 2013

Eingereicht am

Mitglieder der Promotionskommission:

Vorsitzender: Prof. Dr. W. Rössler

Gutachter: Prof. Dr. H. Wiendl

Gutachter: Prof. Dr. E. Buchner

Tag des Promotionskolloquiums:

Doktorurkunde ausgehändigt am:

Meinen Eltern, Ulrike und Christiane

Il faut imaginer Sisyphe heureux.

Albert Camus

Table Of Content

1	Summary	4
2	Zusammenfassung	7
3	Introduction.....	10
3.1	The Immune System: Protection and Menace	10
3.1.1	Multiple Sclerosis: Autoimmune Attack of the Central Nervous System ...	11
3.1.2	Neuromyelitis Optica/Devic's Disease: Another Demyelinating Disorder.....	12
3.1.3	Experimental Autoimmune Encephalomyelitis: Studying Multiple Sclerosis	13
3.1.4	The Devic Mouse: A Transgenic Mouse Model for Spontaneous Autoimmune Neuroinflammation	14
3.2	T-Cells in Autoimmunity.....	16
3.2.1	A Revised T-Cell Repertoire: From the Thymus to the Periphery	16
3.2.2	CD4 ⁺ T helper Subsets in Autoimmunity	19
3.2.3	Autoimmune Responses in the Pathogenesis of MS and EAE	22
3.3	Co-Signaling in T-cell Activation	26
3.3.1	Co-Signaling Molecules of the B7 and CD28 Families.....	26
3.3.2	The Programmed Death-1 Receptor and its Ligands.....	27
3.3.3	The PD-1/B7-H1 Pathway in Autoimmunity	30
4	Objectives	34
5	Material and Methods	35
5.1	Material.....	35
5.1.1	Chemical	35
5.1.2	Biochemicals, Media and Supplements	36
5.1.3	Kits	36
5.1.4	Cell Culture Media.....	37
5.1.5	Buffers and Solutions.....	37
5.1.6	PCR Primers for Genotyping.....	39
5.1.7	Antibodies for Flow Cytometry	40
5.1.8	Antibodies for Histology.....	41
5.1.9	Consumables	41
5.1.10	Laboratory Equipment and Instruments.....	42
5.1.11	Software	44
5.2	Animals and Bioassays	44
5.2.1	Experimental Animals	44
5.2.2	Genotyping of Mice	44
5.2.3	Serum Collection	46
5.2.4	Spontaneous EAE Model: Devic Mice	46
5.2.5	Adoptive Transfer Experiments.....	46
5.3	Cell Biological Methods.....	47
5.3.1	Cell Culture.....	47
5.3.2	Cell Counting	47
5.3.3	Preparation of Single-Cell Suspensions from Peripheral Organs	47
5.3.4	Isolation of Mononuclear Leukocytes from the CNS	48
5.4	In vitro Assays	48

5.4.1	Proliferation Assay.....	48
5.4.2	Restimulation Assay: Antigen-dependent Cytokine Production	50
5.4.3	In vitro Survival Assay	50
5.4.4	In vitro Migration Assay	51
5.5	Flow Cytometry.....	51
5.5.1	Staining of Cell Surface Molecules	51
5.5.2	Staining of Intracellular Components	52
5.5.3	Cytometric Bead Array	53
5.6	ELISA (Enzyme-Linked Immunosorbent Assay).....	53
5.7	Immunohistochemistry.....	54
5.8	Statistical Analysis	55
6	Results.....	56
6.1	Clinical Features of Devic B7-H1^{+/+} and Devic B7-H1^{-/-} Mice	56
6.1.1	Accelerated and Aggravated Course of Spontaneous EAE-like Disease in Devic B7-H1 ^{-/-} Mice	56
6.1.2	Enhanced Accumulation of CD4 ⁺ T cells and Macrophages in Spinal Cord Lesions of sick Devic B7-H1 ^{-/-} Mice	57
6.2	Immune Responses in Devic B7-H1^{+/+} and Devic B7-H1^{-/-} Mice.....	59
6.2.1	Enhanced Accumulation and Activation of V α 3.2 ⁺ V β 11 ⁺ CD4 ⁺ T cells in the CNS of sick Devic B7-H1 ^{-/-} mice	59
6.2.2	Enhanced Antigen-specific Th1 and Th17 Responses of CNS- infiltrating CD4 ⁺ T cells in Devic B7-H1 ^{-/-} mice.....	61
6.2.3	Unaffected Phenotypes of Peripheral Lymphocytes in Devic B7-H1 ^{-/-} Mice at Disease Maximum	62
6.2.4	Indifferent Levels of MOG-specific Autoantibodies in Devic B7-H1 ^{-/-} Mice	64
6.2.5	Unaffected Cytokine Secretion Pattern of Devic B7-H1 ^{-/-} Splenocytes	64
6.2.6	Enhanced Accumulation of V α 3.2 ⁺ V β 11 ⁺ CD4 ⁺ T Cells in Secondary Lymphoid Organs of sick Devic B7-H1 ^{-/-} mice	65
6.2.7	Increased Thymic Cellularities in Devic B7-H1 ^{-/-} Mice.....	66
6.2.8	Elevated Antigen-induced Proliferation of Devic B7-H1 ^{-/-} Splenocytes.....	67
6.2.9	Hint on Modified Survival Capacities of Devic B7-H1 ^{-/-} Lymphocytes	69
6.2.10	Unaltered <i>in vitro</i> Migratory Behavior of V α 3.2 ⁺ V β 11 ⁺ B7-H1 ^{-/-} T cells..	70
6.2.11	Unaltered <i>in vivo</i> Migratory Behavior of V α 3.2 ⁺ V β 11 ⁺ B7-H1 ^{-/-} T cells...	71
6.2.12	Amplified Th1 Response of Devic B7-H1 ^{-/-} Splenocytes in the Preclinical Phase	75
6.2.13	Higher Expression of LFA-1 on Peripheral CD4 ⁺ T cells in Devic B7- H1 ^{-/-} Mice in the Preclinical Phase	75
7	Discussion	77
8	Abbreviation Directory	86
9	References.....	89
10	Declaration	104
11	Acknowledgments	105
12	Curriculum Vitae.....	107
13	Publications	108

1 Summary

Multiple sclerosis (MS) is an autoimmune disease of the central nervous system (CNS) characterized by inflammatory, demyelinating lesions and neuronal death. Formerly regarded as a variant of MS, neuromyelitis optica (NMO) / Devic's disease is now recognized as a distinct neurological disorder which exhibits characteristic lesions in the optic nerves and the spinal cord sparing the brain. With the introduction of the double-transgenic "Devic mouse" model featuring spontaneous, adjuvant-free incidence of autoimmune neuroinflammation due to the interaction of transgenic MOG (myelin oligodendrocytes glycoprotein)-specific T and B cells, a promising tool was found for the analysis of factors triggering or preventing autoimmunity. The co-inhibitory molecule B7-H1 has been proposed to contribute to the maintenance of peripheral tolerance and to confine autoimmune inflammatory damage via the PD-1/B7-H1 pathway in models of induced CNS autoimmunity. The influence of B7-H1 on spontaneously occurring neuroinflammation was thought to be elucidated in the present study using the Devic mouse model.

Compared to Devic B7-H1^{+/+} mice, Devic B7-H1^{-/-} mice developed clinical symptoms with a remarkably higher incidence rate and faster kinetics emphasized by deteriorated disease courses and a nearly quadrupled mortality rate. These observations already indicated a potentially immune-modifying role of B7-H1 in the pathogenesis of this EAE-like disease. Remarkably enlarged immune-cell accumulation in the CNS of Devic B7-H1^{-/-} mice, in particular of activated MOG-specific CD4⁺ T cells, correlated with the more severe clinical features. Our studies showed that the CNS not only was the major site of myelin-specific CD4⁺ T-cell activation but also that B7-H1 expression within the target organ significantly influenced T-cell activation and differentiation levels. Analysis at disease maximum furthermore revealed augmented accumulation of MOG-specific CD4⁺ T cells in the peripheral lymphoid organs of Devic B7-H1^{-/-} mice which we partly attributed to increased T-cell proliferation rates. Transgenic MOG-specific B cells of Devic B7-H1^{-/-} mice activated MOG-specific CD4⁺ T cells in vitro more efficiently than B cells of Devic B7-H1^{+/+} mice. These observations indicated a relevant immune-modulating role of B7-H1 on APCs (antigen-presenting cells) in the investigated mouse model. We also assumed altered thymic selection processes to be

involved in increased peripheral CD4⁺ T-cell numbers of Devic B7-H1^{-/-} mice as we found more thymocytes expressing the transgenic MOG-specific T-cell receptor (TCR). Moreover, preliminary in vitro experiments hinted on an enhanced survival of TCR^{MOG}-transgenic CD4⁺ T cells of Devic B7-H1^{-/-} mice. Elevated levels of MOG-specific CD4⁺ T cells in the periphery of Devic B7-H1^{-/-} mice could have entailed the higher quantities in the CNS. However, mechanisms such as CNS-specific proliferation and/or apoptosis/survival could also have caused the observed higher T-cell accumulation in the CNS. These possibilities should be addressed in future investigations. Judging from in vitro migration assays and adoptive transfer experiments on RAG-1^{-/-} recipient mice, migratory behavior of MOG-specific CD4⁺ T cells of diseased Devic B7-H1^{+/+} and Devic B7-H1^{-/-} mice seemed not to differ. However, enhanced expression of the transmigration-relevant integrin LFA-1 on encephalitogenic CD4⁺ T cells in young symptom-free Devic B7-H1^{-/-} mice might hint on temporally differently pronounced transmigration capacities during the disease course. Moreover, we attributed the earlier conversion of CD4⁺ T cells into Th1 effector cells in Devic B7-H1^{-/-} mice during the initiation phase to the lack of co-inhibitory signaling via PD-1/B7-H1 possibly leading to an accelerated disease onset. Full blown autoimmune inflammatory processes could have masked these slight effects of B7-H1 in the clinical phase. This assumption was supported by the fact that, at peak of the disease, Th1 and Th17 effector functions of peripheral CD4⁺ T cells were comparable in both mice groups. Moreover, judging from titers of MOG-specific IgG1 and IgM antibodies, alterations in humoral immunity were not detected at disease maximum. Therefore, clinical differences could not be explained by altered T-cell or B-cell effector functions at disease maximum. B7-H1 rather seemed to take inhibitory effect in the periphery during the initiation phase only and consistently within the target organ by parenchymal expression.

In summary, our observations indicate that B7-H1 plays a relevant role in the regulation of T-cell responses in this mouse model for spontaneous CNS autoimmunity. By exerting immune-modulating effects in the preclinical as well as the clinical phase of the disease, B7-H1 contributed to the confinement of the immunopathological tissue damage in Devic B7-H1^{+/+} mice mirrored by later disease onsets and lower disease scores. As a model for spontaneous autoimmunity featuring a close to 100 % incidence rate, the Devic B7-H1^{-/-} mouse may prove instrumental in clarifying disease-triggering and -limiting factors and in validating novel therapeutic approaches in the field of

autoimmune neuroinflammation, in particular the human Devic's disease.

2 Zusammenfassung

Multiple Sklerose (MS) ist eine Autoimmunerkrankung des zentralen Nervensystems (ZNS), die durch entzündliche, demyelinisierende Läsionen und neuronalen Tod gekennzeichnet ist. Einst als Variante der MS betrachtet, gilt die Neuromyelitis optica (NMO) / Devic-Krankheit mittlerweile als eigenständige neurologische Erkrankung, bei der charakteristische Läsionen in den Sehnerven und im Rückenmark jedoch nicht im Gehirn auftreten. Mit der Einführung des doppelt-transgenen "Devic Maus"-Modells, bei dem es zur spontanen, Adjuvans-freien Inzidenz von autoimmuner Neuroinflammation aufgrund von wechselwirkenden transgenen MOG (Myelin-Oligodendrozyten-Glykoprotein)-spezifischen T- und B-Zellen kommt, wurde ein vielversprechendes Werkzeug für die Analyse von Faktoren gefunden, die Autoimmunität auslösen bzw. hemmen können. Das ko-inhibitorische Molekül B7-H1 trägt über den PD-1/B7-H1 Signalweg vermeintlich zur Aufrechterhaltung peripherer Toleranz bei und vermag, entzündungsbedingte Schädigung des Zielorgans in Tiermodellen der induzierten ZNS-Autoimmunität einzudämmen. Der Einfluss von B7-H1 auf spontan auftretende Neuroinflammation sollte in der vorliegenden Arbeit anhand des Devic-Mausmodells erläutert werden.

Devic B7-H1^{-/-} Mäuse entwickelten im Vergleich zu Devic B7-H1^{+/+} Mäusen klinische Symptome, die mit deutlich höherer Inzidenz und schnellerer Kinetik einhergingen, unterstrichen von verstärkten Krankheitsverläufen und einer nahezu vervierfachen Sterblichkeit. Diese Beobachtungen wiesen bereits auf eine potentiell immunmodifizierende Rolle von B7-H1 in der Pathogenese der EAE-ähnlichen Erkrankung hin. Eine bemerkenswert erhöhte Akkumulierung von Immunzellen im ZNS von Devic B7-H1^{-/-} Mäusen, insbesondere von aktivierten MOG-spezifischen CD4⁺ T-Zellen, korrelierte mit den schwerwiegenderen klinischen Merkmalen. Unsere Untersuchungen zeigten nicht nur, dass die Aktivierung von myelin-spezifischen CD4⁺ T-Zellen hauptsächlich im ZNS stattfand, sondern auch, dass die Expression von B7-H1 im Zielorgan maßgeblich den T-Zell-Aktivierungs- und -Differenzierungsgrad beeinflusste. Die Analyse am Krankheitsmaximum offenbarte ferner eine verstärkte Akkumulierung von MOG-spezifischen CD4⁺ T-Zellen in peripheren Lymphorganen von Devic B7-H1^{-/-} Mäusen, die wir zum Teil auf eine erhöhte T-Zell-Proliferation

zurückzuführen. Transgene MOG-spezifische B-Zellen der Devic B7-H1^{-/-} Mäuse aktivierten effizienter als B-Zellen der Devic B7-H1^{+/+} Mäuse MOG-spezifische CD4⁺ T-Zellen. Dies deutete auf eine wichtige immunmodulierende Rolle von B7-H1 auf APZs (Antigen-präsentierenden Zellen) in diesem Mausmodell hin. Außerdem nahmen wir an, dass veränderte Selektionsprozesse im Thymus zu den höheren CD4⁺ T-Zellzahlen in der Peripherie beitrugen, da wir mehr Thymozyten vorfanden, die den transgenen MOG-spezifischen T-Zell-Rezeptor (T-cell receptor, TCR) exprimierten. Zusätzlich deuteten vorläufige in vitro Experimente auf ein verbessertes Überleben von TCR^{MOG}-transgenen CD4⁺ T-Zellen aus Devic B7-H1^{-/-} Mäusen hin; ein Mechanismus, der ebenso zur verstärkten peripheren T-Zell-Akkumulierung geführt haben könnte. Eine erhöhte Anzahl von MOG-spezifischen CD4⁺ T-Zellen in der Peripherie von Devic B7-H1^{-/-} Mäusen könnte die größeren Mengen im ZNS nach sich gezogen haben. Jedoch könnten auch Mechanismen wie ZNS-spezifische Proliferation und/oder Apoptose bzw. Überleben zu der beobachteten verstärkten T-Zell-Anreicherung im ZNS beigetragen haben. Diese Möglichkeiten sollten in zukünftigen Untersuchungen genauer analysiert werden. Anhand von in vitro-Migrationsassays und Adoptiver Transfer-Experimenten in RAG-1^{-/-} Empfängermäusen schlossen wir darauf, dass das Migrationsverhalten von MOG-spezifischen CD4⁺ T-Zellen von Devic B7-H1^{-/-} Mäusen nicht verändert war. Allerdings deutet die verstärkte Expression des transmigrationsrelevanten Intergins LFA-1 auf enzephalitogenen CD4⁺ T-Zellen in jungen, symptomfreien Devic B7-H1^{-/-} Mäusen auf im Krankheitsverlauf zeitlich verschieden ausgeprägte Transmigrationskapazitäten hin. Die frühere Differenzierung von peripheren CD4⁺ T-Zellen in Th1-Effektorzellen in Devic B7-H1^{-/-} Mäusen während der Initiationsphase schrieben wir der fehlenden inhibierenden Wirkung des PD-1/B7-H1 Signalwegs zu, was zum beschleunigten Krankheitsbeginn im Vergleich zu Devic B7-H1^{+/+} Mäusen geführt haben könnte. Stark ausgeprägte autoimmune Entzündungsreaktionen am Krankheitsmaximum maskierten jedoch wahrscheinlich diese schwachen Effekte von B7-H1. Dies wurde durch die Tatsache untermauert, dass am Krankheitsmaximum Th1- und Th17-Effektorfunktionen von peripheren CD4⁺ T-Zellen in beiden Mausgruppen vergleichbar ausgeprägt waren. Evident am Titer von MOG-spezifischen IgG1 und IgM-Antikörpern bestanden des Weiteren am Krankheitsmaximum keine Unterschiede in der humoralen Immunität. Die beobachteten klinischen Unterschiede konnten demnach nicht durch veränderte periphere T-Zell- oder

B-Zell-Effektorfunktionen in dieser Krankheitsphase erklärt werden. Vielmehr scheint B7-H1 in der Peripherie ausschließlich während der Initiationsphase der Krankheit und fortwährend im Zielorgan durch seine parenchymale Expression inhibierenden Einfluss zu nehmen.

Zusammenfassend zeigen unsere Beobachtungen, dass B7-H1 eine relevante Rolle in der Regulierung von T-Zell-Antworten in dem vorliegenden Mausmodell für spontane ZNS-Autoimmunität spielt. Durch immunmodulierende Effekte in der präklinischen sowie der klinischen Phase der Krankheit trug B7-H1 zu der Begrenzung der immunpathologischen Gewebeschädigung in Devis B7-H1^{+/+} Mäusen bei, sichtbar an einem späteren Krankheitsbeginn und leichteren Verlauf. Als Tiermodell für spontane ZNS-Autoimmunität mit nahezu 100 %iger Inzidenz könnte sich die Devis B7-H1^{-/-} Maus als hilfreich bei der Klärung krankheitsauslösender und -limitierender Faktoren erweisen sowie bei der Validierung neuer therapeutischer Ansätze im Bereich der autoimmunen Neuroinflammation, insbesondere der Devis-Krankheit im Menschen.

3 Introduction

3.1 The Immune System: Protection and Menace

The immune system of higher vertebrates consists of two components: the innate and the adaptive immunity. The innate immunity provides an immediate, non-specific defense against external pathogens like viruses, bacteria and fungi. In parallel to first line defense, another key role of the innate immune system is the activation of the adaptive immune response. An effective immune response depends on the accurate interaction and mutual regulation of innate and adaptive immunity. This ideally leads to the elimination of the threatening pathogen or at least to the control of the pathogenic condition with as little damage to the host organism as possible (reviewed by Dempsey et al., 2003; Janeway and Medzhitov, 2002).

Unlike the innate immunity, the adaptive branch of the immune system is characterized by specific protection against pathogens. Its cellular components, i.e. T and B lymphocytes, recognize pathogen-derived antigenic structures via specific cell-surface receptors. Upon antigen-encounter, B lymphocytes exert their protective function primarily by producing antigen-specific antibodies, a process referred to as humoral immunity. On the one hand, T-cell response involves the killing of pathogens, pathogen-infected cells or tumor cells and, on the other hand, the contribution to the maturation of other immune cells. Moreover, the adaptive immunity provides immunological memory which ensures a stronger immune response each time a certain antigen is re-encountered. The primary, adaptive response often takes days to develop whereas the secondary, memory response acts within hours (reviewed by Dempsey et al., 2003; Janeway and Medzhitov, 2002). Adaptive immunity, however, is also the source of allergy and autoimmunity. Depending on the expression pattern of the specific antigen, autoreactive lymphocytes may induce organ-specific or systemic autoimmune reactions. Type I diabetes is an example for an organ-specific autoimmune disease: autoreactive lymphocytes recognize their epitopes on insulin-producing β -cells in the pancreas whereupon β -cells are attacked and consequently, insulin production drops (reviewed by Knip and Siljander, 2008). In systemic autoimmune diseases such as systemic lupus erythematosus (SLE), the target antigen is ubiquitously expressed throughout the body which leads to acute and chronic tissue inflammation and damage

of multiple end-organs (reviewed by Fu et al., 2011).

3.1.1 Multiple Sclerosis: Autoimmune Attack of the Central Nervous System

Multiple sclerosis (MS) is an organ-specific autoimmune disease of the central nervous system (CNS) leading to impairment of physical and cognitive functions in the affected individual. Affecting more than 2.5 million people worldwide, MS is the most significant inflammatory autoimmune disease of the CNS. Women are twice as often affected than men with the disease commonly developing during young adulthood (Weinshenker et al., 1989). The clinical phenotype of MS comprises a variety of symptoms such as impaired vision, sensory deficits, paralysis, and disorders in coordination and in cognitive functions which may be partly reversible but follow an unpredictable course (reviewed by Compston and Coles, 2002). The clinical courses of MS vary from relapsing-remitting (RR), progressive-relapsing (PR), primary progressive (PP) to secondary progressive (SP) forms with or without superimposing relapses. RR is the most common course of MS characterized by episodes of disease deterioration alternating with periods of recovery and stable phases in between. The RR course is often followed by a secondary progressive course characterized by gradual neurologic deterioration. Continuous disease progression from onset is typical for PP-MS and is observed in between relapses in patients with PR course (Confavreux et al., 2000; Weinshenker et al., 1989).

To date, the exact pathogenesis of MS still remains unclear but a correlation between the development of MS and certain MHC genes (major histocompatibility complex) among other hereditary factors have been discussed (reviewed by Compston, 1999; Olerup and Hillert, 1991). Moreover, environmental factors might trigger MS development such as infections with exogenous pathogens. So-called molecular mimicry is a phenomenon based on the structural similarity between epitopes on infectious agents or other exogenous substances and on self-antigens. As a result of the pathogen-specific immune response, an autoaggressive T-cell attack to host structures is induced (reviewed by Albert and Inman, 1999). Additionally, immune responses may start to target epitopes distinct from and non-cross-reactive with the dominant epitope which are either located on the same or even on other proteins; a process called epitope spreading. Tissue injury occurring after the primary immune response probably causes this phenomenon by uncovering previously cryptic epitopes. Expanded autoaggressive

T-cell responses are the consequence (reviewed by Vanderlugt and Miller, 1996).

MS is presumably initiated by autoreactive T and B cells targeting components of the myelin sheath of oligodendrocytes resulting in acute focal inflammatory demyelination and axonal loss with limited remyelination. Typical pathological features of MS are multifocal lesions throughout the white matter of the CNS displaying sharply defined sclerotic plaques, inflammatory infiltrates composed of oligoclonal T cells, macrophages, occasional B cells and plasma cells, gliosis, axonal damage and neuronal death (reviewed by Lassmann et al., 2007; Sospedra and Martin, 2005). Demyelination and axonal damage lead to impairment of saltatory axonal conduction which explains many clinical features. The anatomical localization and histopathological characteristics of CNS lesions vary according to the respective clinical subtype of MS. For a long time, IFN- γ -secreting Th1 CD4⁺ T cells have been allocated the central role in the pathogenesis of MS. However, recent findings in animal models and studies on MS patients revealed that IL-17-secreting Th17 CD4⁺ T cells are also critically involved in the induction of CNS tissue inflammation and autoimmunity (Langrish et al., 2005; Matusiewicz et al., 1999). Only recently, the involvement of CD8⁺ T cells in the pathogenesis of MS has been paid attention to. Evidence has been drawn for example from studies with MS patients revealing that both CD4⁺ and CD8⁺ T cells invaded CNS lesions, clonally expanded and also accumulated in CSF and blood (Babbe et al., 2000; Wallstrom et al., 2000). Even though MS has long been regarded a predominantly T cell-mediated autoimmune disease, evidence is emerging that humoral immunity significantly contributes to the pathogenesis, too, as B cells, plasma cells and immunoglobulins are frequently found in MS lesions (Correale and de los Milagros Bassani Molinas, 2002).

3.1.2 Neuromyelitis Optica/Devic's Disease: Another Demyelinating Disorder

For a long time, it has been a matter of debate whether neuromyelitis optica (NMO) is a variant of MS or a distinct neurological disorder. Today, however, several clinical, laboratory, immunological and pathological characteristics have been identified that clearly distinguish NMO from MS (reviewed by Asgari et al., 2011). Named after Eugène Devic who in 1894 allocated lost vision to inflammation of the optic nerve or the spinal cord in diverse patients, NMO is also referred to as Devic's disease (Devic, 1895). NMO patients exhibit inflammatory and demyelinated foci characteristically

restricted to the optic nerve and the spinal cord without any involvement of the brain. Most NMO patients first develop optic neuritis, followed by myelitis at a later time point while the intervals between both manifestations vary. Monophasic and also relapsing disease courses of NMO have been described (Wingerchuk et al., 1999). The presence of highly specific serum autoantibodies (NMO-IgGs) which react with the water channel aquaporin 4 (AQP4) further differentiates NMO from MS (Lennon et al., 2005). AQP4 is an integral protein of astrocytic plasma membranes located in the foot processes at the blood-brain-barrier (BBB). It was identified as the predominant water channel in the CNS and has been allocated a dominant role in pathophysiological conditions such as brain edema and focal cerebral ischemia (Amiry-Moghaddam et al., 2004; Manley et al., 2000; Vajda et al., 2002). NMO-IgGs deriving from peripheral B cells are assumed to activate complement and to cause the inflammatory demyelination and necrosis seen in NMO (reviewed by Asgari et al., 2011). In Asia, opticospinal MS (OSMS) accounts for approximately one third of the cases of MS. With selective but severe involvement of the optic nerves and spinal cord, this form exhibits similar features as the relapsing form of NMO in Western populations (Misu et al., 2002).

3.1.3 Experimental Autoimmune Encephalomyelitis: Studying Multiple Sclerosis

Animal models are essential tools for studying immunological and pathological mechanisms. In the 1920s, autoimmune spinal cord inflammation was for the first time induced in rabbits by inoculation with human spinal cord homogenate (Koritschoner R. S., 1925). Since then, the experimental autoimmune encephalomyelitis (EAE) was produced in several different species including primates and rodents and its resemblance to human demyelinating diseases was soon appreciated. By now, EAE has turned into a widely used animal model for the human autoimmune disease MS reflecting its immunological and neuropathological key features being inflammation, demyelination, gliosis, axonal damage and neuronal death (reviewed by Gold et al., 2006). So-called active induction of EAE in mice is achieved by adjuvant-supported immunization of susceptible mouse strains with myelin-derived peptides such as peptides derived from MBP (myelin basic protein), MOG (myelin oligodendrocyte protein) and PLP (proteolipid protein) representing effective autoantigens. Before subcutaneous injection, the respective peptide is emulsified with complete Freund's adjuvant (CFA) composed of mineral oil and heat-killed mycobacterium tuberculosis which amplifies innate

immune responses. Simultaneous peritoneal injection of pertussis toxin results in weakening the BBB thereby allowing access of myelin-specific T cells to the CNS which subsequently initiate an autoimmune attack of target structures within the myelin sheath (Miller and Karpus, 2007). Depending on the susceptibility of the respective mouse strain and the applied immunization protocol, the different courses of MS can be reproduced. Accordingly, a relapsing-remitting course of the disease is elicited in SJL mice by the immunization with PLP₁₃₉₋₁₅₁ peptide while C57BL/6 mice undergoing MOG₃₅₋₅₅ peptide-induced EAE show chronic-progressive paralysis (reviewed by Gold et al., 2006). The clinical features of classical EAE comprise the characteristic, ascending paralysis starting with loss of tail tonus, followed by weakness of the hind legs, the forelegs and finally by the complete paralysis of all limbs (Miller and Karpus, 2007). Classical EAE is associated with inflammatory lesions predominantly located in the white matter of the spinal cord. In contrast, non-classical or atypical EAE is associated with inflammation rather of the brain than the spinal cord. Its clinical phenotype is characterized by gait impairment and continuous and unrelenting axial-rotation (ataxia) (Wensky et al., 2005). In the pathogenesis of EAE, Th1 cells have been allocated a key role. This view was supported by the observation that passive induction of EAE is achieved by the transfer of pre-activated, encephalitogenic Th1 cells into naïve recipient mice which models the effector phase of EAE (Stromnes and Goverman, 2006). Today, however, it is well appreciated that Th17 cells are crucially involved, too. IL-17-deficient mice, for example, develop EAE with delayed onset and diminished severity (Komiyama et al., 2006). Likewise, administration of IL-17-neutralizing antibodies to immunized mice prevents a full-blown development of EAE (Langrish et al., 2005). Moreover, MOG-specific Th17 cells were shown to be capable of inducing EAE upon adoptive transfer (Jäger et al., 2009).

3.1.4 The Devic Mouse: A Transgenic Mouse Model for Spontaneous Autoimmune Neuroinflammation

Most of the current knowledge regarding principal mechanisms of neuroinflammation in MS and therapeutic interventions has been gathered from animal studies on induced EAE. In recent years, models of spontaneous EAE which occurs in non-immunized mice of strains with a certain genetic background were more and more focused on. Among others, mice transgenic for myelin-specific T-cell receptors (TCR) seem to be a

useful tool to gain further insight into the complex pathogenesis of MS. Transgenic mice (on B10.PL background) with a TCR-specificity for MBP, for example, spontaneously develop EAE-like symptoms with a frequency <15 % under conventional animal housing conditions. They exhibit characteristic demyelinated inflammatory lesions within the CNS (Goverman et al., 1993; Lafaille et al., 1994). With the introduction of a novel double-transgenic TCR^{MOG} x IgH^{MOG} mouse model by Bettelli et al. and Krishnamoorthy et al., the bidirectional interaction between myelin-specific T cells and myelin-specific B cells and their contribution to autoimmune neuroinflammation was targeted for the first time (Bettelli et al., 2006; Krishnamoorthy et al., 2006). In TCR^{MOG}-transgenic mice, the majority of CD4⁺ T cells express the rearranged variable regions of the TCR α (V α 3.2) and β chains (V β 11) of a pathogenic T-cell clone obtained from MOG₃₅₋₅₅-immunized C57BL/6 mice. Consequently, V α 3.2⁺ V β 11⁺ CD4⁺ T cells recognize MOG₃₅₋₅₅-peptide in the context of MHC class II molecules I-A^b. Spontaneous optic neuritis occurs in more than 30 % and spontaneous, low-grade EAE is seen in approximately 4 % of TCR^{MOG}-transgenic mice (bred on C57BL/6 background) (Bettelli et al., 2003). Due to a gene knock-in in the VDJ (Variable, Diverse, Joining) heavy chain region, IgH^{MOG}-transgenic mice express a myelin-specific B-cell receptor (BCR) which carries the heavy chain of the demyelinating MOG-binding antibody 8.18C5 (Litzenburger et al., 1998). Consequently, about 30 % of B cells recognize a conformational epitope of MOG and secrete high titers of MOG-specific serum antibodies in their effector function as plasma cells. IgH^{MOG}-transgenic mice (on C57BL/6 background) do not show any spontaneous EAE-like symptoms. However, MOG₃₅₋₅₅ peptide-induced EAE exhibits faster kinetics in these mice (Litzenburger et al., 1998). The presence of MOG-specific B and T cells in double-transgenic TCR^{MOG} x IgH^{MOG} mice was shown to result in a massive production of MOG-specific IgG1 (immunoglobulin G1) antibodies on the one hand and in enhanced proliferation and activation of TCR^{MOG}-transgenic T cells on the other hand. Between 50-60 % of these mice spontaneously develop severe EAE-like symptoms at the age of about 42nd-46th days (Bettelli et al., 2006; Krishnamoorthy et al., 2006). Inflammatory lesions are predominantly located in the optic nerves and spinal cords but not in the brains of affected mice; a lesion distribution pattern strongly resembling that of human Devic's disease/NMO. Due to this finding, these double-transgenic mice are often referred to as Devic or opticospinal EAE (OSE) mice (Bettelli

et al., 2006; Krishnamoorthy et al., 2006).

3.2 T-Cells in Autoimmunity

Autoimmunity is typically initiated by autoreactive T cells that produce proinflammatory cytokines inducing inflammation and also provide T-cell help to autoreactive B cells. In turn, activated autoreactive B cells produce autoreactive antibodies which entail further inflammation and damage within the target tissue. During T-cell development, autoreactive T cells are supposed to be deleted by so-called central tolerance processes in the thymus. Additional mechanisms of peripheral tolerance apply when T cells targeting self-antigens appear in the periphery. These tolerance mechanisms include the elimination of autoaggressive T cells by apoptosis or their conversion into a non-responsive or anergic state preventing them from exerting effector functions (reviewed by Anderton and Wraith, 2002; Goverman, 2011).

3.2.1 A Revised T-Cell Repertoire: From the Thymus to the Periphery

B and T cells originate from hematopoietic stem cell precursors generated in the fetal liver and the bone marrow. Whereas B cells finish their maturation process in the bone marrow, T-lymphoid progenitor cells migrate into the thymic parenchyma where they evolve via several stages from double-negative (DN) $CD4^- CD8^-$ over double-positive (DP) $CD4^+ CD8^+$ into single-positive (SP) $CD4^+$ or $CD8^+$ thymocytes. Finally, they leave the thymus as mature naïve $CD4^+$ or $CD8^+$ T cells and recirculate between blood and secondary lymphoid organs until they encounter their specific antigen.

Orderly selection and differentiation processes within the thymic parenchyma shall ensure a repertoire of functional and self-tolerant peripheral lymphocytes (reviewed by Germain, 2002; Takahama, 2006). Throughout T-cell development in the thymus, adequate signaling upon TCR engagement to self-peptide/MHC complexes on stromal cells is crucial. Signaling via the TCR $\alpha\beta$ complex which is first expressed at the DP stage of thymocyte maturation controls the fate of DP thymocytes in the thymic cortex. Low-avidity interactions to self-peptide/MHC complexes presented by cortical epithelial cells and DCs induce the survival and further differentiation of DP thymocytes (positive selection) (Fig. 1). Conversely, high-avidity interactions elicit signals that trigger apoptosis (negative selection). Moreover, if the induced TCR signal does not exceed a certain threshold, DP thymocytes fail to upregulate cell survival

genes and die through neglect (Fig. 1). These selection processes contribute to the enrichment of functional T cells that potentially target foreign antigens and prevent putative autoaggressive T cells from entering the periphery. Positively selected DP thymocytes differentiate into MHC I-restricted $CD8^+$ or MHC II-restricted $CD4^+$ SP thymocytes and relocate to the medulla where additional selection and maturation processes follow including further deletion of T cells reactive for tissue-specific antigens and the generation of regulatory T cells (reviewed by Anderton and Wraith, 2002; Nikolich-Zugich et al., 2004). Despite central tolerance mechanisms, however, autoreactive T cells happen to escape from selection processes and enter the peripheral T-cell repertoire where they may pose a serious threat to the organism (Liblau et al., 1991; Sun et al., 1991).

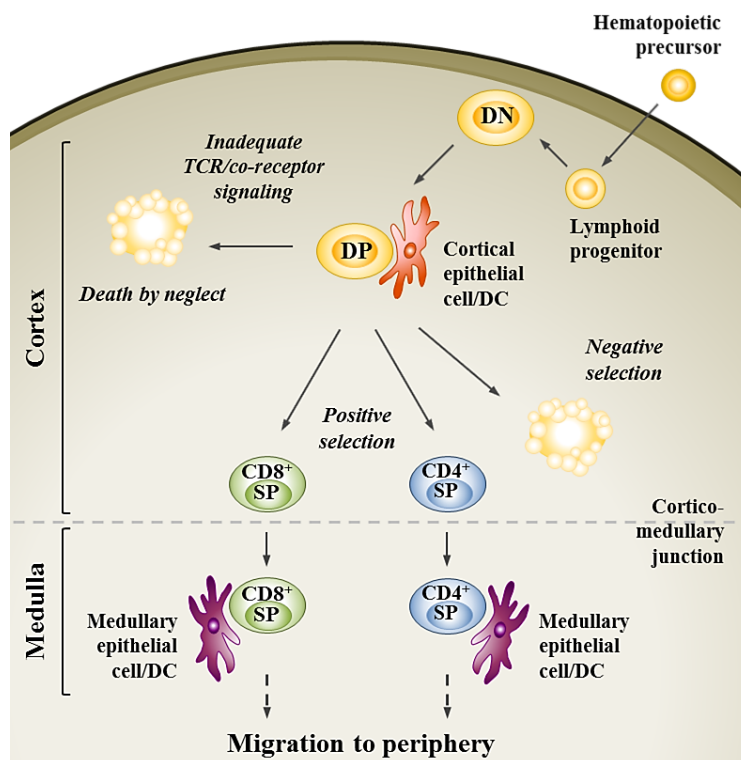


Fig. 1. T-cell selection in the thymus. Bone marrow-derived precursors enter the thymus and undergo T-cell development via consecutive stages of phenotypic maturation. The early committed thymocytes are characterized by lacking expression of TCR, CD4 and CD8 and therefore named DN thymocytes (double-negative). $CD4^+$ $CD8^+$ DP (double-positive) thymocytes developing in the thymic cortex are selected for their TCR avidity to self-peptide/MHC complexes presented by cortical epithelial and dendritic cells (DC). Insufficient TCR/co-receptor signaling induces apoptosis (death by neglect). Excessive signaling levels induce apoptosis in a so-called negative selection process to eliminate putative autoreactive cells. Positive selection due to an intermediate level of TCR signaling leads to the development of $CD8^+$ and $CD4^+$ SP thymocytes. After further selection and maturation processes of SP thymocytes in the thymic medulla, mature naïve T cells are released into the periphery. (Figure adapted from Takahama, 2006)

The membrane-anchored antigen-specific TCR of mature naïve T cells is composed of two immunoglobulin (Ig)-like chains. The vast majority of T cells (95 %) carries TCRs consisting of $\alpha\beta$ heterodimers and recognizes peptide antigens or rarely haptens in conjunction with MHC proteins presented on the surface of APCs (antigen-presenting cells). Soluble antigens can only be detected by a small population (2-5 %) of T cells expressing TCRs composed of both γ and δ chains. The TCR chains consist of a constant and a variable region. The latter in turn comprises three (hypervariable) complementarity determining regions (CDRs) which mediate the interaction to the antigen/MHC complex. The structural diversity of the TCRs is mainly based on the somatical gene rearrangement by the recombination-activating genes -1 and -2 (RAG-1, RAG-2) enzymes during T-cell development. Recombination of gene segments for the variable (V), joining (J), diversity (D) and the constant (C) regions in the case of the β chain and for the V-J-C regions in the case of the α chain guarantees receptor diversity on the one hand. On the other hand, mechanisms such as the random pairing of TCR α and β chains contribute to diversification as well as. Thereby, a great variability of particular antigen specificities is provided which allows recognition of almost any antigenic structure that can potentially be associated with infectious pathogens. The human TCR $\alpha\beta$ repertoire is estimated at a diversity of about 2.5×10^7 different TCR clonotypes (reviewed by Fearon and Locksley, 1996; Nikolich-Zugich et al., 2004).

In order to form a functional, signal-mediating TCR complex, the TCR $\alpha\beta$ chains associate with the CD3 complex consisting of one γ , one δ , two ϵ and two ξ chains all of which are required for signal transduction through ITAMs (immunoreceptor tyrosine-based activation motifs). Upon antigen-recognition, ITAMs of CD3 ξ chains are phosphorylated by the co-receptor associated tyrosine kinase Lck (and to a lesser extent by Fyn) upon which the enzyme ZAP-70 (zeta chain associated protein), another member of the spleen protein tyrosine kinase family, is bound via its SH2-domains (src-homology 2). ZAP-70 phosphorylates the transmembrane protein linker of activated T cells (LAT) which in turn serves as a docking site to other signaling proteins. Subsequent activation of signaling cascades leads to the transcription of several gene products with T-cell activation as the final outcome (reviewed by Bromley et al., 2001; Smith-Garvin et al., 2009).

3.2.2 CD4⁺ T helper Subsets in Autoimmunity

In autoimmunity, the allegedly most relevant players are CD4⁺ T cells which comprise a number of phenotypically and functionally distinct subsets. T-cell interaction with antigen-loaded APCs results in an antigen-specific T-cell activation with clonal expansion, affinity maturation and the exertion of effector functions (reviewed by Janeway, 2001). CD4⁺ T cells depend on antigen presentation by MHC class II molecules whose expression is limited to professional APCs and a few other cell types like endothelial and thymic epithelial cells referred to as non-professional APCs. The cell-surface co-receptor CD4 binds simultaneously with the antigen-specific TCR to antigen/MHC complexes presented by APCs. Hereby, the TCR complex-mediated signal is intracellularly induced. Among others, T helper (Th) cells are characterized by CD4 expression. Th cells exert essential functions in acquired immunity such as promoting B-cell antibody class switching, activation and expansion of cytotoxic CD8⁺ T cells and activation of APCs (reviewed by Bevan, 2004; Fearon and Locksley, 1996; Janeway, 2001).

The classification of CD4⁺ T effector cells into Th subsets is based on their characteristic cytokine production patterns. The direction of the CD4⁺ T-cell differentiation following foreign or self-antigen recognition is influenced by several factors including the duration and the strength of the TCR signal (reviewed by Abbas et al., 1996; Zhou et al., 2009). Strong TCR stimulation and high concentrations of antigen promote Th1 differentiation. In contrast, weak signals and low dose of antigen induce the differentiation into Th2 cells (reviewed by Constant et al., 1995; Iezzi et al., 1998). Following antigen recognition, interleukin-2 (IL-2) is produced by activated CD4⁺ T cells and serves as an important T-cell proliferation, differentiation and survival factor (reviewed by Dittel, 2008). The nature of the activating APCs and accordingly the prevailing cytokine profile which fundamentally directs differentiation into subpopulations is also influenced by several maturation signals. In a proinflammatory environment, innate immune cells such as DCs and macrophages produce IL-12 which functions as “instructive” cytokine that differentiates CD4⁺ T cells into inflammatory Th1 cells (Fig. 2). Interferon- γ (IFN- γ) secreted by natural killer (NK) cells promotes IL-12 production by APCs and consequently Th1 differentiation. In turn, IFN- γ induces the expression of IL-12 receptors on T cells (reviewed by Abbas et al., 1996; Zhou et al., 2009). Th1 cells characteristically produce IFN- γ , IL-2, tumor necrosis factor- α

(TNF- α) and - β (TNF- β , lymphotoxin- α) and others and boost cell-mediated immunity and inflammation. By activating macrophages, Th1 cells promote the elimination of intracellular pathogens. However, an excessive response of Th1 cells to self-antigens is might be the origin of organ-specific autoimmune diseases such as diabetes mellitus type 1, RA and MS as well as in inflammatory reactions such as granulomas (reviewed by Jager and Kuchroo, 2010).

Th2 differentiation is induced by IL-4 (Fig. 2). Th2 cells in turn produce cytokines such as IL-4, IL-5, IL-9, IL-10, IL-13 and IL-25, antagonize IFN- γ and inhibit the activation of macrophages. Moreover, Th2 cells promote especially those immune responses which are mediated by the antibody isotypes IgG1 and IgE, by mast cells and eosinophils as it is the case in parasitic infections, asthma and allergy, and chronic T-cell activation (e.g. SLE) (reviewed by Jager and Kuchroo, 2010; Zhou et al., 2009).

Recently, Th17 cells were identified as another distinct subset of CD4⁺ T helper cells (Fig. 2). Producing IL-17 (IL-17A), IL-17F, IL-21 and IL-22, Th17 cells regulate chemokine expression and tissue inflammation and are particularly linked to tissue neutrophil recruitment through the induction of granulocyte colony-stimulating factor (G-CSF) and IL-8 (reviewed by Dong, 2008). This cell subset mediates host defensive mechanisms to various infections especially extracellular bacterial and fungal infections and is involved in the pathogenesis of many autoimmune diseases (reviewed by Ghoreschi et al., 2011; Jager and Kuchroo, 2010). CD4⁺ T-cell activation in presence of IL-6 and transforming growth factor- β (TGF- β) leads to the induction of Th17 cells; IL-21 and IL-23 further promote Th17 differentiation (Fig. 2). Formerly considered as solely Th1-mediated, autoimmune diseases such as RA, MS, SLE, and inflammatory bowel disease are at least in part triggered by Th17 cells (reviewed by Ghoreschi et al., 2011; Jager and Kuchroo, 2010).

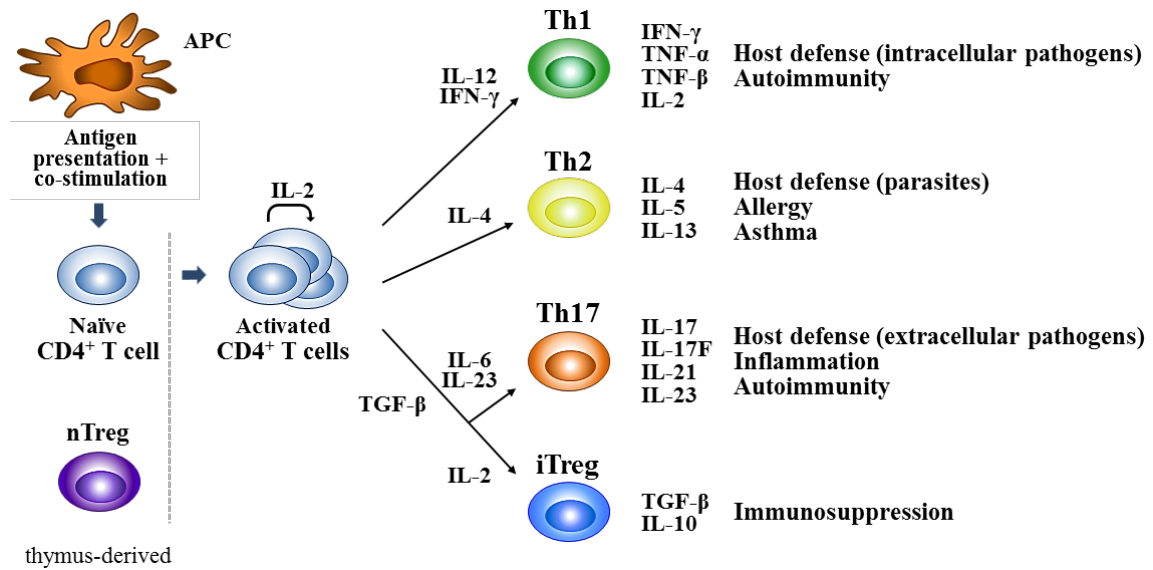


Fig. 2. Differentiation of CD4⁺ T-cell subsets. Antigen-presentation and co-stimulation by APCs induce naïve CD4⁺ T cells to produce IL-2 as an autocrine growth and survival factor. Depending on the prevailing cytokine milieu, activated CD4⁺ T cells differentiate into Th1, Th2, Th17 or iTreg cells, secrete cell lineage-specific cytokines and promote distinct immune responses. Like naïve CD4⁺ T cells, nTreg cells naturally emerge from the thymus. (Figure adapted from Dong, 2008)

The primary effector T-cell response targeting the offending pathogen is often followed by the occurrence of Treg cells which play an essential role in the induction and maintenance of immune homeostasis and peripheral tolerance (reviewed by Curotto de Lafaille and Lafaille, 2009; Sakaguchi et al., 2008). They are classified into two major categories: the naturally occurring CD4⁺ CD25⁺ regulatory T cells (nTreg) and the peripherally TGF- β -induced iTreg cells (Fig. 2) (Chen et al., 2003). During T-cell development, thymocytes whose TCRs bind self-peptide/MHC complexes with high affinity but do not undergo deletion during thymic selection processes potentially emerge as nTreg cells (Jordan et al., 2001). Regarding their development, survival and maintenance of function, Treg cells crucially depend on the presence of IL-2. An efficient competition of Treg cells sequestering IL-2 from effector T cells has been discussed (de la Rosa et al., 2004; Scheffold et al., 2005). Treg cells are characterized by the constitutive expression of CD25 (α chain of IL-2 receptor) and the robust expression of the transcription factor FoxP3 (forkhead box P3). Whereas CD25 is also expressed by activated effector T cells, FoxP3 is -at least in the murine system- an exclusive marker for the identification of Treg cells at the molecular level. FoxP3 is a transcriptional repression factor of the forkhead/winged-helix family and is critically

involved in specifying and maintaining the functional program of Treg cells (Fontenot et al., 2003; Hori et al., 2003). Treg cells exert their immune-suppressive function in an antigen-unspecific and cell contact-dependent manner. Secretion of immune-suppressive cytokines like TGF- β , IL-10 and IL-35 has been proposed. As a consequence, Treg cells are able to diminish the proliferation of naïve T cells, their differentiation into effector T cells and to restrain effector functions of differentiated CD4⁺ and CD8⁺ T cells, NK cells, B cells, macrophages and DCs (reviewed by Curotto de Lafaille and Lafaille, 2009; Sakaguchi et al., 2008).

3.2.3 Autoimmune Responses in the Pathogenesis of MS and EAE

For a long time, CD4⁺ T cells were believed to be the central players in the pathogenesis of MS and EAE. Nowadays, it is perceived that the pathogenic mechanisms are much more complex and that various cell types of both the acquired and the innate immune system contribute in several ways. Nevertheless, due to the immunization protocol of EAE, antigen-presentation is mainly mediated by MHC class II molecules and thus, the primary T-cell response in this model is restricted to myelin-specific CD4⁺ T cells (Ben-Nun et al., 1981). Even in healthy individuals, autoreactive myelin-specific T cells occur in the peripheral T-cell repertoire due to leaky tolerance mechanisms (Liblau et al., 1991; Sun et al., 1991). In MS pathogenesis, autoreactive T and B cells might be primed in the peripheral lymphoid organs either by endogenous antigens released from the CNS or by cross-reactive antigens from infectious agents. In actively induced EAE, professional APCs including DCs, macrophages and B cells migrate towards the source, take up and intracellularly process the myelin-derived peptides and present the autoantigens on their cell surface (reviewed by Gold et al., 2006). As a consequence to the antigen encounter, APCs secrete proinflammatory cytokines and chemokines which again induce an increased expression of membrane-bound adhesion molecules on APCs such as CD54 (ICAM-1, Intercellular Adhesion Molecule 1) and co-stimulatory molecules like CD40, CD80 (B7-1) and CD86 (B7-2). In secondary lymphoid organs, mature APCs present antigen/MHC I and antigen/MHC II complexes together with co-stimulatory molecules to antigen-specific T cells which receive the co-stimulatory signals via CD28, ICOS (Inducible Co-stimulator) or others (reviewed by Dempsey et al., 2003). Priming of naïve CD4⁺ T cells including their antigen-specific activation, expansion and differentiation into Th1 and Th17 effector T cells takes place during the

induction phase of actively-induced EAE. There, T-cell differentiation is strongly influenced by IL-12 produced by APCs after interaction of their TLR (Toll-like Receptors) with mycobacteria contained in “complete Freund’s adjuvant” in the immunization emulsion (Tsuji et al., 2000). T cells up-regulate the cell-surface expression of activation-associated molecules such as CD69 and CD44, of cytokine receptors including CD25 and secrete IL-2 as autocrine growth and differentiation factor (Robb, 1984; Ziegler et al., 1994). The adhesion molecules LFA-1 (Lymphocyte Function-associated Antigen -1) and VLA-4 (Very Late Antigen -4) are increasingly expressed during the induction phase (Dopp et al., 1994). These integrins stabilize the antigen/MHC-TCR ligation and mediate the adhesion to other immune cells, endothelial cells, fibroblasts and extracellular matrix proteins via their respective ligands ICAM (Intercellular Adhesion Molecule) and VCAM (Vascular Cell Adhesion Molecule). The “immunological synapse” between APCs and T cells, i.e. the simultaneous antigen-presentation, co-stimulation and adhesion via membrane-bound receptors, triggers the intracellular TCR complex-mediated signaling cascades (reviewed by Bromley et al., 2001; Smith-Garvin et al., 2009). APCs finalize their maturation process by upregulating the expression of co-stimulatory molecules, the secretion of IL-12, IL-18 and others and the release of chemokines such as IL-8, CCL3 (MIP-1 α) and CCL4 (MIP-1 β) (reviewed by Dempsey et al., 2003). After the induction phase of EAE, the effector phase takes effect starting with the circulation of activated myelin-specific T cells through the body in search for their target antigen. Mediated via LFA-1/ICAM-1 and VLA-4/VCAM-1 interaction, effector T cells adhere to brain endothelial cells and extravasate across the BBB into the CNS perivascular space and parenchyma. These interactions between encephalitogenic T cells with endothelial cells are the key determinants of migration of activated immune cells into the target tissue (reviewed by Engelhardt, 2006). Immunocytochemical studies of human brain tissue proved the expression of VCAM-1 in chronic active lesions and on endothelial and microglial cells of MS patients but not of healthy individuals (Cannella and Raine, 1995). First shown in EAE-affected mice, blocking of VLA-4 or VCAM-1 by monoclonal antibodies resulted in the inability of effector T cells to cross the BBB (Baron et al., 1993). The administration of natalizumab, a monoclonal antibody highly specific for VLA-4 on T cells, B cells and monocytes, turned out to be very effective in the treatment of active RR MS as the relapse-rate and the disability progression were both significantly

reduced (Polman et al., 2006). Lymphocyte trafficking is further supported by matrix metalloproteinases and the release of chemokines by endothelial and CNS-resident cells which recruit effector cells that express distinct cell-surface chemokine receptors. Thus, entry of primed neuroantigen-specific T cells into the CNS is directed by both integrin-dependent adhesion to the luminal vascular wall and chemokine-driven migration through the BBB. The expression of the chemokine receptors CCR1-5 and CCR8, CXCR2 and CXCR3 was found on CNS-infiltrating T cells after induction of EAE (Fife et al., 2001; Matejuk et al., 2000). Additionally, highly inflamed MS lesions were found to exhibit increased levels of CCR5 and its ligands (Balashov et al., 1999). CCR5 is primarily expressed by Th1 cells but also by monocytes/macrophages and immature DCs and ligates inflammatory chemokines such as CCL3 (MIP1- α), CCL4 (MIP1- β), CCL5 (RANTES) and CCL8 (MCP-2). These chemokines are produced by neurons, astrocytes, microglia and endothelial cells under inflammatory conditions (Izikson et al., 2000; Karpus et al., 1995). Recently, CXCL12, a ligand for CXCR7 and CXCR4, has been shown to be critical for the CNS entry of CXCR4-expressing lymphocytes during EAE induction as loss of CXCL12 from abluminal surfaces of the BBB results in minor cell accumulation in the CNS parenchyma of the CNS (Cruz-Orengo et al., 2011). CXCL12 expression increases during autoimmune disease and CXCR4 participates in the localization, proliferation, and activation of effector lymphocytes in inflamed tissue (Garcia-Vicuna et al., 2004). Amelioration of disease in a variety of murine models of autoimmunity has been accomplished via permanent treatment with a CXCR4 signaling antagonist suggesting that CXCR4 ligation is required during the expression of certain autoimmune diseases (Lukacs et al., 2002).

During MS and EAE pathogenesis, infiltrating effector T cells are believed to be re-activated by CNS-resident APCs like microglial cells and astrocytes as well as by infiltrating mononuclear phagocytes like DCs and macrophages that present immunodominant epitopes of myelin-derived proteins. In turn, T cells produce chemokines and cytokines hereby inducing further activation of APCs and the infiltration of other immune cells into the CNS parenchyma (reviewed by Goverman, 2009). Cytotoxic CD8⁺ T lymphocytes (CTLs) are able to directly damage cells which express and present myelin-derived antigens by MHC I molecules. Cytotoxicity is mediated by FasL (Fas ligand) interacting with Fas receptor on target cells, by perforin (pore-forming protein) and granzymes which in turn activate caspases, proteases that

play an essential role in apoptosis (Fig. 3) (reviewed by Gutcher and Becher, 2007; Petermann and Korn, 2011). Autoreactive B cells that re-encounter myelin antigens mature to plasma cells secreting antigen-specific antibodies which might subsequently damage the myelin sheath either via complement activation or by direct activation of downstream signaling mechanisms (Fig. 3). Demyelination of CNS axonal tracts is further triggered by the phagocytic activity of activated mononuclear cells and by the inflammatory and cytotoxic effects of cytokines released by T cells and APCs (e.g., $\text{IFN-}\gamma$, $\text{TNF-}\alpha$, $\text{TNF-}\beta$, IL-17 and nitric oxide/NO) (Fig. 3).

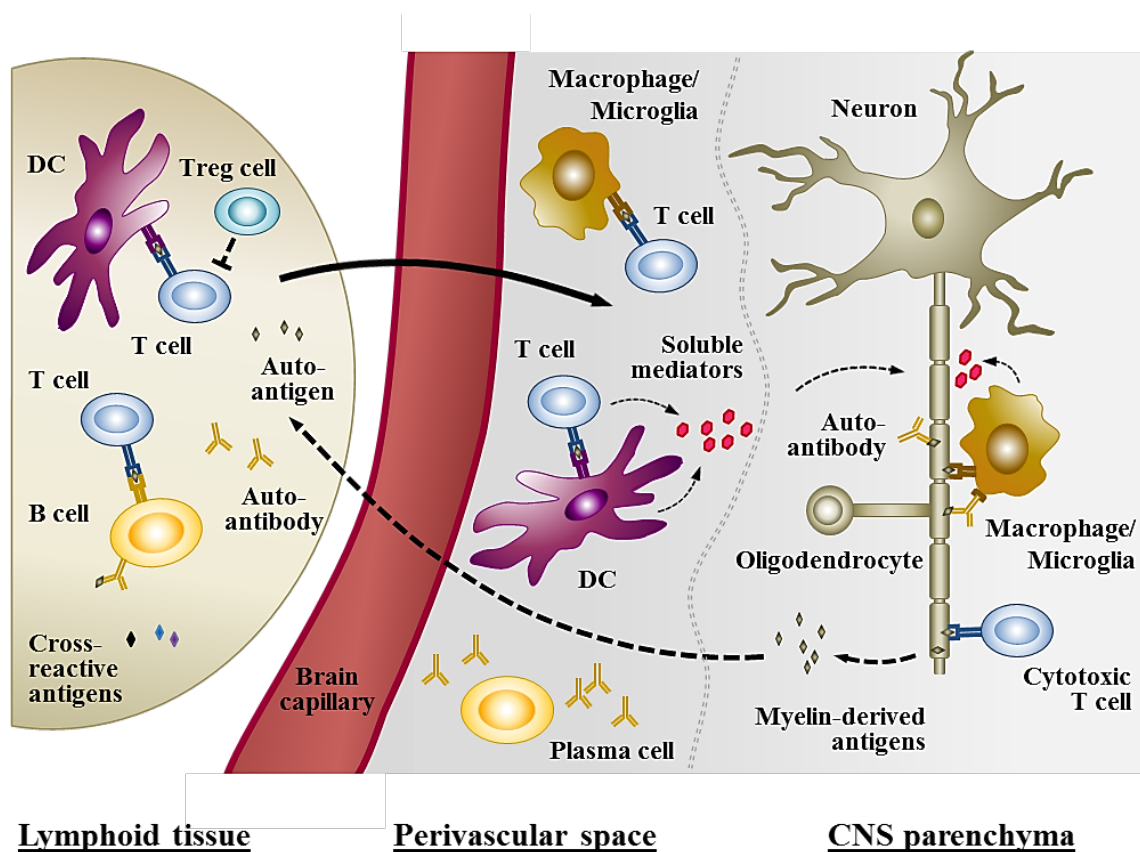


Fig 3. Current concepts of the pathogenesis of MS/EAE. Myelin-specific T and B cells are primed in peripheral lymphoid tissue by myelin-derived autoantigens released from the CNS or by cross-reactive antigens deriving from infectious agents. Activated lymphocytes migrate across the BBB into the CNS parenchyma. T cells are re-activated by APCs such as activated microglia or infiltrating DCs in the perivascular space and secrete proinflammatory cytokines attracting other immune cells. B cells that re-encounter myelin antigens mature to plasma cells secreting autoantibodies which subsequently induce damage to the myelin sheath either via complement activation or by opsonization of myelin. Mediated by FasL, perforin and granzyme, cytotoxic CD8^+ T cells directly damage cells that express and present myelin antigens by MHC I molecules. Macrophages/microglia contribute to neuronal damage by secretion of several proinflammatory mediators as well as by phagocytosis of the myelin sheath. (Figure adapted from Goverman, 2009)

3.3 Co-Signaling in T-cell Activation

Antigen-presentation to T cells by professional APCs is a critical step in the initiation of T-cell-mediated immune responses. The “two signal model” of T-cell activation claims that for the initiation of effective T-cell responses as well as for the maintenance of peripheral self-tolerance the antigen-specific stimulation of the TCR by antigen/MHC complexes, so-called signal 1, is required. Simultaneously, a second, antigen-independent signal, so-called signal 2, is needed which is mediated via co-signaling molecules (reviewed by Bretscher, 1999; Lafferty and Gill, 1993). Co-signaling molecules on APCs may either provide co-stimulatory signals that promote T-cell activation or co-inhibitory signals that inhibit T-cell responses and mediate T-cell tolerance at the level of naïve but also of effector and memory T cells and Treg cells. Without signal 2, antigen-specific engagement of the TCRs results in inefficient T-cell activation, anergy or apoptosis (reviewed by Chen, 2004; Wells et al., 2001). Additionally, the prevailing cytokine milieu influencing T-cell differentiation and completing the polarization of T-cell responses is often referred to as signal 3 of T-cell activation (reviewed by Gutcher and Becher, 2007).

3.3.1 Co-Signaling Molecules of the B7 and CD28 Families

A large variety of co-receptors has been described which mediate “signal 2” between APCs and T cells. The ligation of B7 molecules on professional APCs to members of the CD28 receptor family on T cells delivers either co-stimulatory or co-inhibitory signals influencing the T-cell response accordingly (reviewed by Subudhi et al., 2005). Both B7 and CD28 families comprise type I transmembrane proteins classified into the Ig superfamily. CD80 and CD86 are the first identified members of the B7 family (reviewed by Bluestone, 1995). The interaction of CD80 and CD86 on professional APCs such as macrophages and DCs with CD28, a co-receptor that is constitutively expressed on most T cells, leads to an enhanced activation, accelerated cell cycle progression, T-cell survival and clonal expansion promoted by enhanced IL-2 production and upregulation of the anti-apoptotic protein bcl-XL (reviewed by Chambers, 2001). The primary function of CD28 is lymphocyte activation but it is substantially involved in the maintenance of peripheral tolerance, too. Under the influence of CD28 signaling the development and maintenance of Treg cells are directed, the expression of immune-inhibitory molecules such as CTLA-4 (Cytotoxic T-

Lymphocyte Antigen 4) increases and the CD4⁺ T-cell response can be shifted towards an autoimmune-protective Th2 phenotype (reviewed by Guo et al., 2008; Webb and Feldmann, 1995). CD80 and CD86 also ligate the receptor CTLA-4 which is exclusively present on activated T cells and which binds its ligands with higher affinities than CD28. The engagement of CTLA-4 delivers a negative signal to the activated T cell by inhibition of IL-2 synthesis and induction of cell cycle arrest and thus counteracts and terminates the ongoing T-cell response. Another member of the CD28 family is the co-stimulatory receptor ICOS which is increasingly expressed upon T-cell activation. In contrast to CD28, ICOS-mediated co-stimulation does not (or not optimally) induce IL-2 production but enhances the secretion of IL-4, IL-5, IL-10, IFN- γ and TNF- α suggesting that ICOS primarily functions to induce T-cell effector functions (reviewed by Chambers, 2001). In the past few years, another co-inhibitory signaling pathway conveyed by members of the B7 and CD28 families has been increasingly described: the pathway of PD-1 and its ligands B7-H1 and B7-DC.

3.3.2 The Programmed Death-1 Receptor and its Ligands

First identified as a gene upregulated in a murine T-cell hybridoma undergoing cell death, the membrane-standing PD-1 receptor (Programmed Death-1, CD279) is found on activated T and B lymphocytes as well as on activated NKT cells (natural killer T cells), monocytes, DCs and a subset of thymocytes (Agata et al., 1996). PD-1 is a member of the CD28-like receptor family and shares some structural homologies with CD28, CTLA-4 and ICOS such as the extracellular IgV-like (immunoglobulin variable) domain (Ishida et al., 1992; Zhang et al., 2004). However, PD-1 differs from the other CD28-family members for example in the gene locus (Shinohara et al., 1994). It is a Type I transmembrane protein of 268 amino acids with an extracellular domain of 147, a transmembrane domain of 27 and a cytoplasmatic tail of 94 amino acids (Ishida et al., 1992). Different from CD28, CTLA-4 and ICOS, PD-1 occurs as a monomer on the cell surface partly due to the lack of cysteine residues forming disulfide bridges (Zhang et al., 2004). The cytoplasmatic tail contains two phosphorylation sites located in an immunoreceptor tyrosine-based inhibitory motif (ITIM) and an immunoreceptor tyrosine-based switch motif (ITSM). Upon ligand binding and simultaneous antigen-specific activation of the TCR complex, the protein tyrosine phosphatases SHP-1 and -2 (Src Homology Phosphatase) are recruited to these motifs (Fig. 4) (Chemnitz et al.,

2004; Latchman et al., 2001; reviewed by Riley, 2009). SHP-1 and -2 dephosphorylate and thereby deactivate downstream effector proteins of the antigen-receptor signaling cascade including phosphatidylinositol-3 kinase (PI3K), phospholipase C-(PLC) γ 2, and extracellular signal-regulated kinase (ERK) thereby restricting the extent of the TCR-mediated T-cell activation (Fig. 4) (Latchman, Wood et al. 2001; Chemnitz, Parry et al. 2004).

The two PD-1 ligands (PD-Ls), the B7-family members B7-H1 (B7 homologue 1, PD-L1, CD274) and B7-DC (PD-L2, CD273), show distinct expression patterns. B7-H1 is constitutively expressed at low levels in lymphoid cells like resting T and B cells, in myeloid cells as macrophages and in dendritic cells. Its expression gets upregulated in an inflammatory milieu determined by the presence of IFN- γ , LPS, GM-CSF (granulocyte-macrophage colony-stimulating factor) or IL-4 (Liang et al., 2003). Additionally, B7-H1 is found on non-hematopoietic cells including vascular endothelial cells, glial cells in the inflamed brain, in non-lymphoid organs like pancreas, heart and lung as well as in “immune-privileged” organs such as placenta (Petroff et al., 2003). In contrast, the expression of B7-DC on hematopoietic cells is mainly restricted to macrophages and DCs but is also upregulated upon activation with IFN- γ , GM-CSF and IL-4 (Ishida et al., 2002; Latchman et al., 2001; Liang et al., 2003; Rodig et al., 2003; Yamazaki et al., 2002).

The role of B7-H1 and B7-DC in negatively regulating T-cell responses mediated via their mutual receptor PD-1 was demonstrated in numerous *in vitro* studies (Bennett et al., 2003; Carter et al., 2002; Freeman et al., 2000; Latchman et al., 2001). Freeman et al. showed that the engagement of PD-1 on murine and human T cells by human B7-H1 Ig leads to a dose-dependent blockade of CD3-mediated T-cell proliferation and cytokine production (Fig. 4) (Freeman et al., 2000). Even though T-cell cytokine production was restrained in general upon PD-1/B7-H1 ligation, IL-10 secretion was found to be induced potentially contributing to the negative regulation of T-cell-mediated immunity (Dong et al., 1999). Recently, CD80 was identified as another receptor for B7-H1. The interaction was shown to inhibit T-cell activation characterized by diminished expression of cell-surface activation markers, decreased T cell proliferation and reduced cytokine production *in vitro* (Butte et al., 2007). Albeit plenty of studies described an inhibitory effect of the PD-1/PD-Ls pathway, contradictory results have been reported claiming a co-stimulatory role on T-cell functions. T-cell

proliferation was induced after binding of B7-H1 Ig to its cognate receptor(s) in the presence of polyclonal stimuli or allogeneic antigens (Dong et al., 1999). Likewise, *in vivo* T-cell proliferation of adoptively transferred OVA-specific (ovalbumin) so-called OT-I CD8⁺ T cells in OVA-transgenic mice was enhanced by the injection of B7-H1 Ig fusion protein (Subudhi et al., 2004). The contradictory results concerning the PD-1/PD-Ls pathway might be explained by the existence of a third receptor for B7-H1 and B7-DC which promotes T-cell activation as suggested by Kanai et al. (Kanai et al., 2003). Moreover, agonistic vs. antagonistic effects of the antibodies as well as the genetic background of experimental mice used in the studies evidentially influence the outcome (Wang et al., 2005).

In vivo studies have shown that cancer-cell associated B7-H1 expression prevented tumor rejection in a murine adoptive transfer model by inducing T-cell apoptosis or by rendering tumor cells more resistant to cytolysis (Dong et al., 2002; Iwai et al., 2002). The expression of both B7-H1 and B7-DC on several types of tumor cells has therefore been recognized as a tumor strategy that has evolved to evade the host's immunity. As a consequence, high expression levels on human tumors often entail negative outcome due to inhibition of effector T-cell responses (reviewed by Okazaki and Honjo, 2007).

The co-inhibitory function of the PD-1/PD-Ls pathway is best characterized in connection with adaptive immunity but several studies also validated the regulation of innate immunity for example of DC-mediated immune responses during infection with *Listeria monocytogenes* in the mouse (Yao et al., 2009). Since B7-H1 and B7-DC expression is broadly distributed throughout the body, the biological significance of the PD-1/B7-H1 and PD-1/B7-DC pathway has been assigned to numerous immune responses including tumor and infectious immunity, immunological privilege and autoimmunity.

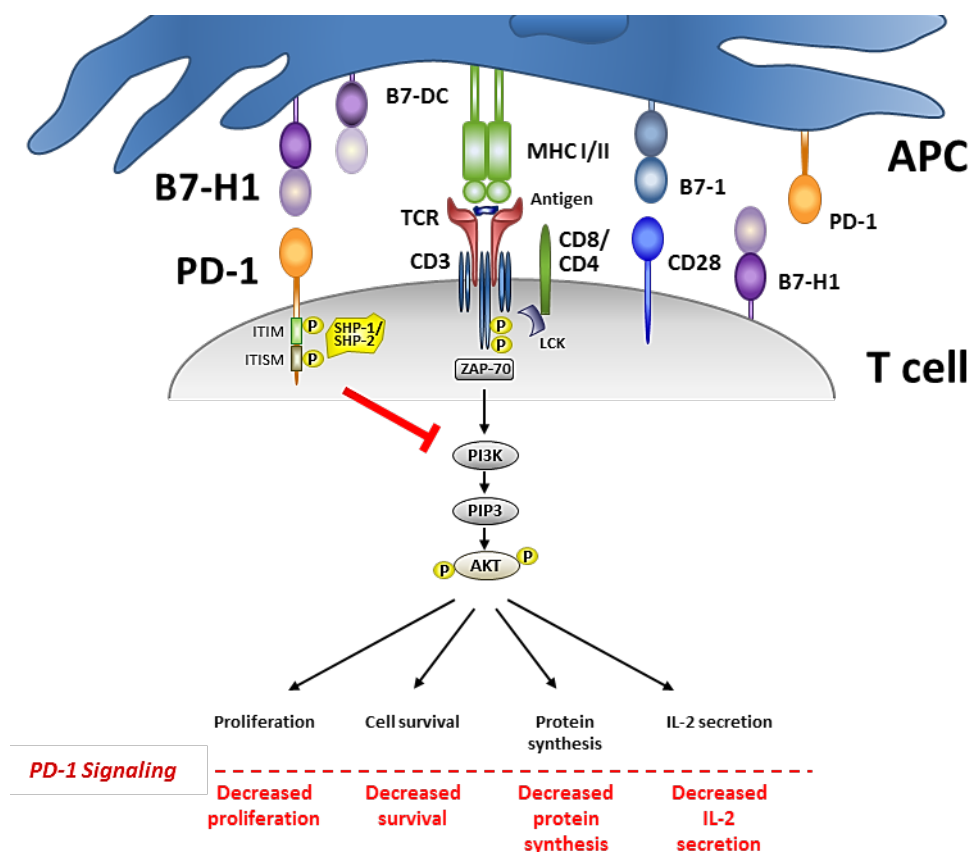


Fig. 4. PD-1 signaling in T cells. Following TCR engagement by antigen/MHC I or antigen/MHC II complexes, CD8/CD4 co-receptor-associated kinase Lck is activated leading to phosphorylation of CD3 ζ -chains and ZAP-70. Activated ZAP-70 initiates downstream signaling cascades that induce T-cell proliferation and survival, protein synthesis and IL-2 production. Ligation of PD-1 on T cells by B7-H1 on APCs leads to tyrosine phosphorylation of ITIM and ITSM in the cytoplasmic tail of the PD-1 receptor. Here, the protein tyrosine phosphatases SHP-1 or SHP-2 are recruited to. This induces dephosphorylation of downstream signaling molecules which effectively attenuates the PI3K and Akt pathway and thereby restricts the extent of T-cell activation (Red bar and text indicate consequences of PD-1-mediated signaling). (Figure adapted from Francisco et al., 2010)

3.3.3 The PD-1/B7-H1 Pathway in Autoimmunity

The PD-1/PD-Ls pathway has been suggested a role in T-cell development and central tolerance mechanisms. B7-DC is expressed on thymic medullary epithelial cells in mice whereas B7-H1 is found on cortical epithelial cells of the thymus and on thymocytes. Moreover, PD-1 is expressed on CD4⁻ CD8⁻ DN thymocytes at the time point of TCR β chain gene rearrangement during T-cell maturation (Liang et al., 2003; Nishimura et al., 1996; Nishimura et al., 2000). The injection of anti-CD3 monoclonal antibodies was shown to significantly increase the expression of PD-1 in murine double-negative thymocytes implying a role of PD-1 in the β selection process (Nishimura, Agata et al.

1996). Moreover, PD-1/B7-H1 ligation modulates selection during the transition from double-negative to double-positive CD4⁺ CD8⁺ thymocytes as the loss of either PD-1 or B7-H1 was shown to increase the number of double-positive thymocytes (Keir et al., 2005; Nishimura et al., 2000). Findings in PD-1 deficient mice (C57BL/6-Pdcd-1^{-/-}) suggest that the PD-1/PD-Ls pathway plays a critical role in the prevention of autoimmunity: about half of the mice developed lupus-like arthritis and glomerulonephritis with increasing age (Nishimura et al., 1998; Nishimura et al., 1999). Alterations in thymic development and central tolerance mechanisms but also in induction and maintenance of peripheral tolerance mechanisms could have contributed to this autoimmune phenotype. In a model for tissue-specific autoimmunity - the NOD (non-obese diabetic) mouse model for diabetes -, the disruption of the PD-1/B7-H1 pathway in prediabetic mice by the administration of blocking monoclonal antibodies seriously accelerated the pathogenesis of diabetes with precipitated insulinitis and secretion of proinflammatory T-cell cytokines. These results indicated that the PD-1/B7-H1 signaling pathway profoundly maintained peripheral tolerance in this mouse model (Ansari et al., 2003; Keir et al., 2006). Moreover, studies with bone marrow chimeras supported the view that parenchymal expression of B7-H1/B7-DC mediated tissue-specific tolerance. Studies with bone marrow chimeras demonstrated that B7-H1/B7-DC expression only on APCs was insufficient to prevent the early onset diabetes in NOD mice which had been transferred prediabetic wildtype (wt) T cells. In contrast, B7-H1/B7-DC expression on transplanted islets protected against immunopathology mediated by transferred autoreactive CD4⁺ T cells (Keir et al., 2006). Loss of PD-1 on autoreactive CD8⁺ T cells was shown to enhance T-cell activation and expansion upon encounter with self-antigen-presenting DCs (Keir et al., 2007). Immunohistochemical analysis of C57BL/6 mice in the acute phase of MOG₃₅₋₅₅-induced EAE detected the expression of PD-1, B7-H1 and B7-DC on mononuclear cells accumulating within the meninges. Moreover, B7-H1 expression was up-regulated on endothelial cells, astrocytes and microglial cells in the inflamed CNS (Liang et al., 2003; Magnus et al., 2005). Blocking the interaction between PD-1 and its ligands proved a critical role of this pathway in EAE. The administration of anti-PD-1 or anti-B7-DC blocking monoclonal antibodies during the induction phase of MOG₃₅₋₅₅-induced EAE in C57BL/6 mice led to accelerated onset and more severe disease course, increased inflammatory infiltrates within the CNS and increased numbers of MOG-reactive T

cells and antibodies (Salama et al., 2003). Studies on PD-1-, B7-H1- and B7-DC-deficient mice revealed that PD-1 and predominantly B7-H1 and not B7-DC were responsible for influencing the severity of EAE in various mouse strains (Carter et al., 2007; Latchman et al., 2004; Ortler et al., 2008). Passively induced EAE by adoptive transfer of wt encephalitogenic T cells into B7-H1^{-/-} compared to wt recipient mice led to exacerbated disease in mice lacking B7-H1 expression. The disease course was even more severe when B7-H1^{-/-} recipient mice received T cells from B7-H1^{-/-} donor mice. These results underlined the importance of B7-H1 expression on APCs and host tissue and also on T cells in crucially inhibiting naïve and effector T cell responses (Latchman et al., 2004).

Treg cells have been identified as another important mechanism of peripheral tolerance by suppressing proliferation of and cytokine production by activated T cells (reviewed by Sakaguchi et al., 2008). Both PD-1 and B7-H1 are highly expressed on the Treg population hinting at an involvement of this pathway in Treg-mediated functions (Baecher-Allan et al., 2003; Krupnick et al., 2005). Indeed, adoptive transfer studies suggest that B7-H1 plays a critical role in the induction and maintenance of iTreg cell development as iTreg conversion of transferred CD4⁺ FoxP3⁻ T cells was markedly lower in B7-H1^{-/-} B7-DC^{-/-} RAG^{-/-} than in wt RAG^{-/-} recipient mice (Francisco et al., 2009).

A correlation of SNP (Single Nucleotide Polymorphism) in the encoding PDCD1 gene with various autoimmune diseases in humans such as for SLE, RA and MS has been assumed (Kroner et al., 2005; Prokunina et al., 2002; Prokunina et al., 2004). One polymorphism has been described to be located in a binding site for the transcription factor Runx1 (runt related transcription factor 1) which plays an important role in the regulation of hematopoiesis. This polymorphism has been associated with high IFN- γ levels in MS patients due to the loss of PD-1-mediated inhibition which might occur due to decreased stability of mRNA or expression level of PD-1 (Kroner et al., 2005). In addition, antibodies against B7-H1 were found in patients with RA potentially contributing to a dysregulation of T-cell responses (Dong et al., 2003). Upregulation of B7-H1 expression was also pronounced to represent a counter-mechanism that confines parenchymal inflammation in human autoimmunity. Studies by Ortler et al. supported this hypothesis by revealing a considerable expression of B7-H1 in CNS specimens of MS patients which was largely absent in non-pathological CNS tissue (Ortler et al.,

2008).

All together, these data suggest an important role of the PD-1/B7-H signaling pathway in the induction and maintenance of peripheral T-cell tolerance thereby contributing to the protection from autoimmunity.

4 Objectives

The role of B7-H1 in the maintenance of immune tolerance and in the confinement of immune responses has been studied comprehensively in animal models. In the present study, we thought to elucidate the role of B7-H1 in the pathogenesis of spontaneous CNS autoimmunity. To do so, the double-transgenic $\text{TCR}^{\text{MOG}} \times \text{IgH}^{\text{MOG}}$ /Devic mouse model was used which characteristically develops spontaneous neuroinflammation due to the interaction of myelin-specific B cells and myelin-specific CD4^+ T cells.

This study was undertaken with the following objectives.

1. To establish the Devic mouse model under the prevailing animal housing and breeding facilities.
2. To characterize the influence of B7-H1 deficiency on the clinical course of spontaneous EAE-like disease by introducing B7-H1 knock-out in Devic mice.
3. To elucidate predominantly the influence of B7-H1 deficiency on myelin-specific CD4^+ T-cell responses and secondly on myelin-specific B-cell responses during the EAE-like disease.

5 Material and Methods

5.1 Material

5.1.1 Chemical

2-mercaptoethanol	Gibco (Invitrogen), Karlsruhe
3,3', 5,5' tetramethylbenzidine (TMB)	Sigma-Aldrich, Steinheim
Acetic acid	J.T. Baker, Griesheim
Agarose	Sigma-Aldrich, Steinheim
Ammonium chloride	Merck, Darmstadt
Aqua ad iniectabilia	B. Braun Melsungen
Aquatex®	Merck, Darmstadt
Brefeldin A (GolgiPlug™)	BD Biosciences, Heidelberg
Calcium chloride	Sigma-Aldrich, Steinheim
Cell Proliferation Dye eFluor® 670	eBioscience, San Diego, USA
DNA ladder, 100 bp	PEQLAB, Erlangen
dNTP Solution Mix	PEQLAB, Erlangen
Diaminobenzidine (DAB)	Kementec, Copenhagen, Denmark
Dimethyl sulfoxide (DMSO)	C. Roth, Karlsruhe
Ethanol	J.T. Baker, Griesheim
Ethidium bromide	Sigma-Aldrich, Steinheim
Ethylenediaminetetraacetate (EDTA)	Sigma-Aldrich, Steinheim
Heparin-sodium (25 000 I.E.)	Ratiopharm, Ulm
Hydrogen peroxide	Merck, Darmstadt
Isopentane	Sigma-Aldrich, Steinheim
MicroScint™-20, 1L	PerkinElmer, Rodgau
Paraformaldehyde (PFA)	Sigma-Aldrich, Steinheim
Percoll	GE Healthcare Europe GmbH, Freiburg
Potassium chloride	Merck, Darmstadt
Potassium bicarbonate	Merck, Darmstadt
Potassium dihydrogen phosphate	Merck, Darmstadt
Sodium azide	Merck, Darmstadt
Sodium chloride	Merck, Darmstadt

Sodium phosphate	Merck, Darmstadt
Sodium pyruvate	Gibco (Invitrogen), Karlsruhe
Streptavidin-HRP complex	R&D Systems
Taq DNA polymerase	Invitrogen, Karlsruhe
Tissue-Tek® OCT™ compound	DiaTec, Hallstadt
Triton X-100	Sigma-Aldrich, Steinheim
Tris acetate	C. Roth, Karlsruhe
Trypan blue	Sigma-Aldrich, Steinheim
Tween-20	Sigma-Aldrich, Steinheim

If not indicated differently, all suppliers are located in Germany.

5.1.2 Biochemicals, Media and Supplements

1x PBS (0.1 M)	PAA Laboratories, Pasching
[³ H] thymidine	Amersham, Piscataway, USA
Bovine serum albumin (BSA)	Sigma-Aldrich, Steinheim
Fetal calf serum (FCS)	PAA Laboratories, Pasching
Geneticin	Gibco (Invitrogen), Karlsruhe
Gentamicin	Gibco (Invitrogen), Karlsruhe
HEPES	Gibco (Invitrogen), Karlsruhe
L-glutamine	Gibco (Invitrogen), Karlsruhe
MOG ₃₅₋₅₅	purified by R. Volkmer, Charité, Berlin
MOG ₁₋₁₂₅	purified by A. Weishaupt, Neurologische Klinik und Poliklinik, Würzburg
Non-essential amino acids (NEAA)	Lonza, Basel, Switzerland
Streptomycin	Gibco (Invitrogen), Karlsruhe
RPMI 1640	PAA Laboratories, Pasching

If not indicated differently, all suppliers are located in Germany.

5.1.3 Kits

CD45R (B220) MicroBeads	Miltenyi, Bergisch Gladbach
BD Cytotfix/Cytoperm Plus Fixation/Permeabilization Kit	BD Biosciences, Heidelberg
BD Cytometric Bead Array(CBA)	BD Biosciences, Heidelberg

Mouse Th1/Th2/Th17 Cytokine Kit	BD Biosciences, Heidelberg
Calibrite beads	
CD4 ⁺ T cell Isolation Kit II	Miltenyi, Bergisch Gladbach
DNeasy Blood & Tissue kit	Qiagen, Hilden
Mouse IFN- γ (DuoSet ELISA Development Kit)	R&D Systems, Wiesbaden-Nordenstadt
Mouse IL-17 (DuoSet ELISA Development Kit)	R&D Systems, Wiesbaden-Nordenstadt
Mouse Regulatory T cell Staining Kit	eBioscience, San Diego, USA
StreptABComplex Duo Reagent Set	DakoCytomation, Glostrup, Denmark

If not indicated differently, all suppliers are located in Germany.

5.1.4 Cell Culture Media

Culture media:	RPMI 1640
	10 % FCS
	2 mM L-glutamine
	1 mM sodium pyruvate
	100 U/mL penicillin
	10 μ g/mL streptomycin
	50 μ M 2-mercaptoethanol
	10 mM HEPES
Freezing media:	90 % FCS
	10 % DMSO

5.1.5 Buffers and Solutions

ACK buffer (Ammonium-Chloride-Potassium; erythrocytes lysing buffer)	150 mM ammonium chloride 10 mM potassium bicarbonate 0.1 mM EDTA pH adjusted to 7.4
Annexin V Buffer (10x)	0.1 M HEPES 1.4 M sodium chloride 25 mM calcium chloride

	pH adjusted to 7.4
ELISA reagent diluent (IFN- γ)	0.1 % BSA 0.05 % Tween-20 in 1x PBS pH adjusted to 7.4
ELISA reagent diluent (IL-17)	1 % BSA in 1x PBS pH adjusted to 7.4
ELISA blocking buffer	1 % BSA 0.05 % sodium azide in 1x PBS pH adjusted to 7.4
ELISA wash buffer	0.05 % Tween-20 in 1x PBS pH adjusted to 7.4
FACS buffer	0.1 % BSA 0.1 % sodium azide in 1x PBS pH adjusted to 7.4
MACS buffer	0.5 % BSA 2 mM EDTA in 1x PBS pH adjusted to 7.4
1x PBS (0.1 M)	0.14 M sodium chloride 2.7 mM potassium chloride 3.2 mM sodium phosphate 1.5 mM potassium dihydrogen phosphate pH adjusted to 7.4

50x TAE buffer	2 M tris acetate
	1 M acetic acid
	50 mM EDTA
	pH adjusted to 8.0

5.1.6 PCR Primers for Genotyping

Gene/Transgene	B7-H1 wt
Forward primer (5'-3')	AGAACGGGAGCTGGACCTGCTTGCGTTAG
Reverse Primer (5'-3')	ATTGACTTTCAGCGTGATTCGCTTGTAG
Annealing temperature	60 °C
Replication cycles	40
Band size	250 bp
Gene/Transgene	B7-H1 ko
Forward primer (5'-3')	TTCTATCGCCTTCTTGACGAGTTCTTCTG
Reverse Primer (5'-3')	ATTGACTTTCAGCGTGATTCGCTTGTAG
Annealing temperature	60 °C
Replication cycles	40
Band size	450 bp
Gene/Transgene	IgH wt
Forward primer (5'-3')	TCT CTT CTA TGC TTT CTT TGT CCC
Reverse Primer (5'-3')	GTC ATT GTT CCA CAT TCT GTT CC
Annealing temperature	62 °C
Replication cycles	35
Band size	560 bp
Gene/Transgene	IgH^{MOG} tg
Forward primer (5'-3')	GCA TCC TGA TAC CTG ACG CA
Reverse Primer (5'-3')	GGA GAC TGT GAG AGT GGT GCC T
Annealing temperature	62 °C
Replication cycles	35
Band size	700 bp

Gene/Transgene	TCR^{MOG} tg
Forward primer (5'-3')	CCC GGG CAA GGC TCA GCC ATG CTC CTG
Reverse Primer (5'-3')	GCG GCC GCA ATT CCC AGA GAC ATC CCT CC
Annealing temperature	68 °C
Replication cycles	35
Band size	700 bp
Gene/Transgene	RAG-1 wt
Forward primer (5'-3')	GAGGTTCCGCTACGACTCTG
Reverse Primer (5'-3')	TGGATGTGGAATTGTTGCGAG
Annealing temperature	58 °C
Replication cycles	35
Band size	470 bp
Gene/Transgene	RAG-1 ko
Forward primer (5'-3')	CCGGACAAGTTTTTCATCGT
Reverse Primer (5'-3')	TGGATGTGGAATTGTTGCGAG
Annealing temperature	58 °C
Replication cycles	35
Band size	530 bp

All primers were purchased from Sigma-Aldrich, Steinheim, Germany.

5.1.7 Antibodies for Flow Cytometry

Antigen	Specificity	Clone	Format	Source
B7-H1	rat anti-mouse	MIH5	PE	BD Biosciences
CD4	rat anti-mouse	GK1.5	FITC	BD Biosciences
CD4	rat anti-mouse	RM4-5	PerCp	BD Biosciences
CD4	rat anti-mouse	RM4-5	APC	BD Biosciences
CD8a	rat anti-mouse	53-6.7	FITC	BD Biosciences
CD8a	rat anti-mouse	53-6.7	PE	BD Biosciences
CD8a	rat anti-mouse	53-6.7	PerCp	BD Biosciences
CD8a	rat anti-mouse	53-6.7	APC	BD Biosciences

CD11b	rat anti-mouse	M1/70	PE	BD Biosciences
CD25	rat anti-mouse	PC61	APC	BD Biosciences
CD44	rat anti-mouse	IM7	FITC	BD Biosciences
CD45R/B220	rat anti-mouse	RA3-6B2	PE	BD Biosciences
CD62L	rat anti-mouse	MEL-14	APC	BD Biosciences
CD69	hamster anti-mouse	H1.2F3	FITC	BD Biosciences
CD184 (CXCR4)	rat anti-mouse	2B11	FITC	BD Biosciences
CD195 (CCR5)	rat anti-mouse	C34-3448	PE	BD Biosciences
FoxP3	rat anti-mouse/rat	FJK-16s	APC	eBioscience
IL-17	rat anti-mouse	TC11-18h10	PE	BD Biosciences
IFN-γ	rat anti-mouse	XMG1.2	APC	BD Biosciences
Vα3.2^{b,c}	rat anti-mouse	RR3-16	FITC	BD Biosciences
Vβ11	rat anti-mouse	RR3-15	FITC	BD Biosciences
Vβ11	rat anti-mouse	RR3-15	PE	BD Biosciences
Annexin V			FITC	BD Biosciences

BD Biosciences, Heidelberg, Germany; eBioscience, San Diego, USA

5.1.8 Antibodies for Histology

Primary antibodies

Antigen	Format	Specificity	Clone	Source
CD4	purified	rat anti-mouse	YTS191.1	Serotec
CD11b	purified	rat anti-mouse	OX-42	Serotec

Secondary antibody

Isotype	Format	Specificity	Clone	Source
IgG	biotinylated	goat anti-rat	polyclonal	Serotec

Serotec, Oxford, UK

5.1.9 Consumables

1.5 ml / 2 ml tubes

Eppendorf, Wesseling-Berzdorf

15 ml / 50 ml tubes

BD Biosciences, Heidelberg

Cell culture flasks	Greiner Bio-One, Frickenhausen
Cell culture plates	Nunc, Wiesbaden
Cell strainer, 40µm pore size	BD Biosciences, Heidelberg
Centrifuge tubes	Greiner Bio-One, Frickenhausen
Combination tips	Eppendorf, Wesseling-Berzdorf
CryoTubes™	Nunc, Wiesbaden
Diabetes syringes	BD Biosciences, Heidelberg
Disposable syringes	B. Braun Melsungen
ELISA plates (Maxisorp ® flat-bottom 96 well plate)	Nunc, Wiesbaden
Glass slides (SuperFrost®)	Langenbrinck, Teningen
Gloves	Cardinal Health, Baesweiler
Needles	BD Biosciences, Heidelberg
MACS columns (MS, LS)	Miltenyi, Bergisch Gladbach
Microtiter plates (ELISPOT)	Millipore, Schwalbach
Petri dishes	Sarstedt, Nümbrecht
Plastic pipettes	Corning, New York, USA
Polyester Membrane Transwell- clear Inserts	Corning Costar, Bodenheim
ScintiPlate-96 Tissue Culture	PerkinElmer, Rodgau-Jügesheim
Tips	Sarstedt, Nümbrecht
Scalpel	B. Braun Melsungen
Sterile filter	Nalgene, Hereford, UK

If not indicated differently, all suppliers are located in Germany.

5.1.10 Laboratory Equipment and Instruments

Agarose gel chamber (Sub Cell GT)	Biorad, München
Analytical scales	Sartorius, Göttingen
Autoclave	Vakulab HP Münchener Medizin Mechanik GmbH, Planegg
β-scintillation counter (TopCount NXT)	PerkinElmer, Rodgau-Jügesheim
Camera (for gel documentation)	Intas Science Imaging Instruments GmbH, Göttingen

Cell Counter and Analyzer (Casy® Model TT)	Roche, Grenzach-Wyhlen
Cell Harvester	Connectorate AG, Dietikon, Switzerland
Centrifuges	Heraeus, Hanau Eppendorf, Wesseling-Berzdorf Hettich centrifuges, Adelsried
Cryostat	Leica, Wetzlar
Dissecting instruments	Fine Science Tools, Heidelberg
ELISA Reader	Multiskan EX Image Labsystems, Helsinki, Finland
Flow cytometer (FACSCalibur)	BD Biosciences, Heidelberg
Freezer	Liebherr, Biberach an der Riss
Heat block (Thermoblock TDB-120)	Hartenstein, Würzburg
Hemocytometer, Neubauer chamber	C. Roth, Karlsruhe
Incubator	Heraeus, Hanau
Laminar flow hood	Heraeus, Hanau
Light microscope	Zeiss, Jena
MACS separator	Miltenyi, Bergisch Gladbach
Magnetic stirrer	IKA Labortechnik, Staufen
PCR cycler (lab cycler)	Senso Quest, Göttingen
pH-meter	WTW, Weilheim
Photomicroscope	Axioplan 2 Zeiss, Jena
Pipettes	Abimed, Langenfeld Eppendorf, Wesseling-Berzdorf
Pipetting aid	Brand, Wertheim
Power supply (Power Pac 300 HC)	Biorad, München
Refrigerator	Liebherr, Biberach an der Riss
Shaker	E. Bühler, Hechingen
UV transilluminator	Intas Science Imaging Instruments GmbH, Göttingen
Vortex mixer	A. Hartenstein, Würzburg
Water bath	Köttermann laboratory technology, Uetze
X-Ray irradiation unit RT 200	C.H.F. Müller, Hamburg

If not indicated differently, all suppliers are located in Germany.

5.1.11 Software

Excel	Microsoft Corporation, Redmond, USA
FCAP Array™ software	Softflow Inc., Burnsville, USA
FlowJo 7.6.1	Treestar, Inc., Ashland, USA
Graph Pad Prism 5	Graph Pad Software, La Jolla, USA
Gel Capture Recording Software	Intas Science Imaging Instruments GmbH, Göttingen, Germany

5.2 Animals and Bioassays

5.2.1 Experimental Animals

Wild type C57BL/6 mice were purchased from Harlan Winkelmann Company (Borchen, Germany). RAG-1^{-/-} mice were purchased from Charles River Laboratories (Sulzfeld, Germany). B7-H1^{-/-} mice were generated by L. Chen (Baltimore, USA) and a breeding pair of these was provided by P. Knolle (Bonn) for the in-house breeding. TCR^{MOG}-transgenic (also referred to as 2D2) mice were generated and provided by V. Kuchroo (Boston, USA). IgH^{MOG}-transgenic (also referred to as Th) mice were generated and provided by T. Litzemberger (Martinsried, Germany).

Mice were kept under conventional animal housing conditions in the animal facility of the University Hospital of Würzburg, Department of Neurology, according to German guidelines for animal care. All experiments were conducted according to animal experimental ethics committee guidelines and were approved by the local authorities (Regierung von Unterfranken). Mice were euthanized for organ dissection by CO₂ gassing.

5.2.2 Genotyping of Mice

Transgenic animals were genotyped by conventional polymerase chain reaction (PCR) of genomic DNA extracted from a piece of tail. Mice tail tips were clipped at about 25 days of age and genomic DNA was extracted using the DNeasy Blood & Tissue kit according to the manufacturer's protocol. A small piece of tail was incubated in ATL tissue digestion buffer containing proteinase K at 55 °C overnight until completely lysed. Then, 400 µl of buffer AL-ethanol mixture were added and mixed well. After

transfer into a DNeasy Mini spin column, the mixture was centrifuged at $\geq 6000 \times g$ for 1 min. Next, 500 μl buffer AW1 were added on the spin column and centrifuged for 1 min at $\geq 6000 \times g$. Thereafter, 500 μl buffer AW2 were added on the spin column and centrifuged at RT at 20,000 $\times g$ for 3 min. After each centrifugation step, flow-through was discarded and the used collection tube replaced by a clean one. Finally, 200 μl buffer AE were pipetted on the DNeasy Mini spin column, incubated at RT for 1 min and then centrifuged for 1 min at $\geq 6000 \times g$ to elute the DNA into a clean microcentrifuge tube. Purified DNA samples were stored at $-20 \text{ }^\circ\text{C}$.

With standard PCR methods and the accordant PCR primers, transgenic DNA was amplified. The typical PCR mixture consists of:

- 1 μl genomic DNA
- 2.5 μl 10x buffer
- 0.5 μl 10 μM sense primer
- 0.5 μl 10 μM anti-sense primer
- 0.5 μl 10 mM dNTPs
- 0.3 μl Taq polymerase (5 units/ μl)
- fill up to 25 μl aqua ad iniectionabilia

The typical PCR program consists of 35 cycles:

- 3 min 94 $^\circ\text{C}$ Hot Start
- 40 s 94 $^\circ\text{C}$ denaturation
- 40 s ... $^\circ\text{C}$ annealing (see 5.1.6 *PCR Primers for Genotyping* for specific annealing temperature of the respective primers)
- 1 min 72 $^\circ\text{C}$ elongation
- Final elongation 10 min, 72 $^\circ\text{C}$
- Pause 10 $^\circ\text{C}$

Afterwards, PCR products were loaded on a 2 % agarose gel (in 1x TAE buffer) containing 0.5 $\mu\text{g/ml}$ ethidium bromide. The DNA samples were separated by electrophoresis and bands were detected by a UV transilluminator (Intas Science Imaging Instruments GmbH). Genotypes were determined according to presence or absence of distinct single or multiple bands (for PCR product size, see 5.1.6 *PCR Primers for Genotyping*).

5.2.3 Serum Collection

Blood samples were taken from mice which had been euthanized by CO₂ gassing. Samples were allowed to clot for 5-6 h at 4 °C. Serum was collected after centrifugation (400 x g, 4 °C, 10 min) and stored at -20 °C until further analysis.

5.2.4 Spontaneous EAE Model: Devic Mice

The spontaneous EAE model using double-transgenic TCR^{MOG} x IgH^{MOG} mice (also referred to as Th x 2D2/OSE/Devic mice) was extensively described previously by Bettelli et al (J Clin Invest, 2006) and Krishnamoorthy et al. (J Clin Invest, 2006). Due to the TCR^{MOG} transgene, these mice harbor CD4⁺ T cells with TCR specificity for the MOG₃₅₋₅₅ peptide. The IgH^{MOG} transgene leads to the presence of B cells which recognize a conformational epitope of the MOG protein and secrete high titers of MOG-specific serum antibodies. In the present study, double-transgenic F1 animals (Devic B7-H1^{+/+} mice) resulting from crossing transgenic IgH^{MOG} x B7-H1^{+/+} mice with transgenic TCR^{MOG} x B7-H1^{+/+} mice and double-transgenic Devic B7-H1^{-/-} mice resulting from crossing transgenic IgH^{MOG} x B7-H1^{-/-} with transgenic TCR^{MOG} x B7-H1^{-/-} were bred to investigate the role of B7-H1 on the spontaneous EAE-like disease. The mice were frequently weighed and examined for clinical signs.

Clinical scoring of animals was conducted according to the classical EAE disease determination:

- 0 healthy
- 1 flaccid tail
- 2 impaired righting reflex and/or gait
- 3 one paralyzed hind limb
- 4 hind limb paralysis (both) and limp torso
- 5 moribund or death after preceding clinical disease

5.2.5 Adoptive Transfer Experiments

For investigation of *in vivo* migration and homing of TCR^{MOG}-specific CD4⁺ T cells, lymph nodes (LN) and spleens of sick Devic B7-H1^{+/+} mice and Devic B7-H1^{-/-} mice were collected and single-cell suspensions prepared as described below. RAG-1^{-/-} mice were immobilized in a plexiglas restrainer and 10*10⁶ cells (suspension of LN cells and

splenocytes) were adoptively transferred by injection in the lateral tail vein. Recipient mice were observed for 15-20 days. Then, lymphoid organs and CNS of recipient mice were collected, single-cell suspensions were prepared and investigated with flow-cytometry and transferred into restimulation assays as described below.

5.3 Cell Biological Methods

5.3.1 Cell Culture

Murine organs were harvested as described below and primary cells were isolated under sterile conditions working at a laminar flow. Cells were incubated in sterile filtrated cell culture media in an incubator at 37 °C and 5 % CO₂. Centrifugation steps of cell suspensions were carried out at 300 x g, 6 min, 4 °C, unless otherwise stated.

5.3.2 Cell Counting

Cell numbers were determined by CASY® Cell Counter + Analyzer System Model according to the manufacturer's manual. Cell suspensions were diluted in CASY buffer (1:500). The amount of cells (cells/ml) was automatically calculated out of three cycles of measurement. Alternatively, cells were counted using a 0.4 % trypan blue solution and a Neubauer hemocytometer. Trypan blue enters dead cells through the porous membrane and intercalates with the DNA. Consequently, dead cells appear blue under the light microscope whereas vital cells are not dyed. Appropriately diluted cell suspensions were mixed with trypan blue solution (1:1), applied into the chamber of the hemocytometer and living cells were counted in all four large quadrants at 40x magnification. The calculation of cell number was obtained using the following formula: Number of cells counted/4 x dilution factor x 10⁴=cells/ml. The calculation of specific cell populations was based on the number achieved by CASY® Cell Counter and on the percentages of specific cells from the total cell population acquired by flow cytometry.

5.3.3 Preparation of Single-Cell Suspensions from Peripheral Organs

Primary cells were obtained from spleens, LN and thymi of mice which had been euthanized by CO₂ gassing. Cell isolation was performed under sterile conditions using a laminar flow hood. Organs were removed and transferred into cell culture dishes (35 mm diameter) filled with 2 ml 1x PBS. For each individual mouse, single-cell

suspensions were then generated by mashing the respective organ through a nylon cell strainer (40 μm pore size) using a 2 ml syringe plunger followed by adequate rinsing with 1x PBS. Cell suspensions were centrifuged (300 x g, 4 °C, 6 min), resuspended in 1x PBS and transferred on a cell strainer for a second time to clean the cell suspension of debris. As for splenocyte and LN cell suspensions, red blood cells were lysed by resuspending the respective cell pellet with 5 ml ACK buffer and incubating at RT for 3 min. The lysis process was stopped by adding 15 ml of culture media followed by a centrifugation step (300 x g, 4 °C, 6 min). The resulting cell pellet was resuspended in 1x PBS, the cell number was determined as described above and the cells were transferred into further assays.

5.3.4 Isolation of Mononuclear Leukocytes from the CNS

Brains and spinal cords were collected from transcardially perfused mice. Therefore, the chest of euthanized mice was cut open, the right atrium was punctured and about 10 ml of cold 1x PBS containing 125 I.E. heparin-sodium solution was injected into the left ventricle to flush the whole blood circuit. CNS tissue of each single mouse was dissected, transferred into a cell culture dish filled with 2 ml of 1x PBS and cut into smaller pieces using surgical scissors. The tissue was further homogenized by aspirating the suspension for at least 10 times using a 2 ml syringe. The resulting homogenate was transferred into a 15 ml tube which was then filled up with 1x PBS and centrifuged (300 x g, 4 °C, 6 min). The pellet was resuspended with 3 ml of 50 % Percoll solution (in 1x PBS) and overlaid by 3 ml of 30 % Percoll solution (in 1x PBS). The Percoll density gradient was centrifuged (500 x g, RT, 30 min) without brake. Then, the interface of the density gradient where mononuclear leukocytes accumulated was transferred into a new 15 ml tube, washed in 1x PBS, centrifuged (300 x g, 4 °C, 6 min) and resuspended in 1x PBS for further analysis.

5.4 In vitro Assays

5.4.1 Proliferation Assay

To address antigen-dependent proliferation of TCR^{MOG}-specific CD4⁺ T lymphocytes *in vitro*, splenocytes were isolated as described above and labeled with Cell Proliferation Dye eFluor® 670. This dye binds to any cellular proteins containing primary amines. As lymphocytes divide, the dye is distributed equally among daughter cells so that cell

divisions can be followed by successive halving of the fluorescence intensity of the dye. For labeling, cells were diluted to 10×10^6 cells/ml in sterile 1x PBS and mixed while vortexing in a 1:1 ratio with a 10 μ M solution of eFluor® 670. After incubation at 37 °C in the dark for 10 min, the labeling process was stopped by adding 5x the volume of cold cell culture media and incubating on ice for 5 min. After 2-3 washing steps with cell culture media, cells were seeded in a 96 well plate with 2.5×10^5 cells/well in 200 μ l culture media. MOG₃₅₋₅₅ peptide was added as antigen-specific stimulus in the following concentrations: 0, 0.1, 1, 10, and 50 μ g/ml. After 60 h, cells were harvested and cell surface molecules were co-stained using appropriate fluorescence-labeled monoclonal antibodies. The cell division rates were detected by flow cytometry.

Alternatively, antigen-dependent cell proliferation was detected by incorporation of radioactively labeled [³H] thymidine. The principle of this assay is that during cell proliferation, newly synthesized DNA incorporates supplied [³H] thymidine. The amount of radioactivity in a sample is directly proportional to the cell proliferation rate. To measure cell proliferation, splenocytes were isolated, seeded and cultivated in presence of MOG₃₅₋₅₅ peptide in a 96 well plate as described above. The cells were cultivated for 60 h, the last 6-12 h in presence of [³H] thymidine (1.25 μ Ci/well). Using a Cell Harvester, cells were gathered onto a filter plate (ScintiPlate-96 Tissue Culture) by rinsing the wells with water. Thereby, radioactively labeled DNA bound to the filter membrane whereas not-incorporated [³H] thymidine was flushed out. After 30 min of drying, 20 μ l of scintillation liquid (MicroScint™-20) were added to each cavity and radioactivity was measured by a β -scintillation counter (TopCount NXT). The results were given as counts per minute (cpm). To assess CD4⁺ T-cell proliferation exclusively induced by B cells, CD4⁺ T cells and irradiated B220⁺ B cells were cultured (in a 10:1 ratio) in presence of different MOG₃₅₋₅₅ peptide concentrations for 60 h. T-cell proliferation was evaluated by [³H] thymidine uptake as described above. CD4⁺ T cells were isolated from splenocytes and LN cells using CD4⁺ T cell Isolation Kit II according to the manufacturer's manual. Single-cell suspensions were incubated with a biotinylated antibody cocktail against cell surface antigens CD8a, CD11b, CD11c, CD19, CD45R (B220), CD49b (DX5), CD105, MHC-class II and Ter-119. After washing, anti-biotin MicroBeads were added and incubated at 4°C for 30 min. After washing, the cell suspension was transferred onto MACS columns placed in a magnetic MACS separator and untouched CD4⁺ T cells were eluted. B cells were isolated

accordingly using anti-B220⁺ (CD45R) MicroBeads. The viability and purity of the cells were evaluated by flow cytometric analysis.

5.4.2 Restimulation Assay: Antigen-dependent Cytokine Production

To investigate antigen-dependent *in vitro* cytokine production by distinct cells, flow cytometric analysis of cell surface molecules such as V α 3.2 and V β 11 and intracellular cytokines such as IFN- γ and IL-17 was combined. Splenocytes or leukocytes isolated from the murine CNS were isolated as described above and seeded in a 96 well plate with $2,5 \cdot 10^5$ cells/well in 200 μ l culture media (CNS: $1 \cdot 10^4$ cells/well), followed by 20 h incubation time in presence of MOG₃₅₋₅₅ peptide (final concentration: 10 μ g/ml). Brefeldin A was added 6 h before harvest (final dilution of 1:500). Brefeldin A is a fungal metabolite that interferes with the anterograde protein transport from the endoplasmic reticulum to the Golgi apparatus leading to a rapid accumulation of proteins such as cytokines within the cell. After staining of cell surface molecules by fluorescence-labeled monoclonal antibodies (see 5.6.1 *Staining of Cell Surface Molecules*), intracellular cytokine staining was performed as described below (see 5.6.2 *Staining of Intracellular Components*).

Alternatively, ELISA (Enzyme Linked Immunosorbent Assay) was used to investigate antigen-dependent cytokine production. To do so, splenocytes were isolated as described above and seeded at $1 \cdot 10^6$ cells/well in a 48 well plate in 500 μ l cell culture media. MOG₃₅₋₅₅ peptide was added at in a final concentration of 10 μ g/ml. The cell culture supernatant was collected after 60 h incubation time and stored at -20 °C until analysis by ELISA (as described in 5.6 *ELISA*).

5.4.3 In vitro Survival Assay

In apoptotic cells, the membrane phospholipid phosphatidylserine (PS) is characteristically translocated from the inner to the outer leaflet of the plasma membrane. Annexin V, a phospholipid-binding protein with strong and specific affinity to PS, detects apoptotic cells with externalized PS (Vermes et al., 1995). Flow cytometric analysis using FITC-conjugated Annexin V, anti-V β 11-PE and anti-CD4-APC was performed on day 0 and day 4 of *in vitro* cultivation of LN cells to determine the apoptosis rates of TCR^{MOG}-transgenic CD4⁺ T cells over time. To do so, single-cell suspensions of LN of Devic B7-H1^{+/+} and Devic B7-H1^{-/-} mice at disease maximum

were prepared and 3×10^6 cells per well/sample were cultured in a 48 well plate in culture media for four days. FACS analysis was performed as described below (5.5.1 *Staining of Cell Surface Molecules*) using Annexin V buffer (for details see 5.1.5 *Buffers and Solutions*). The relative induction rate of apoptosis in between day 0 and day 4 was calculated for each sample. The mean apoptosis induction rate of TCR^{MOG}-transgenic CD4⁺ T cells of each mice group was calculated out of 2 independent assays. Afterwards, the mean induction rate obtained for the Devic B7-H1^{+/+} mice group was set as 1 and the fold rate for each Devic B7-H1^{-/-} sample was calculated accordingly.

5.4.4 In vitro Migration Assay

To assess the migratory capacity of TCR^{MOG}-specific CD4⁺ T cells of sick Devic B7-H1^{+/+} and Devic B7-H1^{-/-}, LN cells were freshly isolated as described above and resuspended in FCS-free culture media. The upper chamber of a polyester membrane transwell insert (3.0 μ m membrane pore size) was loaded with 100 μ l cell suspension (5×10^5 cells/insert). The lower chamber of the transwell was filled with 500 μ l cell culture media containing 10 % FCS which could be regarded as an unspecific chemoattractant stimulus. After an incubation period of 6-8 h (“short-run migration”) or 18-20 h (“long-run migration”), the transwell inserts were removed and cells that had migrated via the membrane into the lower chamber were collected. The wells were subsequently rinsed twice with 1x PBS to ensure gain of all cells. Afterwards, flow cytometric analysis was performed as described below. For quantification, Calibrite beads were added to each sample prior to measuring by FACS Calibur flow cytometer and cell per bead ratios were determined afterwards for every well. Each sample was run in triplicates.

5.5 Flow Cytometry

5.5.1 Staining of Cell Surface Molecules

In this study, flow cytometry/FACS (Fluorescence Activated Cell Sorting) was used to detect the expression of cell surface molecules, intracellular cytokines and the proliferation and apoptosis rates of cell populations. The principle of operation of flow cytometry is based on the natural scattering of laser light by cellular structures. FSC (forward scatter) correlates with the cell volume and SSC (side scatter) correlates with the morphological complexity such as cytoplasmic granules and membrane roughness.

On the other hand, flow cytometric analysis is based on the fluorescence of dyes that are directly bound to intracellular components or attached to specific antibodies recognizing cell-surface or intracellular molecules. When these dyes are excited at a distinct wavelength they emit light of longer wavelength which is received by detectors. The intensity of emitted light is proportional to the concentration of dye and thus proportional to the amount of molecules detected by the accordant specific monoclonal antibodies. To perform flow cytometric analysis, single-cell suspensions of spleens, LN, thymi and CNS were prepared as described above. About $5 \cdot 10^5$ cells were transferred into a round-bottom FACS tube, resuspended in FACS buffer, washed once with FACS buffer and centrifuged ($300 \times g$, 4°C , 6 min). Hereafter, the cell pellet was resuspended in a volume of $50 \mu\text{l}$ FACS staining buffer containing the appropriate amounts of monoclonal fluorescence-conjugated detection antibodies and incubated with for 30 min at 4°C in the dark. Afterwards, the samples were washed once, centrifuged and resuspended in about $200 \mu\text{l}$ FACS buffer and stored on ice until measurement. In this study, the flow cytometer FACSCalibur was used and data were analyzed with FlowJo Software.

5.5.2 Staining of Intracellular Components

For intracellular staining of the Cell Proliferation Dye eFluor® 670 or the cytokines IFN- γ and IL-17, leucocytes isolated from spleens, LN or CNS were restimulated and treated as described above (see 5.4.1 *Proliferation Assay* and 5.4.2 *Restimulation Assay*). After staining of cell-surface molecules, cells were fixed and permeabilized with the BD Cytofix/Cytoperm Plus Fixation/Permeabilization Kit according to the manufacturer's manual at 4°C for 30 min. After washing in permeabilization buffer, the samples were incubated with the appropriate amount of monoclonal antibodies in $50 \mu\text{l}$ of permeabilization buffer at 4°C in the dark for 30 min. Afterwards, the samples were washed once again in permeabilization buffer, centrifuged and resuspended in about $200 \mu\text{l}$ FACS buffer and stored on ice until measurement.

For the intracellular staining of the transcription factor FoxP3, the „Mouse Regulatory T cell Staining Kit” was used according to the manual. After staining of cell surface molecules, cells were fixed and permeabilized at 4°C for 30 min. The washing step was followed by the incubation with anti-mouse/rat FoxP3 antibody in permeabilization buffer at 4°C for 30 min. After washing in permeabilization buffer, the cells were

resuspended in FACS buffer and stored on ice until measurement.

5.5.3 Cytometric Bead Array

Using the BD Cytometric Bead Array (CBA) Mouse Th1/Th2/Th17 Cytokine Kit the simultaneous quantification (in pg/ml) of seven different cytokines (IL-2, IL-4, IL-6, IFN- γ , TNF, IL-17A and IL-10) in cell culture supernatants was performed. Each bead population is coated with capture antibodies specific for one distinct cytokine and with distinct fluorescence intensities to form the bead array which is resolved in a red channel (ie, FL3 or FL4) of a flow cytometer. During the assay procedure, the cytokine capture beads were mixed with recombinant standards and samples and incubated with the PE-conjugated detection antibodies to form sandwich complexes. The intensity of PE fluorescence of each sandwich complex is in proportion to the amount of bound analyte and thus revealed the concentration of that cytokine. After the acquisition on FACSCalibur, FCAP Array™ software was used to analyze the results.

5.6 ELISA (Enzyme-Linked Immunosorbent Assay)

For detection and quantification of cytokines which had been antigen-dependently produced by splenocytes, cell culture supernatants of restimulation assays were investigated by ELISA. ELISA plates were coated with IL-17- or IFN- γ -specific capture antibodies diluted in 1x PBS according to the manufacturer's manual (R&D Systems, Wiesbaden-Nordenstadt) at RT overnight. Plates were washed, blocked with reagent diluent (as for IL-17 ELISA) or blocking buffer (as for IFN- γ ELISA) at RT for 1 h and washed again. Cell culture supernatants were either left undiluted (IL-17 ELISA) or diluted in reagent diluent (1:10 for IFN- γ ELISA) and incubated in the coated plates at RT for 2 h (100 μ l of sample/well). After thorough washing, 100 μ l of the respective biotinylated detection antibodies diluted in reagent diluent was added and incubated at RT for another 2 h. After extensive washing, streptavidin-HRP (horseradish peroxidase; 1:2000 in reagent diluent) was added and incubated at RT for 20 min. All incubation steps were stopped with 3x washing with ELISA wash buffer. The chromogenic substrate solution (1:1 mixture of Color Reagent A and Color Reagent B) was incubated at RT for 20 min. The reaction was stopped by adding stop solution (2 N H₂SO₄). Hereafter, the color intensity was detected photometrically by a microplate reader at 450 nm wavelength with wavelength correction set to 540 nm (Multiskan EX Image

Labsystems). Running a row of recombinant standards allowed the quantification of cytokines contained in the samples. Each sample was run in duplicates.

For the determination of MOG-specific IgM and IgG1 levels in serum, ELISA plates were coated with MOG₁₋₁₂₅ peptide (10 µg/ml in 1x PBS) at 4 °C overnight. Non-specific binding was assessed using 1x PBS-coated plates. Afterwards, the assay was performed as mentioned above. Serum samples were diluted in reagent diluent (1:500 dilutions for detection of IgM and 1:1000 dilutions for detection of IgG1 isotypes) and incubated at RT for 1 h. After thorough washing, bound Ig was detected by a biotinylated allotype- and isotype-specific anti-mouse Ig and a streptavidin-HRP complex. TMB (tetramethylbenzidine) was used as a color substrate that was measured at 405 nm. Results were reported as OD (optical density).

5.7 Immunohistochemistry

For immunohistochemical assessment of murine tissue, spinal cords were harvested from mice transcardially perfused with 1x PBS as described above (see 5.3.4 *Isolation of Mononuclear Cells from the CNS*). After embedding the material in Tissue-Tek OCT compound, the samples were frozen in liquid nitrogen-cooled isopentane and stored at -20 °C until further analysis. Transverse sections of the spinal cord were cut with a Leica cryostat at -20 °C and the 10 µm thick sections were transferred on glass slides. Before staining, sections were pre-incubated for 30 min in 5 % BSA in 1x PBS to block unspecific binding sites and then incubated with primary antibodies diluted in 1 % normal bovine serum (at 4 °C overnight). Rat anti-mouse CD11b antibodies were used for detection of macrophages/microglia; rat anti-mouse CD4 antibodies were used for the identification of CD4⁺ T lymphocytes. To optimize immunolabeling for CD11b, sections were permeabilized with 0.3 % Triton X-100 after post-fixation with 4 % paraformaldehyd in 1x PBS. To visualize primary antibodies, a biotinylated secondary goat anti-rat antibody was applied for 1 h, followed by a streptavidin-HRP complex. Chromogenic peroxidase substrate solution consisting of diaminobenzidine-HCl (DAB) and 0.2 % hydrogen peroxide was incubated on the sections for about 10 min to visualize the antigen-antibody-complex. The reaction was stopped by rinsing the slides with distilled water. All incubation steps were followed by 3 washing steps in 1x PBS. The tissue sections were finally covered with glass coverslips using mounting media Aquatex®. Microscopic analysis of the immunohistochemical stainings were done with

a Zeiss Axiophot 2 microscope. The immunohistochemical analysis was performed in close cooperation with Dr. Chi Wang Ip.

5.8 Statistical Analysis

The statistical analysis within this study was performed with the statistics tools of the programs GraphPad Prism 5 or Microsoft Excel. To determine the significant difference of two independent groups in one experiment the two-sided Student's t-test was used. The probabilities * $p < 0.05$, ** $p < 0.01$ and *** $p < 0.001$ were regarded as statistically significant.

6 Results

6.1 Clinical Features of Devic B7-H1^{+/+} and Devic B7-H1^{-/-} Mice

6.1.1 Accelerated and Aggravated Course of Spontaneous EAE-like Disease in Devic B7-H1^{-/-} Mice

In the present study, TCR^{MOG}-transgenic mice (also referred to as 2D2) expressing MOG₃₅₋₅₅-specific CD4⁺ T cells and IgH^{MOG}-transgenic mice (also referred to as Th) expressing MOG-specific B cells were crossed with B7-H1^{+/+} mice (all on C57BL/6 background) to generate single-transgenic strains exhibiting a wild type (wt) expression pattern of the cell-surface molecule B7-H1. Subsequently, TCR^{MOG} x B7-H1^{+/+} mice were interbred with IgH^{MOG} x B7-H1^{+/+} mice to obtain double-transgenic Devic B7-H1^{+/+} mice characterized by the simultaneous expression of MOG-specific T and B cells and a wt expression pattern of B7-H1 throughout all tissue. Under conventional animal housing conditions, 71.4 % of Devic B7-H1^{+/+} mice developed EAE-like symptoms which were scored according to the classical EAE determination. First symptoms were loss of tail tonus occurring at the age of about 36 days followed by ascending paralysis from hind to front legs (Fig. 4 A, Tab. 1).

In order to elucidate the role of B7-H1 in this mouse model for spontaneous autoimmune inflammation of the CNS, the clinical course of the disease was monitored in Devic B7-H1^{+/+} and Devic B7-H1^{-/-} mice. The strains TCR^{MOG} x B7-H1^{-/-} and IgH^{MOG} x B7-H1^{-/-} were obtained by crossing each transgenic strain onto B7-H1^{-/-} background (all on C57BL/6 background). Finally, by crossing TCR^{MOG} x B7-H1^{-/-} mice with IgH^{MOG} x B7-H1^{-/-} mice, double-transgenic Devic B7-H1^{-/-} mice were obtained featuring a disrupted PD-1/B7-H1 co-inhibitory pathway. Strikingly, the knock-out (ko) of the B7-H1 gene led to an elevated induction of spontaneous EAE-like disease in almost all Devic B7-H1^{-/-} mice (98 % incidence rate) during the 12 weeks observation time. Clinical symptoms evolved with an abrupt onset and a rapid progression at a significantly younger age (at day 31 on average) compared to Devic B7-H1^{+/+} mice. Moreover, Devic B7-H1^{-/-} mice exhibited a significantly exacerbated disease course with higher clinical scores (3.7±1.0 vs. 2.4±1.7) and higher rates of disease-dependent deaths than the Devic B7-H1^{+/+} control group (22.0 % vs. 5.7 %

mortality) (Fig. 4 B, Tab. 1).

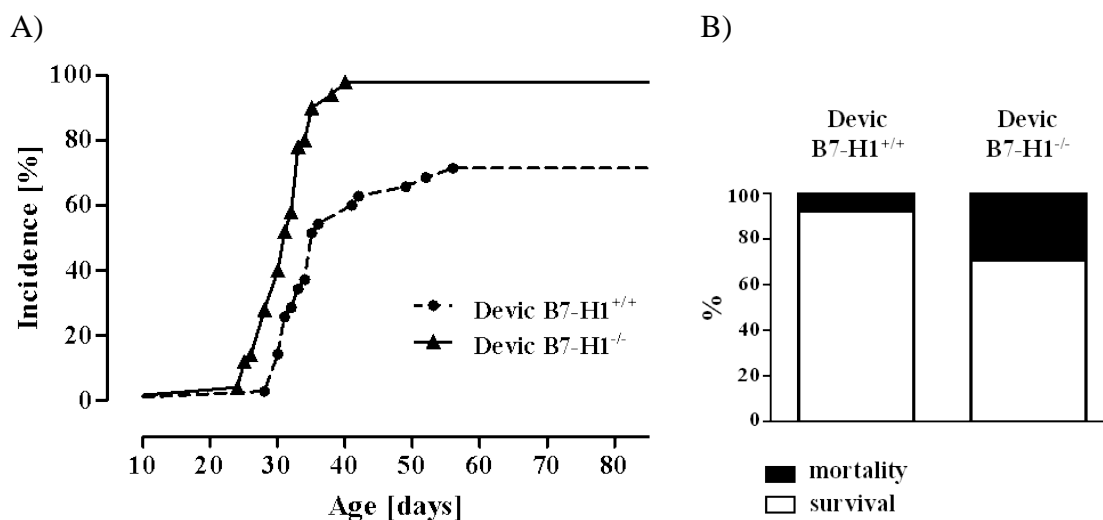


Fig. 4. Incidence of spontaneous EAE-like disease and mortality in Devic B7-H1^{+/+} and Devic B7-H1^{-/-} mice. Devic B7-H1^{+/+} and Devic B7-H1^{-/-} mice bred under conventional animal housing conditions were observed for a period of 12 weeks after birth and regularly scored for A) the incidence of EAE-like disease and B) disease-dependent deaths (mortality).

Group		Devic B7-H1 ^{+/+}	Devic B7-H1 ^{-/-}
Specificity	T cells	MOG	MOG
	B cells	MOG	MOG
B7-H1		wild type	knock-out
Incidence		25/35 (71.4%)	49/50 (98.0%)
Mortality		2/35 (5.7%)	11/50 (22.0%)
Age of onset (days)		35.8 ± 7.1 days	31.2 ± 3.9 days p=0.005
Mean clinical score		2.4±1.7	3.7±1.0 p=0.001

Tab. 1. Summary of clinical features of spontaneous EAE-like disease in double-transgenic Devic B7-H1^{+/+} and Devic B7-H1^{-/-} mice.

6.1.2 Enhanced Accumulation of CD4⁺ T cells and Macrophages in Spinal Cord Lesions of sick Devic B7-H1^{-/-} Mice

In order to investigate the influence of B7-H1 deficiency on immune-cell infiltration into the CNS, immunohistochemical staining was performed on transversal cryosections of spinal cords collected from Devic B7-H1^{+/+} and Devic B7-H1^{-/-} mice at disease maximum. CD4⁺ T cells strongly accumulated in the spinal cord meninges and

parenchyma of sick Devic B7-H1^{+/+} mice. Strikingly, the spinal cord lesions of Devic B7-H1^{-/-} mice exhibited exceedingly vast infiltration of encephalitogenic CD4⁺ T cells compared to those of score-matched Devic B7-H1^{+/+} mice (Fig. 5 A). Likewise, accumulation of CD11b⁺ macrophages was remarkably increased within spinal cord lesions of Devic B7-H1^{-/-} mice compared to Devic B7-H1^{+/+} mice at disease maximum (Fig. 5 B).

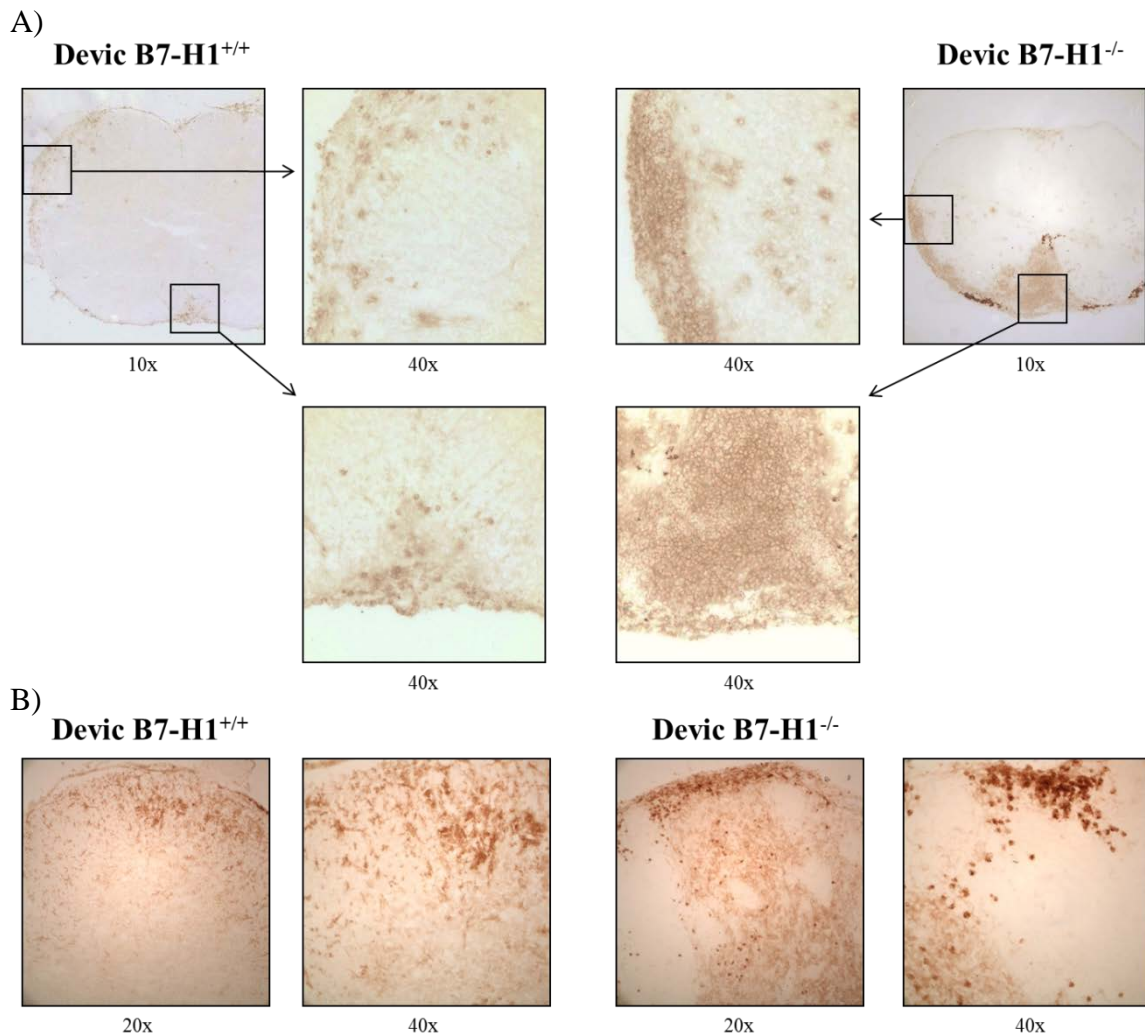


Fig. 5. Infiltration of CD4⁺ T cells and CD11b⁺ macrophages/microglia in spinal cord lesions of sick Devic mice. Transversal cryosections of spinal cords of Devic B7-H1^{+/+} and Devic B7-H1^{-/-} mice at disease maximum were investigated for CD4⁺ T-cell and CD11b⁺ macrophage infiltration using respective primary monoclonal antibodies (detection: DAB staining). A) 10x magnification allows an overview of CD4⁺ T-cell accumulation within the spinal cord meninges and parenchyma. Areas of dense CD4⁺ T-cell accumulation are selected (rectangular gates) and 40x magnified. B) Macrophages/microglia in spinal cord lesions were identified by staining of cell surface CD11b. Representative pictures of multiple experiments are shown (n=4 mice/group). (The immunohistochemical analysis was performed in close cooperation with Dr. Chi Wang Ip)

6.2 Immune Responses in Devic B7-H1^{+/+} and Devic B7-H1^{-/-} Mice

6.2.1 Enhanced Accumulation and Activation of V α 3.2⁺ V β 11⁺ CD4⁺ T cells in the CNS of sick Devic B7-H1^{-/-} mice

The phenotypes of immune cells infiltrating the CNS of sick Devic mice at disease maximum were investigated more closely by flow cytometry. Isolated by a Percoll density gradient, substantial numbers of CNS-infiltrating leukocytes were detected in the CNS of both groups of sick mice. TCR^{MOG}-transgenic CD4⁺ T cells were identified by the expression of the transgenic V α 3.2⁺ and V β 11⁺ TCR chains. The ratio of V α 3.2⁺ V β 11⁺ CD4⁺ T cells within CNS-infiltrating lymphocytes was significantly increased in Devic B7-H1^{-/-} compared to Devic B7-H1^{+/+} mice in the clinical phase of the disease (Fig. 6 A and B). Within gated lymphocytes, B220⁺ B cells and CD8⁺ T cells represented only minor proportions which did not differ notably in between the two groups (Fig. 6 C). It is noteworthy to mention that, generally, the ratio between CD4⁺ and CD8⁺ T cells in TCR^{MOG}-transgenic mice on RAG-1^{+/+} and RAG-2^{+/+} background is clearly biased toward the CD4 compartment compared to non-transgenic littermates (Bettelli et al., 2003). Likewise in TCR^{MOG} x IgH^{MOG} double-transgenic Devic mice, the CD4⁺ T-cell compartment is overrepresented as a result of the TCR^{MOG} transgene. Nevertheless, CD8⁺ T cells develop to a certain amount due to the normal expression of RAG-1 and RAG-2 enzymes that essentially control the rearrangement and recombination of the genes of immunoglobulin and T-cell receptor molecules during the process of VDJ recombination.

As CD4⁺ FoxP3⁺ Treg cells may be able to dampen autoreactive cells and hence confine autoimmunity, we sought to elucidate whether Treg-cell infiltration into the CNS is affected in Devic B7-H1^{-/-} mice potentially contributing to the more severe disease course. However, no major differences in the proportions of Treg cells within gated CNS-infiltrating lymphocytes were detected in between Devic B7-H1^{+/+} and Devic B7-H1^{-/-} mice at maximum phase of disease (Fig. 6 D).

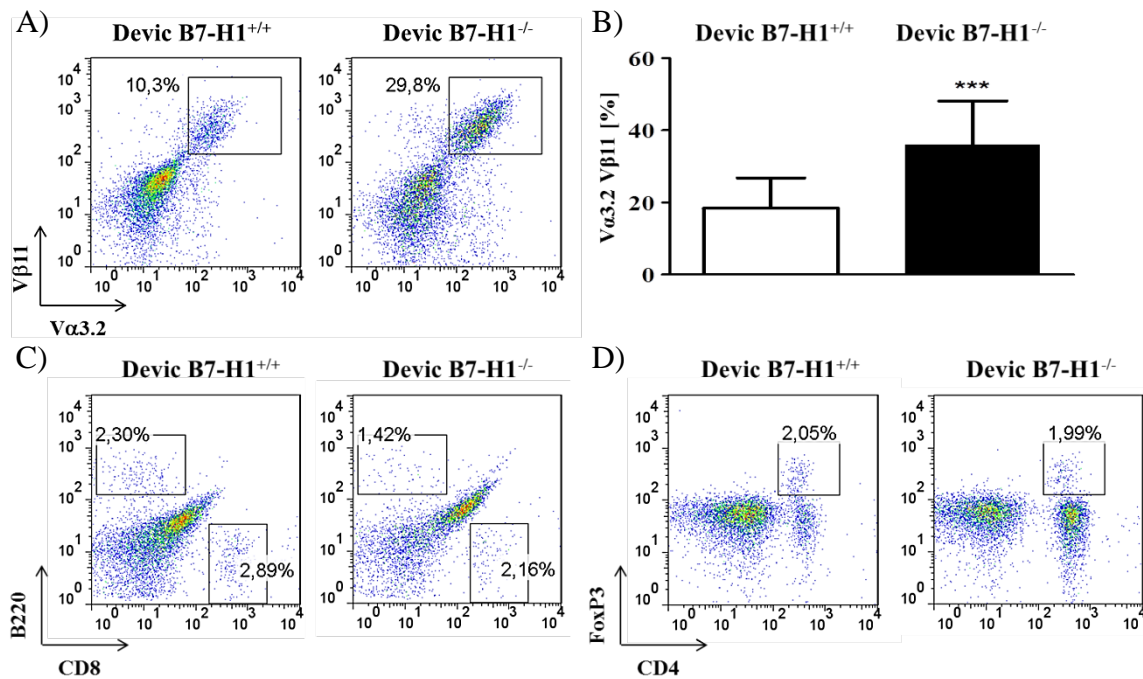


Fig. 6. CNS-infiltrating immune cells. Leukocytes isolated via density gradient from CNS tissue of sick Devic mice were analyzed by flow cytometry. A) CNS-infiltrating TCR^{MOG}-transgenic CD4⁺ T cells are identified by the transgenic V α 3.2⁺ and V β 11⁺ TCR chains. Numbers in rectangular gates indicate the corresponding percentages. B) Mean values of percentages of CNS-infiltrating V α 3.2⁺ V β 11⁺ CD4⁺ T cells of multiple experiments are shown (wt=16, ko=19 mice). Error bars represent SD values (***) p<0.001). C) Percentages of B220⁺ B cells vs. CD8⁺ T cells are indicated in the corresponding rectangular gates (n=5 mice/group). D) The percentages of FoxP3⁺ CD4⁺ Treg cells within CNS-infiltrating lymphocytes are given in the rectangular gates (wt=5, ko=6 mice). Representative FACS profiles are depicted.

The activation levels of CNS-infiltrating V α 3.2⁺ V β 11⁺ CD4⁺ T cells were evaluated by the expression of the T-cell activation markers CD25 and CD69. Higher proportions of CNS-infiltrating V α 3.2⁺ V β 11⁺ T cells isolated from Devic B7-H1^{-/-} mice co-expressed CD25 and CD69 compared to those isolated from Devic B7-H1^{+/+} mice. Even though the fractions of V α 3.2⁺ V β 11⁺ CD4⁺ T cells expressing solely one activation marker were comparable in both groups, the MFIs of CD69 and CD25 were consistently higher in the Devic B7-H1^{-/-} mice group (Fig. 7 A and B). The differential expression of the lymphoid tissue-homing molecules CD44 and CD62L allows evaluating the ratios of naïve, memory and effector T cells. The majority of CNS-derived V α 3.2⁺ V β 11⁺ CD4⁺ B7-H1^{-/-} T cells displayed a CD62L⁻ CD44⁺ effector phenotype. In comparison, a considerably smaller fraction of V α 3.2⁺ V β 11⁺ CD4⁺ B7-H1^{+/+} T cells were effector T cells while a substantial fraction exhibited a CD62L⁺ CD44⁻ naïve phenotype (Fig. 7 C).

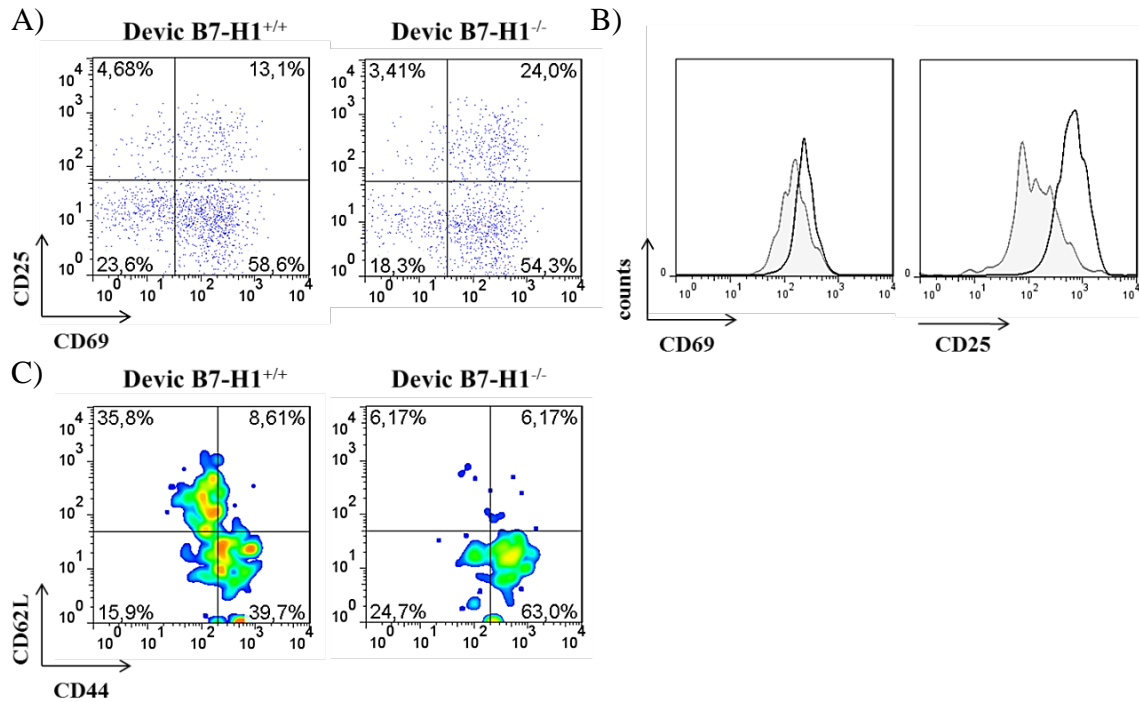


Fig. 7. Activation status of CNS-infiltrating $V\alpha 3.2^+ V\beta 11^+ CD4^+$ T cells. Leukocytes were isolated via density gradient from CNS tissue of sick Devic mice and subsequently stained with fluorescence-labeled monoclonal antibodies against the TCR $V\alpha 3.2$ and $V\beta 11$ chains to identify TCR^{MOG}-transgenic $CD4^+$ T cells. A) $V\alpha 3.2^+ V\beta 11^+ CD4^+$ T cells were gated and analyzed for their expression of CD69 and CD25. Representative FACS profiles show the percentages of $V\alpha 3.2^+ V\beta 11^+ CD4^+$ T cells expressing the cell surface molecules given within the quadrants (n=9 mice/group). B) An exemplary histogram overlay illustrates the MFIs of CD69 and CD25 on CNS-infiltrating $V\alpha 3.2^+ V\beta 11^+ CD4^+$ T cells in Devic B7-H1^{+/+} (grey tinted) vs. Devic B7-H1^{-/-} mice (black line). C) Representative FACS profiles reveal the proportions of CD44⁻ and CD62L-expressing cells within gated $V\alpha 3.2^+ V\beta 11^+ CD4^+$ T cells (n=4 mice/group).

6.2.2 Enhanced Antigen-specific Th1 and Th17 Responses of CNS-infiltrating $CD4^+$ T cells in Devic B7-H1^{-/-} mice

In order to detect a potential impact of B7-H1 deficiency on effector functions within the target tissue, CNS-infiltrating mononuclear cells of sick Devic B7-H1^{+/+} and Devic B7-H1^{-/-} were isolated and investigated for antigen-specific Th1 and Th17 cytokine production *in vitro*. To do so, CNS-derived leukocytes were stimulated with MOG₃₅₋₅₅ peptide, treated with Brefeldin A to suppress cytokine export and subsequently stained for the cell surface molecule CD4 and the intracellular cytokines IL17 and IFN- γ . $CD4^+$ T cells derived from CNS of both sick Devic B7-H1^{+/+} and Devic B7-H1^{-/-} mice secreted IL17 and IFN- γ . Consistently more CNS-infiltrating $CD4^+$ T cells obtained

from Devic B7-H1^{-/-} mice secreted IFN- γ when challenged by MOG₃₅₋₅₅ peptide than those obtained from Devic B7-H1^{+/+} mice (9 % vs. 4-5 %) (Fig. 8). Only slightly more encephalitogenic CD4⁺ T cells obtained from Devic B7-H1^{-/-} mice produced IL17 (10 % vs. 8 %) (Fig. 8).

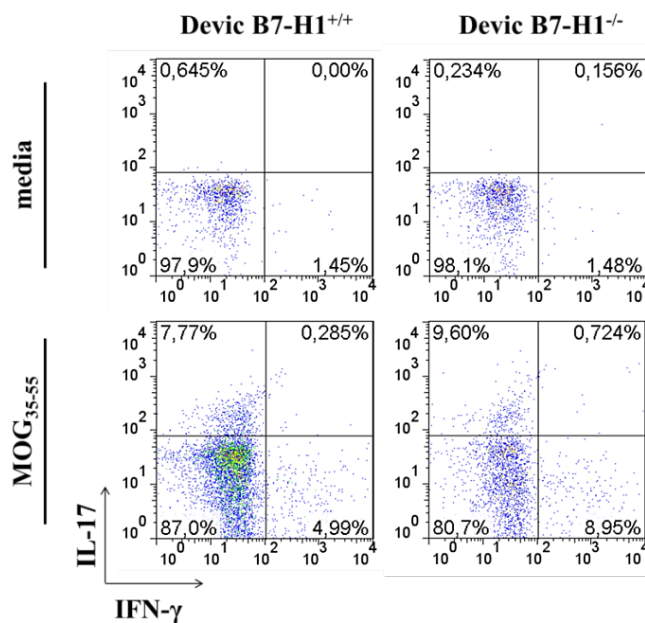


Fig. 8. Th1 and Th17 responses of CNS-infiltrating CD4⁺ T cells.

Leukocytes were isolated by a density gradient from homogenized CNS tissue of sick Devic mice and stimulated with MOG₃₅₋₅₅ peptide (10 μ g/ml) or left untreated overnight, followed by 6 h Brefeldin A treatment. To assess IFN- γ and IL-17 production, cells were stained with fluorescence-labeled anti-CD4 monoclonal antibodies and subsequently permeabilized, fixed and stained for the intracellular cytokines. Representative FACS profiles of CNS-infiltrating CD4⁺ T cells show the percentages of IFN- γ - or IL-17-producing CD4⁺ T cells within the respective quadrants (n=6 mice/group).

6.2.3 Unaffected Phenotypes of Peripheral Lymphocytes in Devic B7-H1^{-/-} Mice at Disease Maximum

Naïve T cells can generally not cross the BBB to infiltrate the CNS unless they get activated before and express several distinct surface molecules. To elucidate whether the absence of B7-H1 influences the activation status of peripheral V α 3.2⁺ V β 11⁺ CD4⁺ T cells in sick Devic mice, the expression of the surface activation markers CD25, CD69, CD44 and CD62L and the chemokine receptors CCR5 and CXCR4 was analyzed. Peripheral V α 3.2⁺ V β 11⁺ CD4⁺ T cells from both sick Devic B7-H1^{+/+} and Devic B7-H1^{-/-} mice exhibited comparably low expression levels of the investigated cell surface molecules (Fig. 9 A, C). In both mice groups, the majority of peripheral V α 3.2⁺ V β 11⁺ CD4⁺ T cells (80-90 %) displayed CD44⁻ CD62L⁺ naïve phenotypes. The frequencies of CD44⁺ CD62L⁻ effector and CD44⁺ CD62L⁺ memory cells were also comparable (Fig. 9 B).

Due to the BCR “knock-in”, IgH^{MOG} x TCR^{MOG}/Devic mice express about 30 % MOG-

specific B cells which contribute to the pathogenesis of the EAE-like disease by acting as APCs and as plasma cells secreting MOG-specific autoantibodies (Bettelli et al., 2006; Krishnamoorthy et al., 2006). Expression of MHC II and CD80 could indicate differences in the antigen-presenting and T-cell activating capacities of peripheral B220⁺ B cells. Analysis of B cells obtained from sick Devic B7-H1^{+/+} and Devic B7-H1^{-/-} mice revealed no difference in the expression of both molecules (Fig. 9 D and E).

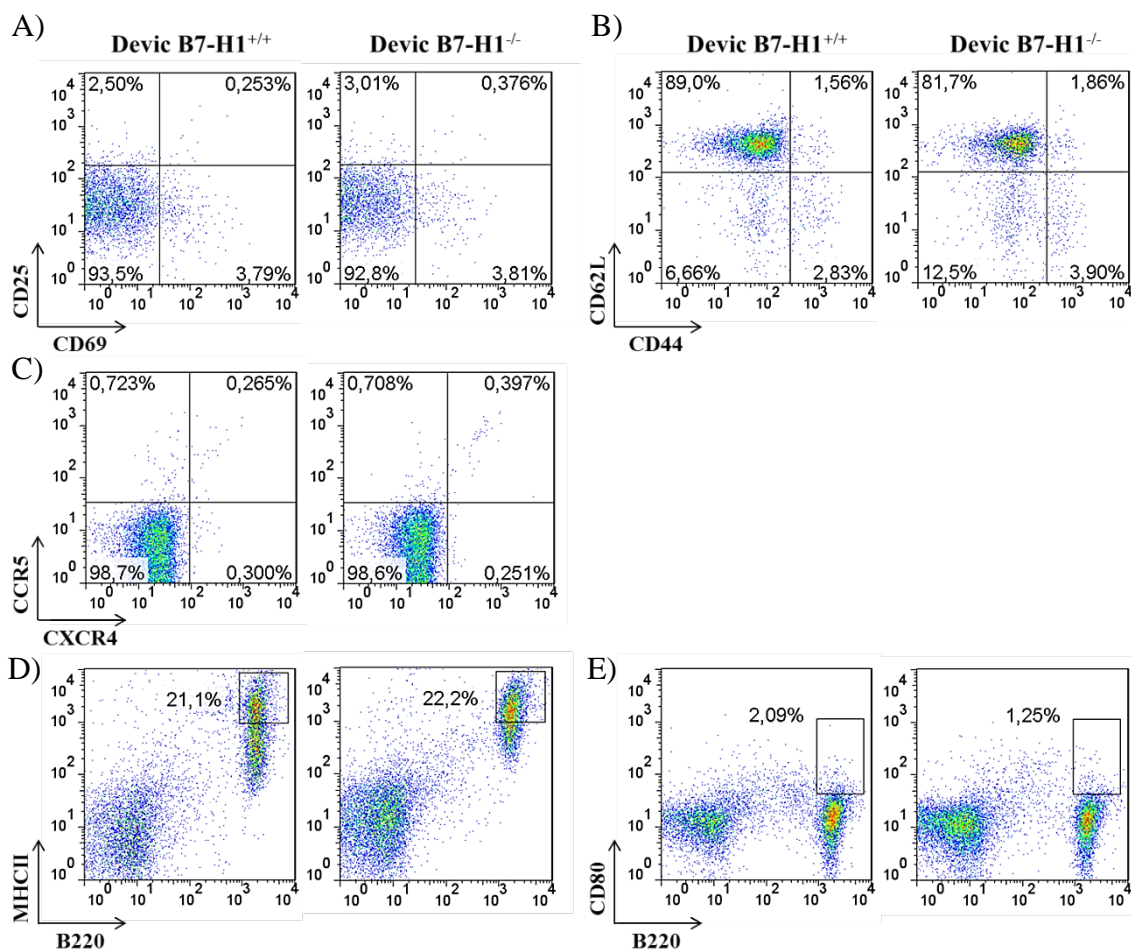


Fig. 9. Activation status of peripheral lymphocytes in Devic mice at disease maximum. Splenocytes obtained from sick Devic mice were stained with fluorescence-labeled monoclonal antibodies and analyzed by flow cytometry. Representative dot plots of gated peripheral lymphocytes are depicted. A) V α 3.2⁺ V β 11⁺ CD4⁺ T cells were analyzed for their expression of CD69 and CD25, B) of CD44 and CD62L, C) of CXCR4 and CCR5. The percentages of V α 3.2⁺ V β 11⁺ CD4⁺ T cells expressing the respective cell surface molecules are indicated within the quadrants (n=13 mice/group). D) B220⁺ B cells were investigated for the expression of MHC II, and E) CD80. Numbers in rectangular gates indicate the percentages of the gated cell population (n=5 mice/group).

6.2.4 Indifferent Levels of MOG-specific Autoantibodies in Devic B7-H1^{-/-} Mice

To analyze whether B7-H1 deficiency influences the conversion of IgH^{MOG}-transgenic B cells into plasma cells, levels of MOG-specific antibodies in serum samples of sick Devic B7-H1^{+/+} and Devic B7-H1^{-/-} mice were measured by ELISA. Both Devic B7-H1^{+/+} and Devic B7-H1^{-/-} mice produced MOG-specific IgM and IgG1 at maximum stage of the disease. The levels, however, did not differ in between the mice groups (Fig. 10 A, B).

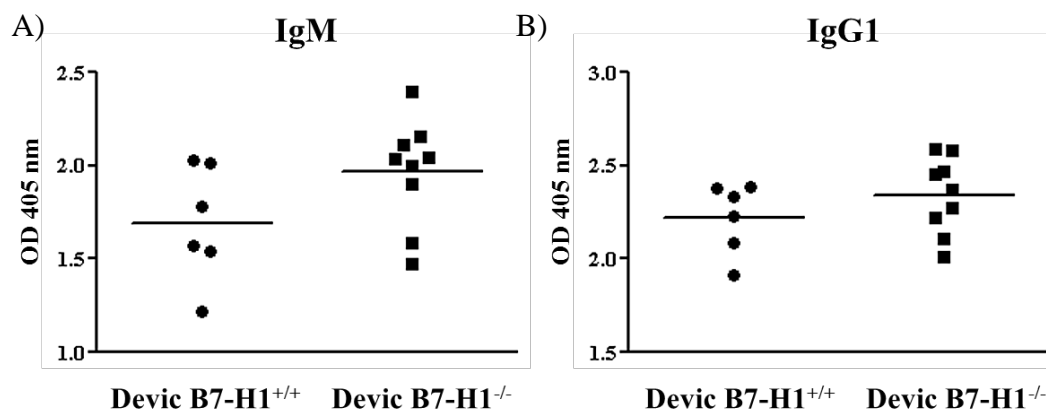


Fig. 10. Levels of MOG-specific serum antibodies. Serum samples collected from Devic B7-H1^{+/+} and Devic B7-H1^{-/-} mice at disease maximum were investigated for the presence of A) MOG-specific IgM and B) MOG-specific IgG1 autoantibodies by an isotype-specific sandwich ELISA. Results are expressed as optical density (OD). Mean values are indicated for each animal group (wt=6, ko=9 mice).

6.2.5 Unaffected Cytokine Secretion Pattern of Devic B7-H1^{-/-} Splenocytes

To investigate whether the absence of B7-H1 modulates the cytokine secretion pattern of MOG-specific T lymphocytes in the periphery and thereby potentially influences the clinical features of the EAE-like disease in Devic mice, splenocytes of Devic B7-H1^{+/+} and Devic B7-H1^{-/-} mice at disease maximum were isolated and restimulated in the presence of MOG₃₅₋₅₅ peptide for 3 days. Similar amounts of IFN- γ and IL-17 were detected in the cell supernatants of splenocytes of both mice groups during ongoing disease (Fig. 11). Moreover, no differences were found in the amounts of the secreted Th1 cytokines TNF- α and IL-2 neither of the Th2 cytokines IL-4 and IL-10 (Fig. 11).

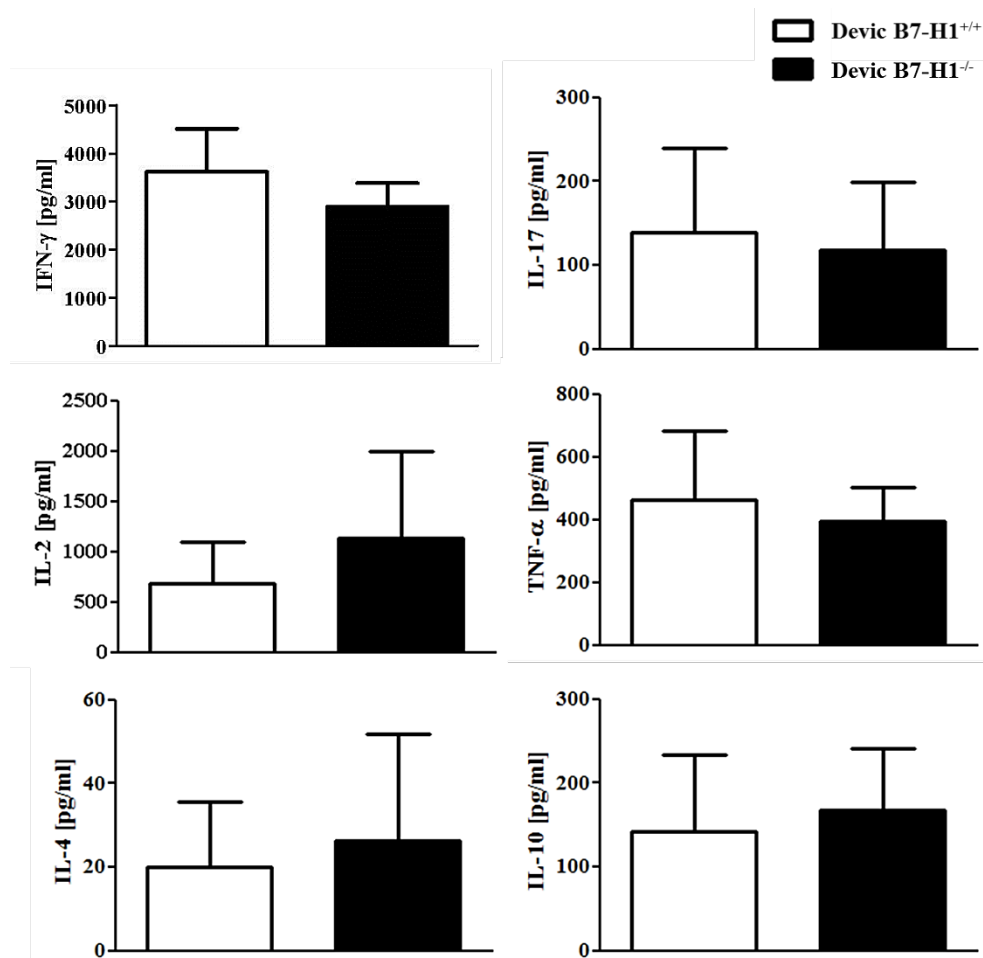


Fig. 11. Cytokine secretion by Devic splenocytes upon MOG₃₅₋₅₅ peptide challenge. Splenocytes of Devic B7-H1^{+/+} and Devic B7-H1^{-/-} mice were isolated at disease maximum and restimulated with MOG₃₅₋₅₅ peptide (10 μ g/ml). Cell supernatants were analyzed for distinct Th1, Th2 and Th17 cytokines amounts by ELISA or CBA (wt=11, ko=14 mice).

6.2.6 Enhanced Accumulation of V α 3.2⁺ V β 11⁺ CD4⁺ T Cells in Secondary Lymphoid Organs of sick Devic B7-H1^{-/-} mice

During dissection of sick Devic mice, LN and spleens seemed macroscopically bigger in Devic B7-H1^{-/-} than in Devic B7-H1^{+/+} mice. Subsequently, single-cell suspensions of these secondary organs were prepared and the total cell numbers determined to detect quantitative differences more precisely. Indeed, the numbers of total LN cells were significantly and of splenocytes considerably higher in Devic B7-H1^{-/-} mice than in Devic B7-H1^{+/+} mice (Fig. 12 A). Next, V α 3.2⁺ V β 11⁺ CD4⁺ T cells present in the secondary lymphoid organs were quantified based on flow cytometry. This analysis

revealed significantly increased absolute numbers of $V\alpha 3.2^+ V\beta 11^+ CD4^+$ T cells within LN cells and splenocytes in between the two Devic mice groups indicating that TCR^{MOG} -transgenic $CD4^+$ T cells accumulated to a larger extent in secondary lymphoid organs of Devic $B7-H1^{-/-}$ than of Devic $B7-H1^{+/+}$ mice (Fig. 12 B).

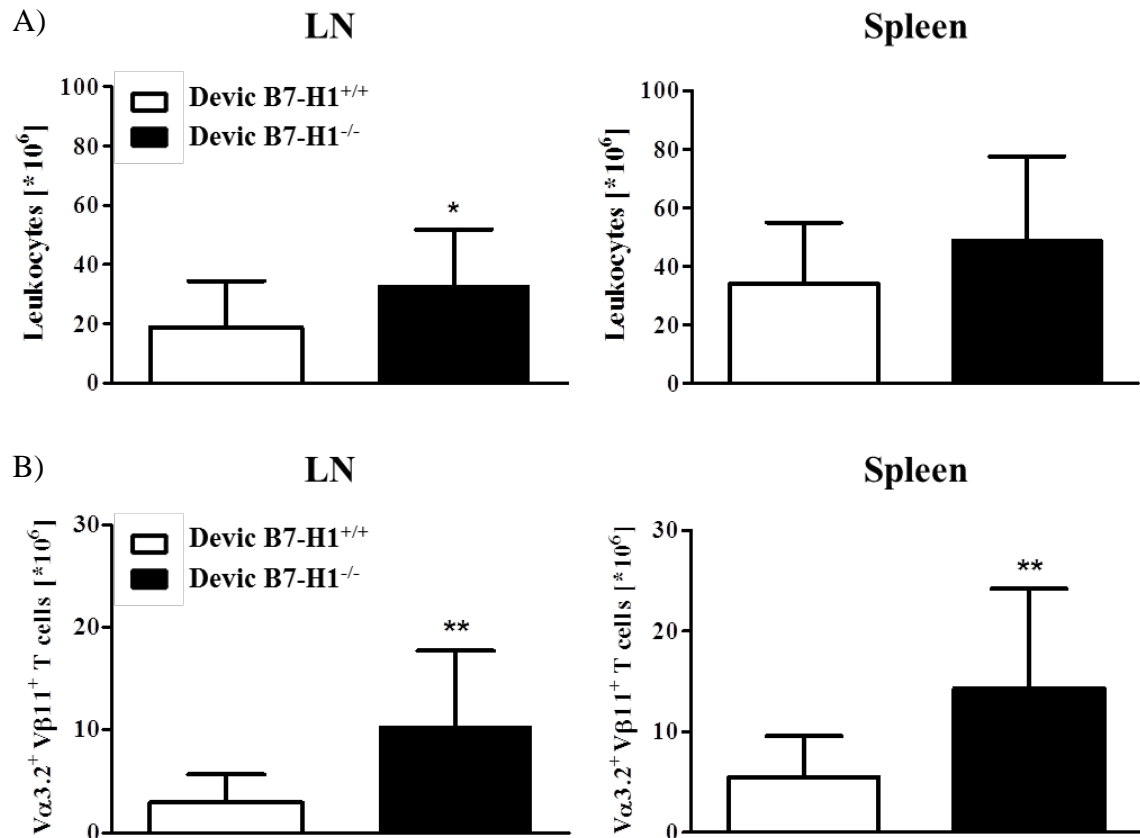


Fig. 12. Cell numbers of LN and spleens of sick Devic mice. A) Single-cell suspensions of LN and spleens obtained from sick Devic $B7-H1^{+/+}$ and Devic $B7-H1^{-/-}$ mice were prepared. The amounts of leukocytes are shown as total numbers (wt=15, ko=23 mice). B) The quantification of $V\alpha 3.2^+ V\beta 11^+ CD4^+$ T cells was based on the total cell numbers and the frequencies of MOG-specific $V\alpha 3.2^+$ and $V\beta 11^+ CD4^+$ T cells determined by flow cytometry (wt=14, ko=20 mice). Bars represent mean values. Error bars indicate SD. * $p < 0.05$, ** $p < 0.01$ compared to Devic $B7-H1^{+/+}$ group.

6.2.7 Increased Thymic Cellularities in Devic $B7-H1^{-/-}$ Mice

Increased cell numbers in secondary lymphoid organs could be the result of diverse mechanisms, for example, of augmented thymic output. To approach this question, the cellularities and cell subsets of thymi of sick Devic $B7-H1^{+/+}$ and Devic $B7-H1^{-/-}$ mice were investigated. Using flow cytometric analysis, no differences in the percentages of $CD4^+ CD8^+ DP$, $CD4^+ SP$ and $CD8^+ SP$ thymocyte subsets or of $V\alpha 3.2^+ V\beta 11^+$

thymocytes were found in between the two mice groups (Fig. 13 A). However, Devic B7-H1^{-/-} mice had significantly more total thymocytes than Devic B7-H1^{+/+} mice (Fig. 13 B). Accordingly, the quantification based on total thymocyte cell numbers and flow cytometric analysis revealed significant higher numbers of thymocytes expressing both TCR^{MOG}-transgenic V α 3.2 and V β 11 chains in Devic B7-H1^{-/-} mice as compared to Devic B7-H1^{+/+} mice (Fig. 13 B).

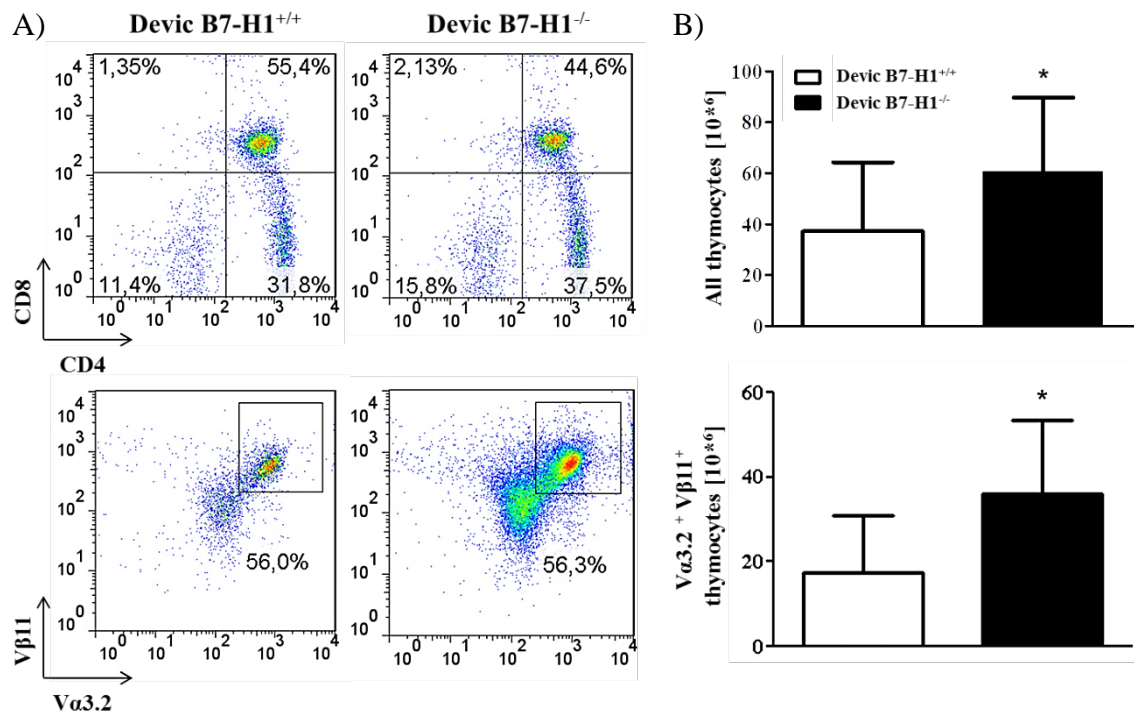


Fig. 13. Thymocyte subsets and cell numbers in sick Devic mice. Thymocytes isolated from sick Devic B7-H1^{+/+} and Devic B7-H1^{-/-} mice were counted, stained with fluorescence-labelled monoclonal antibodies and analysed by flow cytometry. A) Dot plots of CD4/CD8 expression and V α 3.2/V β 11 expression on live thymocytes of a representative animal of each group are shown. B) Total thymocyte cell numbers are displayed (wt=10, ko=18 mice). The quantification of absolute numbers of V α 3.2⁺V β 11⁺ thymocytes is based on the total thymocyte cell numbers and the correlating flow cytometric analysis (wt=10, ko=11 mice). Bars indicate mean values. Error bars indicate SD. * p< 0.05 compared to Devic B7-H1^{+/+} group.

6.2.8 Elevated Antigen-induced Proliferation of Devic B7-H1^{-/-} Splenocytes

Elevated numbers of V α 3.2⁺V β 11⁺CD4⁺T cells in the periphery of Devic B7-H1^{-/-} mice might as well be the consequence of increased proliferation rates of these lymphocytes. In order to clarify whether the lack of B7-H1 influences the proliferative activity of V α 3.2⁺V β 11⁺CD4⁺lymphocytes in this autoimmune-prone mouse model, splenocytes of Devic B7-H1^{+/+} and Devic B7-H1^{-/-} mice were isolated at disease

maximum and restimulated with MOG₃₅₋₅₅ peptide. As measured by the uptake of [³H] thymidine, the proliferation rates of untreated splenocytes and at low antigen doses were minor and comparable in between the two mice groups. At a peptide concentration of 10 µg/ml, proliferation rates increased and the most remarkable difference in between Devic B7-H1^{+/+} and Devic B7-H1^{-/-} splenocytes was detected. Peptide concentrations above, however, did not further raise the levels or the difference of the proliferation rates (Fig. 14 A). As [³H] thymidine incorporation assays only reflect the proliferation of total splenocytes of Devic mice, another method was performed to specifically monitor the impact of B7-H1 deficiency on the proliferation capacity of MOG-specific CD4⁺ T-cells. Using flow cytometry, gradual loss of emission intensity of the Cell Proliferation Dye of CD4⁺ T lymphocytes was detected correlating with their proliferative activities (Fig. 14 B). Increased proliferation rates of encephalitogenic CD4⁺ T cells obtained from Devic B7-H1^{-/-} mice after MOG₃₅₋₅₅ peptide stimulation were assigned to the missing expression of B7-H1. Therefore, these experiments reaffirmed the previously seen inhibitory effect of B7-H1 on antigen-specific proliferation.

To determine whether B7-H1 deficiency influenced the effector function of IgH^{MOG}-transgenic B cells as APCs in this transgenic mouse model, B220⁺ B cells were isolated from Devic B7-H1^{+/+} and Devic B7-H1^{-/-} mice at disease maximum, irradiated and co-cultured with CD4⁺ T cells isolated from the respective mice group in presence of MOG₃₅₋₅₅ peptide. Dose-response proliferation assays revealed that CD4⁺ B7-H^{-/-} T cells proliferated by far more efficiently when presented antigen (MOG₃₅₋₅₅, 10 µg/ml) by B220⁺ B7-H1^{-/-} B cells both obtained from Devic B7-H1^{-/-} mice than CD4⁺ B7-H^{+/+} T cells which were activated by B220⁺ B7-H1^{+/+} B cells isolated from Devic B7-H1^{+/+} mice (Fig. 14 C). Lower antigen doses (1 and 5 µg/ml) were sufficient to induce a considerable CD4⁺ T-cell proliferation which exhibited, however, similar rates in both groups (Fig. 14 C).

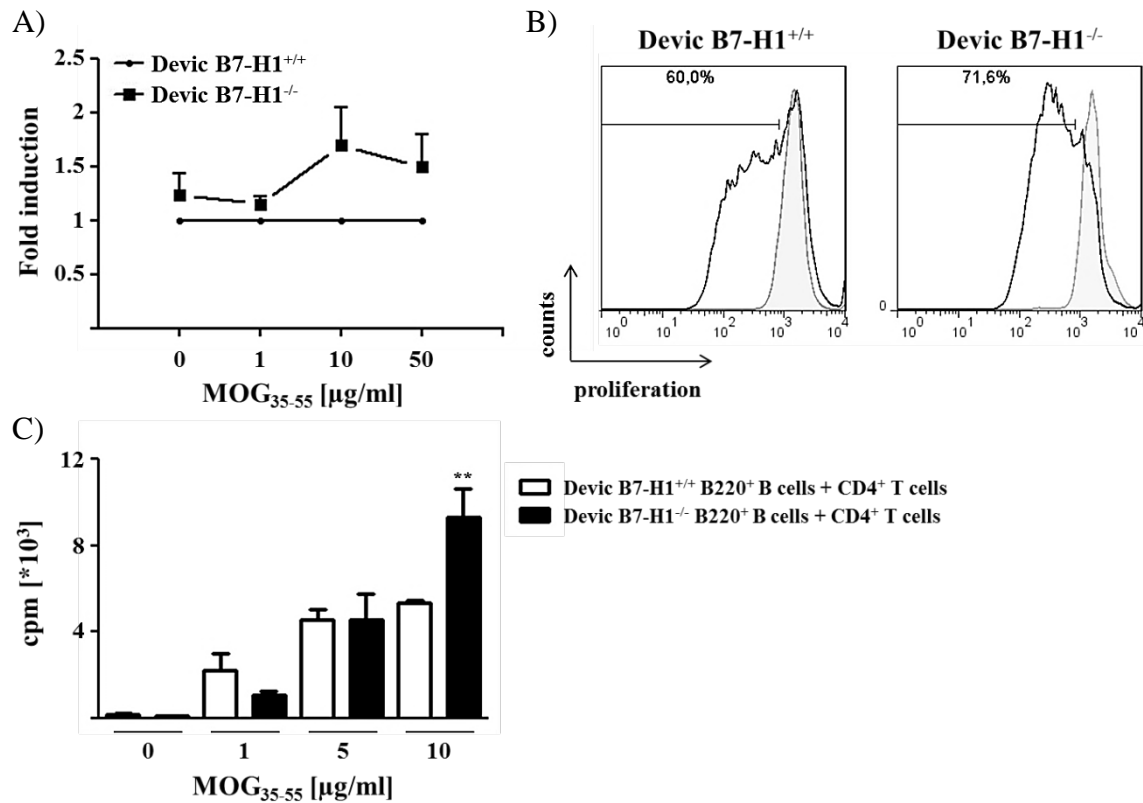


Fig. 14. MOG₃₅₋₅₅-specific proliferation of Devic splenocytes. Splenocytes of Devic B7-H1^{+/+} and Devic B7-H1^{-/-} mice were isolated at disease maximum and restimulated with different doses of MOG₃₅₋₅₅ peptide. A) Cell proliferation was measured by [³H] thymidine incorporation. The mean induction rate was calculated out of three independent assays with cpm values of Devic B7-H1^{+/+} splenocytes set as 1 (n=6 mice/group). Error bars indicate SD. B) Flow cytometric analysis of the gradually decreasing emission intensity of Cell Proliferation Dye eFluor® APC reveals the proliferative activity of gated CD4⁺ T cells within isolated splenocytes of sick Devic B7-H1^{+/+} and Devic B7-H1^{-/-} mice. The depicted histogram is representative for four independent experiments (n=8 mice/group). The grey shaded curve represents the non-stimulated samples; the black curve represents the samples stimulated with MOG₃₅₋₅₅ peptide (10 μg/ml). C) Dose-response proliferation assays based on [³H] thymidine incorporation were also performed with isolated, irradiated B220⁺ B cells and CD4⁺ T cells (1:10 ratio) obtained from the respective mice group. One representative assay is shown (n=5 mice/group).

6.2.9 Hint on Modified Survival Capacities of Devic B7-H1^{-/-} Lymphocytes

Extended survival or increased resistance to apoptosis might also contribute to augmented accumulation of Vα3.2⁺ Vβ11⁺ CD4⁺ T cells in lymphoid of Devic B7-H1^{-/-} mice. We approached this question by preliminary *in vitro* survival assays lasting for 4 days. Fluorescein-conjugated Annexin V was used in flow cytometric analysis performed on day 0 and day 4 of *in vitro* cultivation of LN cells to determine the increase of apoptotic Vα3.2⁺ Vβ11⁺ CD4⁺ T cells over time. We observed that less Vα3.2⁺ Vβ11⁺ CD4⁺ T cells obtained from Devic B7-H1^{-/-} mice underwent apoptosis

than cells from Devic B7-H1^{+/+} mice (Fig. 15). These differences, however, were not significant and should be validated in further analysis.

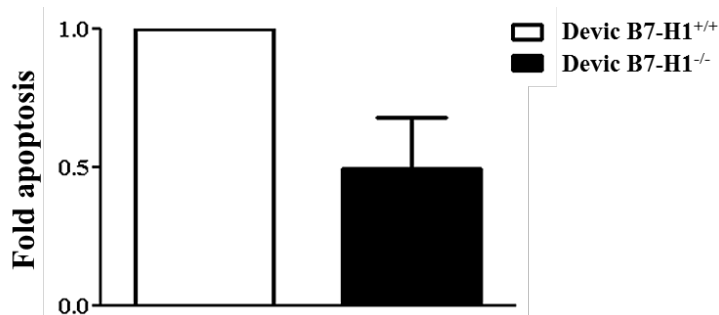


Fig. 15. *In vitro* survival of V α 3.2⁺ V β 11⁺ CD4⁺ T cells. Single-cell suspensions of LN obtained from Devic B7-H1^{+/+} and Devic B7-H1^{-/-} mice at disease maximum were prepared and cultivated in conventional cell culture media for 4 days. Apoptotic TCR^{MOG}-transgenic CD4⁺ T cells were detected by Annexin V-FITC staining on day 0 and 4 and the relative induction rates were calculated for each sample. The mean induction rates were calculated out of 2 independent assays with the Devic B7-H1^{+/+} value set as 1 (n=4 mice/group). Error bars indicate SD.

6.2.10 Unaltered *in vitro* Migratory Behavior of V α 3.2⁺ V β 11⁺ B7-H1^{-/-} T cells

A potential explanation of augmented CD4⁺ T-cell accumulation within the CNS and lymphoid tissues of Devic B7-H1^{-/-} mice could be an altered migratory/homing behavior of V α 3.2⁺ V β 11⁺ CD4⁺ T cells in these mice. In a simplistic *in vitro* experimental setting for cell migration using transwell chambers, V α 3.2⁺ V β 11⁺ CD4⁺ T cells of sick Devic B7-H1^{+/+} and Devic B7-H1^{-/-} mice were investigated for their migratory capacities following an FCS (unspecific chemoattractant) signal (Fig. 16 A). The calculation of V α 3.2⁺ V β 11⁺ CD4⁺ T cells that migrated via a filter from the apical to the basolateral chamber during 8 h incubation time using calibration beads as reference demonstrated that V α 3.2⁺ V β 11⁺ CD4⁺ B7-H1^{-/-} and V α 3.2⁺ V β 11⁺ CD4⁺ B7-H1^{+/+} T cells exhibited similar migratory capacities (Fig. 16 B). Likewise, the migratory activities did not differ in between the two groups of CD4⁺ T cells after 16 h incubation (Fig. 16 C). Moreover, extending the incubation time up to 16 h did not increase the maximum yield of the total of transmigrated cells.

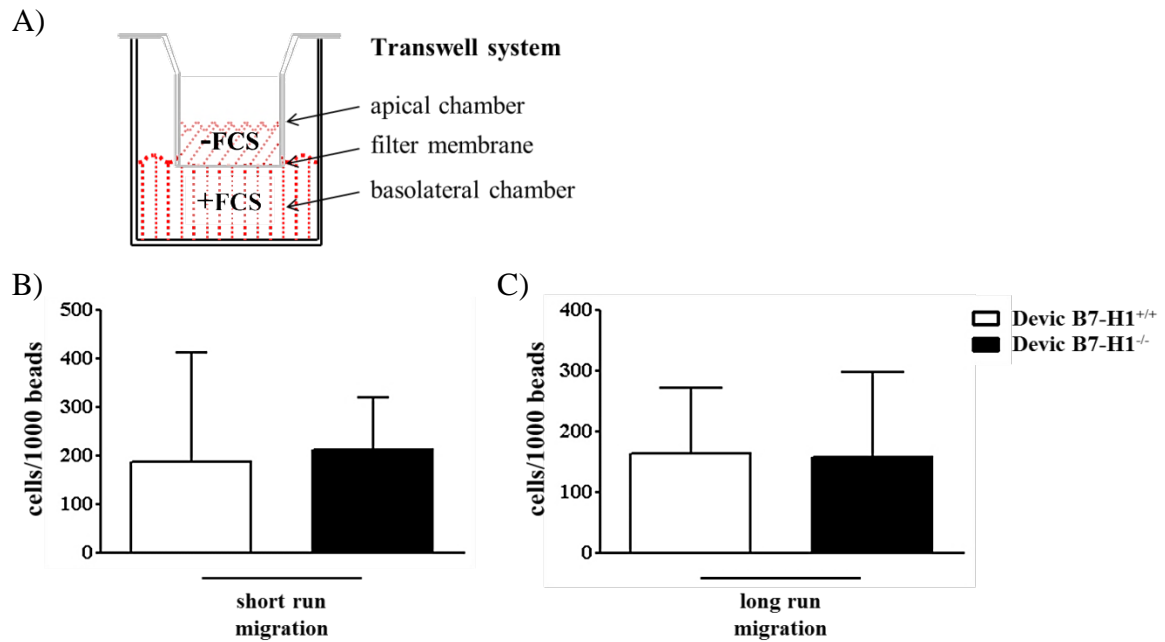


Fig. 16. *In vitro* migration of $V\alpha 3.2^+ V\beta 11^+ CD4^+$ T cells. Lymphocytes of sick Devic B7-H1^{+/+} and Devic B7-H1^{-/-} mice were isolated from LN and transferred into the apical chamber of a transwell plate (5×10^5 cells/transwell). An FCS gradient between the apical and the basolateral chamber served as unspecific chemoattractant stimulus. Transmigrated cells were collected from the basolateral chamber and analyzed by flow cytometry. Calibration beads were used as reference to calculate the cell/bead ratios of transmigrated cells. Each sample was assessed in triplicates. A) Schematic illustration of the transwell system consisting of an apical and a basolateral chamber separated by a filter membrane with 3.0 μ m pore-size. B) After 8 h of incubation time, transmigrated cells were collected and numbers calculated in relation to calibration beads. Mean values of 1 out of 3 independent experiments are shown (n=6 mice/group). C) Likewise, transmigrated cells were collected after 16 h of incubation time and numbers calculated in relation to calibration beads. Mean values of 1 out of 3 independent experiments are shown (n=6 mice/group). Error bars indicate SD.

6.2.11 Unaltered *in vivo* Migratory Behavior of $V\alpha 3.2^+ V\beta 11^+ B7-H1^{-/-}$ T cells

Altered migratory/homing behavior of $V\alpha 3.2^+ V\beta 11^+ CD4^+ B7-H1^{-/-}$ T cells was suspected to lead to the extensively enhanced numbers of MOG-specific $CD4^+$ T cells in the secondary lymphoid organs and the CNS of Devic B7-H1^{-/-} mice compared to Devic B7-H1^{+/+} mice. In parallel to the *in vitro* approach, an adoptive cell transfer model was used to monitor the *in vivo* migratory/homing behavior of MOG-specific $CD4^+$ T cells more precisely. RAG-1^{-/-} mice which do not produce mature T cells or B cells due to the RAG-1 gene knockout were adoptively transferred single-cell suspensions composed of splenocytes and LN cells from sick Devic B7-H1^{+/+} or Devic B7-H1^{-/-} mice. The recipient mice were observed for 16 days after injection.

EAE-like symptoms occurred at a remarkable incidence in both groups of recipient mice during the observation time (60 % incidence in RAG-1^{-/-} recipient mice transferred Devic B7-H1^{+/+} cells, 67 % incidence in RAG-1^{-/-} recipient mice transferred Devic B7-H1^{-/-} cells) (Fig. 17 B, Tab. 2). The clinical features of EAE-like disease such as the age of onset, the mean clinical score and the mean weight loss of sick mice were comparable in both recipient mice groups irrespective of which donor cells they received (Tab. 2).

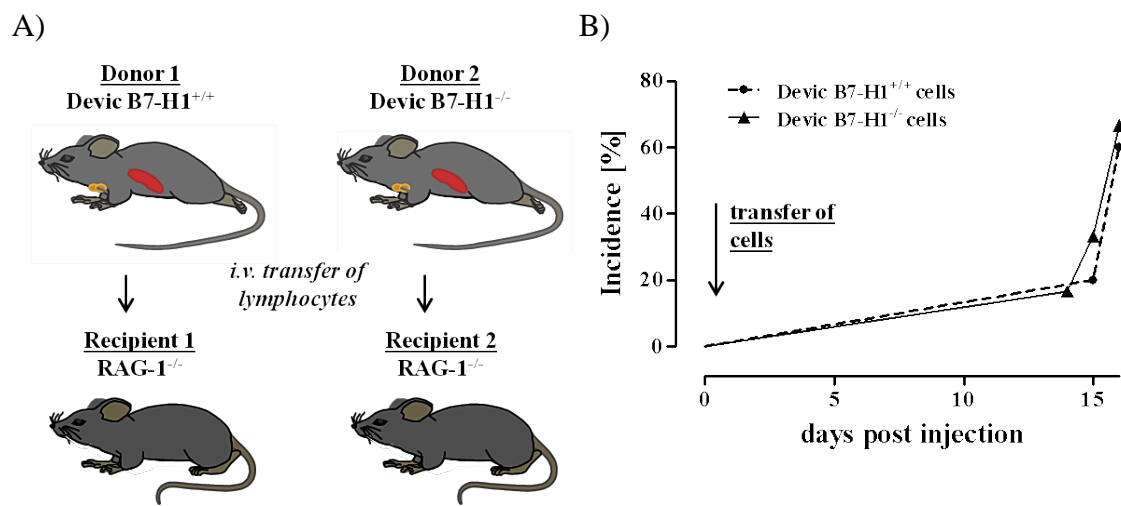


Fig. 17. Adoptive transfer of Devic lymphocytes into RAG-1^{-/-} recipient mice. Single-cell suspensions were prepared from LN and spleens of sick Devic B7-H1^{+/+} and Devic B7-H1^{-/-} mice and i.v. injected into the tail vein of RAG-1^{-/-} recipient mice. A) Schematic illustration of the adoptive cell transfer from sick Devic mice on RAG-1^{-/-} mice. B) RAG-1^{-/-} recipient mice were observed for EAE-like symptoms over a period of 16 days. The graph illustrates the incidence rate in recipient mice receiving Devic B7-H1^{+/+} (dotted line, n=5 mice) or Devic B7-H1^{-/-} lymphocytes (solid line, n=6 mice).

Donor mice	Observation time	Incidence	Age of onset (d.p.i.)	Mean clinical score	Weight loss
Devic B7-H1 ^{+/+}	16 days	3/5 (60%)	15.7 ± 0.6	3 ± 0.5	-2.8 ± 0.7 g
Devic B7-H1 ^{-/-}	16 days	4/6 (67%)	15.3 ± 1	2 ± 1.6	-2.7 ± 2.4 g

Tab. 2. Summary of clinical features of RAG-1^{-/-} recipient mice adoptively transferred either Devic B7-H1^{+/+} or Devic B7-H1^{-/-} lymphocytes (d.p.i. = days post-injection).

After 16 days, LN and CNS tissue of RAG-1^{-/-} recipient mice which had developed clinical EAE-like symptoms were collected and investigated for accumulation and activation levels of transferred cells. V α 3.2⁺ V β 11⁺ B7-H1^{+/+} and V α 3.2⁺ V β 11⁺ B7-H1^{-/-} CD4⁺ T cells had accumulated equally within the secondary lymphoid organs of the respective recipient mice (Fig 18 A). Moreover, in the periphery of RAG-1^{-/-} recipient mice, V α 3.2⁺ V β 11⁺ CD4⁺ T cells consistently exhibited low activation levels judged by expression of CD25 and CD69 independently of which donor group they derived from (Fig 18 A). The CNS of both recipient mice groups were infiltrated by V α 3.2⁺ V β 11⁺ CD4⁺ T cells to a similar extent (Fig. 18 B). In contrast to the periphery, CNS-infiltrating V α 3.2⁺ V β 11⁺ CD4⁺ T cells were highly activated. Still, no considerable differences in the expression levels of CD25 and CD69 were found in between the two recipient mice groups (Fig. 18 B).

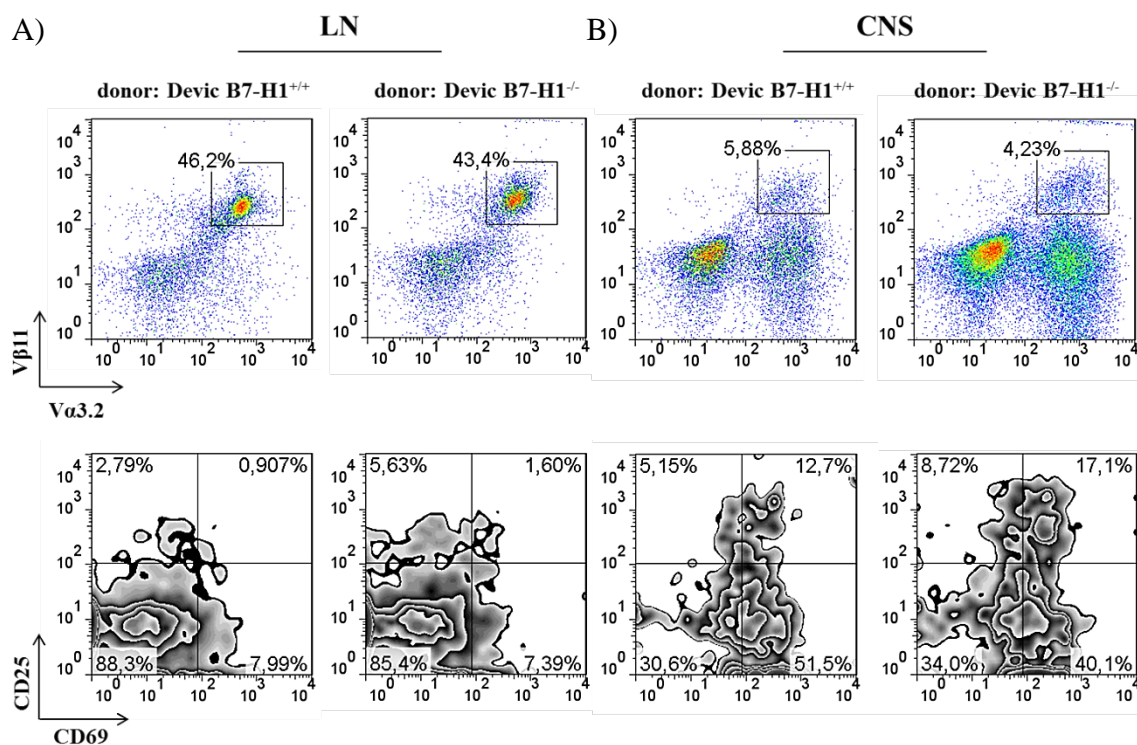


Fig. 18. Accumulation and activation of adoptively transferred encephalitogenic CD4⁺ T cells in RAG-1^{-/-} recipient mice. 16 days after adoptive transfer of Devic cells, single-cell suspensions of LN and CNS tissue obtained from RAG-1^{-/-} recipient mice displaying EAE-like symptoms were prepared and stained with fluorescence-labeled monoclonal antibodies and analyzed by flow cytometry. Representative dot plots are depicted (wt=3, ko=4 mice). A) Within live cells isolated from LN or B) CNS tissue of sick RAG-1^{-/-} recipient mice, V α 3.2⁺ V β 11⁺ CD4⁺ T cells were gated. Expression of activation markers CD25 and CD69 on V α 3.2⁺ V β 11⁺ CD4⁺ T cells was investigated in each recipient mice group.

Furthermore, leukocytes isolated from LN and CNS tissue obtained from RAG-1^{-/-} recipient mice were restimulated with MOG₃₅₋₅₅ peptide to elucidate which Th1 and Th17 differentiation status transferred CD4⁺ T cells acquired in recipient mice. Only marginal secretion of IFN- γ by CD4⁺ T cells obtained from LN was detected irrespective of which donor group they derived of (Fig. 19 A). IL-17 secretion by “peripheral” CD4⁺ T cells could not be observed in either group (Fig. 19 A). CNS-infiltrating CD4⁺ T cells produced IFN- γ and to much smaller extent IL-17 after *in vitro* challenge by MOG₃₅₋₅₅ peptide (Fig. 19 B). Differences in the cytokine production of CD4⁺ T cells derived from Devic B7-H1^{+/+} mice and derived from Devic B7-H1^{-/-} mice isolated from the CNS of sick RAG-1^{-/-} mice were not detected either.

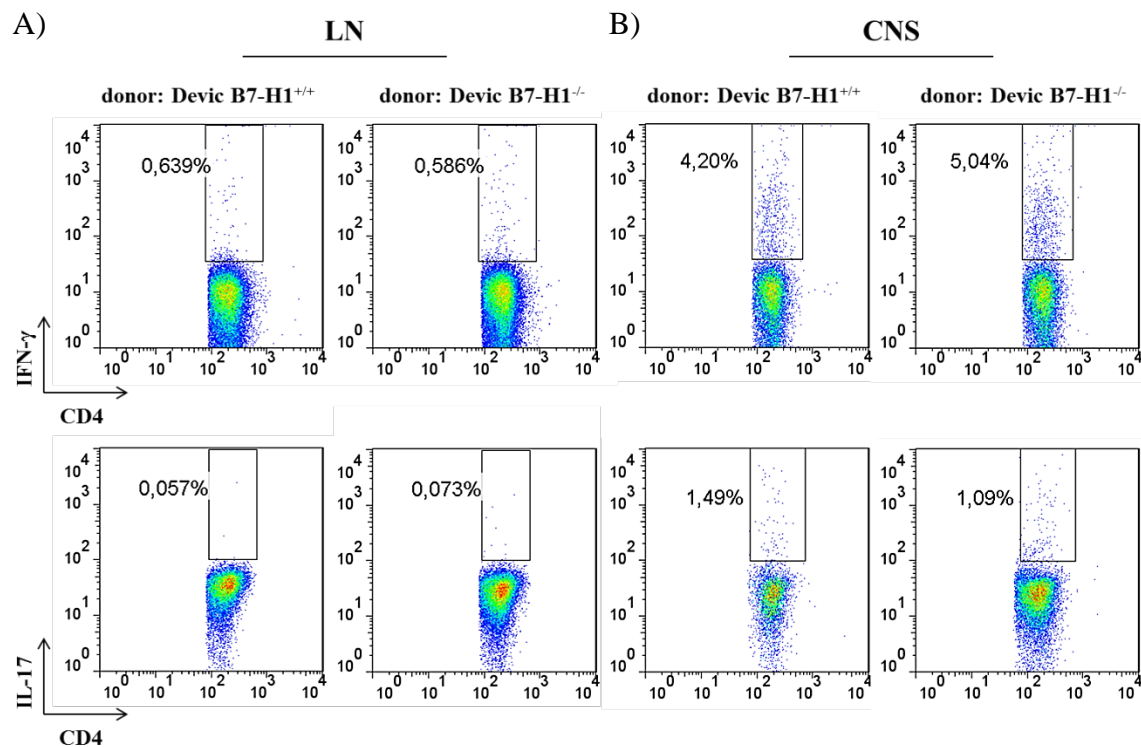


Fig. 19. Cytokine secretion of adoptively transferred CD4⁺ T cells. Leukocytes isolated from LN and CNS tissue of diseased RAG-1^{-/-} recipient mice were stimulated with MOG₃₅₋₅₅ peptide (10 μ g/ml) overnight and treated with Brefeldin A for the last 6 h of incubation. To assess IFN- γ and IL-17 production by CD4⁺ T cells, cells were stained with fluorescence-labeled monoclonal antibodies against CD4, permeabilized, fixed and stained for intracellular cytokines. A) CD4⁺ T cells obtained from LN of RAG-1^{-/-} recipient mice were investigated for IFN- γ and IL-17 secretion. B) Likewise, IFN- γ and IL-17 secreting CD4⁺ T cells were identified within leukocytes obtained from CNS tissue of sick recipient mice. Percentages of the respective cell population are indicated in the corresponding rectangular gates. Representative FACS profiles are depicted (wt=3, ko=4 recipient mice).

6.2.12 Amplified Th1 Response of Devic B7-H1^{-/-} Splenocytes in the Preclinical Phase

Observation of numerous Devic mice over several months allowed to comprehend the course of the disease in Devic mice and to allocate the preclinical phase to the age of approximately 30 days and younger. However, the early and heterogeneous onset of EAE-like disease in Devic B7-H1^{-/-} mice and logistic limitations of an early genotyping impeded analyzing the impact of B7-H1 on early immune responses in symptom-free Devic mice in detail. Restimulation assays were performed with splenocytes of young, symptom-free Devic B7-H1^{+/+} and Devic B7-H1^{-/-} mice to investigate whether the absence of B7-H1 modulates the cytokine secretion pattern of peripheral MOG-specific lymphocytes in the preclinical phase and thereby potentially influences the clinical course of the EAE-like disease. Splenocytes were isolated and restimulated in the presence of MOG₃₅₋₅₅ peptide. The amounts of IFN- γ and IL-17 contained in the cell supernatant were determined by ELISA. Splenocytes of healthy Devic B7-H1^{-/-} mice secreted significantly higher amounts of IFN- γ than of young Devic B7-H1^{+/+} mice upon *in vitro* challenge with MOG₃₅₋₅₅ peptide. The Th17 response was unaffected by B7-H1 deficiency in the preclinical phase (Fig. 20).

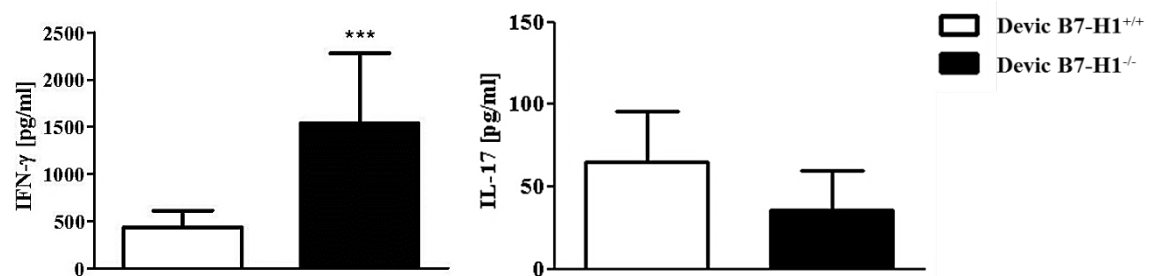


Fig. 20. Cytokine secretion by splenocytes of young, symptom-free Devic mice. Splenocytes of healthy Devic B7-H1^{+/+} and Devic B7-H1^{-/-} mice were restimulated with MOG₃₅₋₅₅ peptide (10 μ g/ml) for 3 days. Cell supernatants were analyzed for the amounts of IFN- γ and IL-17 by ELISA (wt=8, ko=10 mice). Mean values are shown. Error bars indicate SD. *** p < 0.001 compared to Devic B7-H1^{+/+} group.

6.2.13 Higher Expression of LFA-1 on Peripheral CD4⁺ T cells in Devic B7-H1^{-/-} Mice in the Preclinical Phase

Infiltration of encephalitogenic lymphocytes via the BBB into the CNS considerably depends on their responsiveness to chemoattractants, their adhesion to the vascular wall

and their transmigration mediated via cell-surface molecules. LFA-1 on effector T cells is a major factor for the adhesion to brain endothelial cells mediated by LFA-1/VCAM-1 interaction and their extravasation via the BBB into the CNS. Expression of LFA-1 was investigated on peripheral and CNS-infiltrating CD4⁺ T cells of Devic B7-H1^{+/+} and Devic B7-H1^{-/-} mice at disease maximum and before disease onset. Peripheral CD4⁺ T cells of both sick Devic mice groups exhibited remarkable and comparable expression levels of LFA-1 (Fig. 21 A). Moreover, CNS-infiltrating CD4⁺ T cells of both mouse groups showed similar expression levels of LFA-1 even though far more enhanced compared to the levels in the periphery (Fig. 21 C). Remarkably, peripheral CD4⁺ T cells isolated from young and symptom-free Devic B7-H1^{-/-} mice expressed significantly higher levels of LFA-1 than those obtained from healthy Devic B7-H1^{+/+} mice (Fig. 21 B).

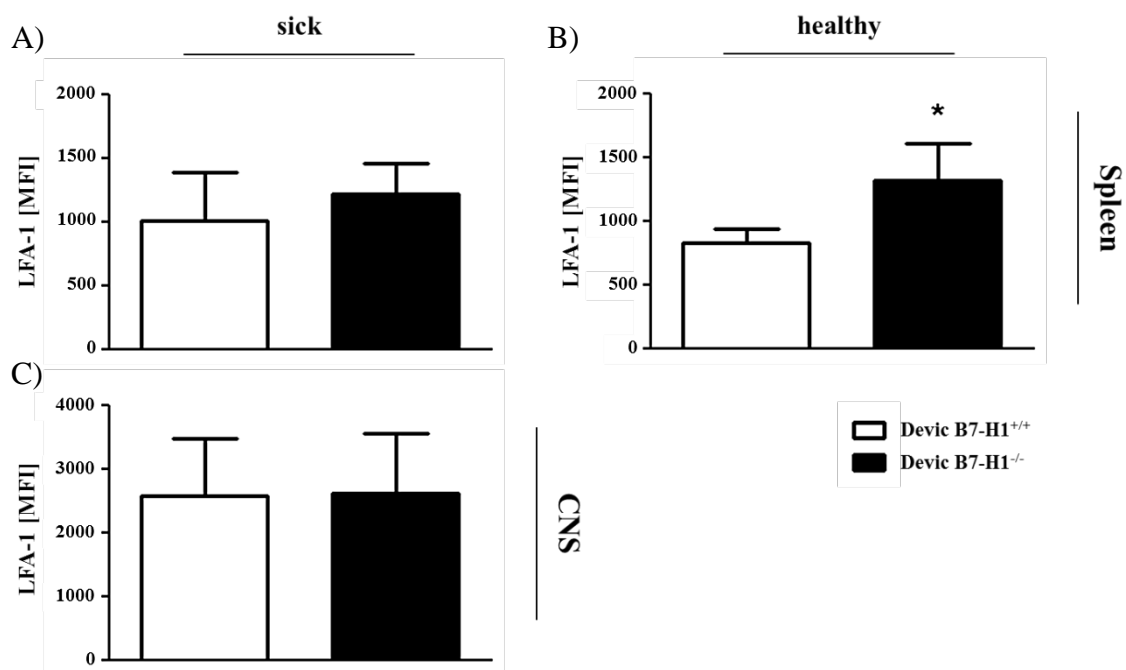


Fig. 21. Average expression levels of LFA-1 on peripheral and CNS-infiltrating CD4⁺ T cells in Devic mice. Splenocytes and CNS-infiltrating mononuclear cells of Devic mice were isolated, stained with fluorescence-labeled monoclonal antibodies against CD4 and LFA-1 and analyzed by flow cytometry. A) The mean LFA-1 expression levels (indicated by MFIs) on peripheral CD4⁺ T cells of diseased mice older than 29 days were analyzed (wt=4, ko=6 mice). B) Likewise, the mean expression levels (indicated by MFIs) of LFA-1 on peripheral CD4⁺ T cells of healthy Devic mice younger than 30 days are shown (n=5 mice/group). * p < 0.05 compared to Devic B7-H1^{+/+} group. C) CNS-infiltrating CD4⁺ T cells of sick mice older than 29 days were also investigated for their LFA-1 expression (n=5 mice/group).

7 Discussion

MS is an autoimmune disease of the CNS characterized by inflammatory, demyelinated lesions and neuronal death causing a variety of symptoms such as paralysis and cognitive impairment with certain recurrent themes but an unpredictable course (reviewed by Compston and Coles, 2002). Actively or passively induced EAE in various mouse strains is a commonly used animal model for studying MS. Mouse models spontaneously developing CNS-specific autoimmune diseases are scarce. A recently described spontaneous EAE mouse model, the TCR^{MOG} × IgH^{MOG} / OSE / Devic mouse, expressing MOG-specific CD4⁺ T and B cells represents a new, very promising tool for the search after disease triggers, for investigating the biology of T-cell/B-cell cooperation in the genesis of autoimmune diseases and for testing novel therapies under homeostatic conditions (Bettelli et al., 2006; Krishnamoorthy et al., 2006). B7-H1, a cell-surface molecule of the B7 family is constitutively expressed by immune and parenchymal cells and has been assigned an important immune-regulatory role by interacting with the PD-1 co-receptor. Both negative and positive regulatory functions of the PD-1/B7-H1 pathway have been described in different experimental systems (reviewed by Francisco et al., 2010).

The clarification of environmental and genetic factors triggering MS has been a central theme in neuroimmunology over the last years. In the present study, 71 % of double-transgenic Devic B7-H1^{+/+} mice developed EAE-like features of spontaneous neuroinflammation under conventional animal housing conditions thereby exceeding published data which stated incidence rates of 50-60 % (Bettelli et al., 2006; Krishnamoorthy et al., 2006). Due to the allegedly same genetic background of the mice used in the studies by Krishnamoorthy et al. and by Bettelli et al. and used in the present study, genetic differences causing this shift can be excluded. However, varying incidence rates of spontaneous autoimmunity are occasionally attributed to variables in animal housing conditions such as the microbial environment, nature of food, maintenance or others. Evidence is growing that the gut commensal flora which might vary according to the environmental conditions influences the immune homeostasis and the development CNS autoimmunity (Berer et al., 2011). Studies on MBP-specific TCR transgenic mice, for example, suggested possible environmental triggers for EAE as 14-

44 % of these mice developed spontaneous EAE under conventional but not under SPF (specific pathogen-free) housing conditions (Goverman et al., 1993). Moreover, it has been concluded from epidemiological studies that exposure to infectious agents such as viruses promote the pathogenesis of MS (reviewed by Das Sarma, 2010; Levin et al., 2010). Accordingly, damage of the myelin sheaths by infectious agents might result in the release of autoantigens which activate autoreactive T cells which in turn initiate an independent secondary inflammatory process. Infectious agents can also activate autoreactive T cells by using the mechanism of molecular mimicry resulting in an autoimmune attack against components of the CNS (reviewed by Sospedra and Martin, 2005). Krishnamoorthy et al. reported insignificant differences in disease incidence rates in between Devic mice kept under SPF conditions (51 %) and in mice housed under conventional conditions (46 %) (Krishnamoorthy et al., 2006). We assumed that during the present study the prevailing housing conditions -even though classified conventional- in its entirety led to higher disease incidence rates in Devic B7-H1^{+/+} mice than previously reported by others. We concluded from our observations that the transgenic Devic mouse model is suitable at the given experimental conditions to investigate the role of B7-H1 in spontaneous CNS autoimmunity.

Devic B7-H1^{-/-} mice developed clinical symptoms with a remarkably higher (close to 100 %) incidence rate and faster kinetics emphasized by deteriorated disease courses and a nearly quadrupled mortality rate than Devic B7-H1^{+/+} mice under the same animal housing conditions indicating a potential disease modifying role of B7-H1 in the pathogenesis of this EAE-like disease. Remarkably enhanced immune-cell accumulation in the CNS of Devic B7-H1^{-/-} mice correlated with the more severe clinical features compared to Devic B7-H1^{+/+} mice which indicates that indeed B7-H1 controls immune responses in this animal model. Our clinical findings agreed well with the described impact of the PD-1/B7-H1 pathway on induced CNS autoimmunity in EAE experiments conducted by others. After abrogation of the PD-1/B7-H1 co-inhibitory pathway by monoclonal antibodies or genetic ablation, the susceptibility for clinical symptoms increased and the disease course worsened in several investigated mouse strains (Latchman et al., 2004; Ortler et al., 2008; Salama et al., 2003). A central role of the PD-1/B7-H1 pathway in the induction and maintenance of immune tolerance toward autoantigens was first concluded when PD-1-deficient mice (on C57BL/6 background) spontaneously developed diverse late onset autoimmune conditions such as

lupus-like proliferative arthritis and glomerulonephritis (Nishimura et al., 1999). Based on this, the primary goal of this study was to elucidate to what degree B7-H1 influences peripheral and CNS-restricted autoimmune responses in a model for spontaneous CNS autoimmunity - the double-transgenic Devic mouse.

Remarkably increased immune-cell accumulation was not only found in the CNS of sick Devic B7-H1^{-/-} mice as compared to Devic B7-H1^{+/+} mice but also in the periphery. Detailed analysis revealed that secondary lymphoid organs of sick Devic B7-H1^{-/-} mice contained significantly higher numbers of MOG-specific V α 3.2⁺ V β 11⁺ CD4⁺ T cells than of Devic B7-H1^{+/+} mice. Multiple factors can be taken into account that might lead to an amplified accumulation of encephalitogenic CD4⁺ T cells such as higher proliferation rates, extended survival and life span or altered homing behaviour of lymphocytes. The PD-1/B7-H1 pathway has previously been allocated to block T-cell proliferation and to restrict T-cell survival (reviewed by Francisco et al., 2010; Keir et al., 2008). In the Devic mouse model, we indeed observed tendencies to amplified MOG-specific proliferation of peripheral CD4⁺ T cells of Devic B7-H1^{-/-} mice. With a closer look on B-cell involvement, it seems as if the absence of B7-H1 largely improved antigen-presenting and T-cell activating capacities of MOG-specific B cells indicating an important role of B7-H1 expression on APCs in this mouse model. Nevertheless, reciprocal interference by B7-H1 on T cells themselves might also contribute to the B7-H1-mediated immune modulation of T-cell proliferation thus additionally contributing to the observed phenotype. We further hypothesized that an altered T-cell survival/life span could contribute to the accumulation of MOG-specific CD4⁺ T cells in Devic B7-H1^{-/-} mice. Judging from preliminary *in vitro* survival experiments, peripheral V α 3.2⁺ V β 11⁺ CD4⁺ T cells of Devic B7-H1^{-/-} mice exhibited a lower sensitivity to apoptosis than those of Devic B7-H1^{+/+} mice. However, these observations would have to be validated in further experiments to verify this mechanism as relevant for augmented cell accumulation. Based on our results, we concluded that the overall higher numbers of encephalitogenic CD4⁺ T cells might be at least partly triggered by a lowered proliferation and increased apoptosis threshold of V α 3.2⁺ V β 11⁺ CD4⁺ T cells in Devic B7-H1^{-/-} mice. To what extent the tissue-specific expression of B7-H1, i.e. expression on T cells, APCs or parenchymal cells, contributes to this result *in vivo* has still to be elucidated.

The PD-1/B7-H1 pathway has been attributed a role in the maintenance of the

peripheral and central tolerance both of which are essential to control autoimmunity (reviewed by Keir et al., 2008). PD-1/B7-H1 interactions have been assumed to be critical to positive selection in thymocyte development indicated by elevated numbers of CD4⁺ CD8⁺ DP and CD4⁺ SP thymocytes in B7-H1 deficient mice (Keir et al., 2005). In TCR^{MOG}-transgenic mice, thymic development is strongly altered compared to non-transgenic littermates as seen in the ratio between CD4⁺ and CD8⁺ SP thymocytes which is biased toward the CD4⁺ compartment (Bettelli et al., 2003). Apart from this shift, we observed a modification of the absolute thymocyte numbers in Devic B7-H1^{-/-} mice compared to Devic B7-H1^{+/+} mice which could very likely be attributed to the elevated numbers of thymocytes expressing both the TCR V α 3.2 and V β 11 chains. Based on this we assumed that the loss of B7-H1 might influence selection of encephalitogenic CD4⁺ T cells in this model for CNS autoimmunity. In fact, increased thymic output could also explain the overall accumulation of encephalitogenic T cells in Devic B7-H1^{-/-} mice. The specific effect of B7-H1 on the selection processes of autoimmune T cells in our model, however, still has to be investigated in more detail and in this connection, the relative contribution of the B7-H1 expression on thymocytes and on parenchymal cells.

Significantly elevated accumulation of V α 3.2⁺ V β 11⁺ CD4⁺ T cells in the CNS of Devic B7-H1^{-/-} compared to Devic B7-H1^{+/+} mice could have been the result of even different mechanisms than in the periphery. These mechanisms might be impaired migration/homing properties of encephalitogenic CD4⁺ T cells, increased capacity to breach the BBB, enhanced CNS-specific proliferation and/or survival. Still, we also took into account that the presence of more V α 3.2⁺ V β 11⁺ CD4⁺ T cells in the periphery of Devic B7-H1^{-/-} mice due to higher proliferative tendencies and lower apoptosis rates might have “simply” entailed quantitatively higher cell numbers in the CNS as compared to Devic B7-H1^{+/+} mice. The relative contribution of proliferation and survival of encephalitogenic CD4⁺ T cells specifically occurring in the CNS was not addressed in the present study but seem potential mechanisms for augmented cell accumulation. Another potential mechanism leading to extended T-cell infiltration into the CNS of Devic B7-H1^{-/-} mice could be an enhanced migratory capacity of encephalitogenic CD4⁺ T cells. It turned out that B7-H1 deficiency on V α 3.2⁺ V β 11⁺ CD4⁺ T cells per se was neither of significance for their *in vitro* migratory nor their *in vivo* homing capacities. These findings support the hypothesis that B7-H1 expression

rather on cells of non-hematopoietic origin (e.g. endothelial cells) could play a role in mediating T-cell transmigration behavior. This, however, still has to be demonstrated in this mouse model. Nevertheless, other mechanisms involved in T-cell/endothelial cell interface and/or organ-specific homing might be altered in Devic B7-H1^{-/-} mice leading to enhanced BBB crossing capacities of encephalitogenic CD4⁺ T cells and, consequently, increased accumulation. This should be investigated in further detail, for example in *in vitro* endothelial layer migration experiments or adoptive transfer experiments in RAG^{-/-} x B7-H1^{-/-} mice.

It has been concluded from studies on actively induced CNS autoimmunity that early priming of neuroantigen-specific CD4⁺ T cells takes place in peripheral lymphoid organs whereupon they proliferate, differentiate into effector T cells, increasingly express a set of activation markers, cytokine and chemokine receptors and adhesion molecules which facilitate the transmigration via the BBB. Re-activation of encephalitogenic CD4⁺ T cells was shown to occur within the CNS where it is conducted by CNS-resident and -infiltrating APCs presenting myelin-derived peptides under inflammatory conditions (Becher et al., 2006; Becher et al., 2000; reviewed by Zozulya et al., 2010). Our studies revealed that CNS-infiltrating Vα3.2⁺ Vβ11⁺ CD4⁺ T cells in both sick Devic B7-H1^{+/+} and sick Devic B7-H1^{-/-} mice displayed a highly activated status whereas in the periphery, activation levels were rather low. Herein, our results went in line with the analysis of T-cell activation degrees in sick Devic mice conducted by others (Bettelli et al., 2006; Krishnamoorthy et al., 2006). Even though the CNS has long been regarded as an immune-privileged organ, it was recently hypothesized that it is immunologically surveyed by non-activated lymphocytes. Adoptive transfer experiments in SJL mice undergoing PLP₁₇₈₋₁₉₁-induced R-EAE, for example, revealed that initial activation of naïve PLP-specific T cells exclusively occurred in the CNS but not in peripheral lymphoid organs (McMahon et al., 2005). Accordingly, the exact site of initial CD4⁺ T-cell activation could not be identified in Devic B7-H1^{+/+} and Devic B7-H1^{-/-} mice in the present study. However, our findings suggest that a re-activation process of myelin-specific CD4⁺ T cells took place in the CNS of Devic B7-H1^{+/+} and Devic B7-H1^{-/-} mice during the course of the disease. In CNS lesions of sick Devic B7-H1^{-/-} mice, Vα3.2⁺ Vβ11⁺ CD4⁺ T cells did not only accumulate to a higher extent but also exhibited higher activation levels than in sick Devic B7-H1^{+/+} mice at maximum of the EAE-like disease. Additionally, more CNS-

infiltrating MOG-specific CD4⁺ T cells in sick Devic B7-H1^{-/-} showed Th1 effector functions than in sick Devic B7-H1^{+/+} mice. As at this stage of the disease these differences in activation levels were not observed in the periphery, our findings suggest that CNS-specific B7-H1 expression could well play a relevant role in counterbalancing local autoimmune T-cell responses and thereby contributes to the confinement of the immunopathological tissue damage in Devic B7-H1^{+/+} mice mirrored by lower disease scores. Adoptive transfer experiments using RAG-1^{-/-} mice as recipients reconfirmed the CNS as the principal CD4⁺ T-cell (re-) activation site since elevated levels of activation were only found in CNS-infiltrating V α 3.2⁺ V β 11⁺ CD4⁺ T cells whereas in secondary lymphoid organs they remained largely naïve. As encephalitogenic V α 3.2⁺ V β 11⁺ CD4⁺ T cells exhibited the same activation and Th differentiation degrees independently of which donors they derived of, we assumed that most likely the expression of B7-H1 on transferred encephalitogenic CD4⁺ T cells themselves did not have any larger impact on these processes within the target tissue. Therefore, we concluded that B7-H1 expression on host-derived non-hematopoietic tissue might be more relevant in mediating T-cell entry and activation in the CNS. Although in the present study we did not elucidate this possibility in more detail, others have shown that expression of B7-H1 on professional CNS-located APCs exerted important immune-regulatory functions by controlling the re-activation of encephalitogenic CD4⁺ T cells in the CNS during the effector phase of murine EAE (Magnus et al., 2005; Salama et al., 2003; Schreiner et al., 2008; Schreiner et al., 2004). Accumulating evidence suggests that B7-H1 expression on CNS-located APCs is even induced during ongoing neuroinflammatory processes thereby maximizing its inhibitory effect. Schreiner et al., for example, demonstrated that B7-H1 was significantly up-regulated by various CNS-infiltrating and -permanent APCs during inflammatory processes and negatively regulated T-cell re-activation during acute relapsing EAE in SJL/J mice (Schreiner et al., 2008). With respect to the adoptive transfer experiments in RAG-1^{-/-} recipient mice used in the present study, B7-H1 expression is presumably “normal” on professional CNS-resident APCs as well as on parenchymal cells such as endothelial cells and therefore very likely influences the (re-) activation of both infiltrating V α 3.2⁺ V β 11⁺ CD4⁺ B7-H1^{-/-} and V α 3.2⁺ V β 11⁺ CD4⁺ B7-H1^{+/+} T cells to the same degree. Concerning the spontaneous EAE model Devic mouse, we concluded that (induced) B7-H1 expression within the CNS of Devic B7-H1^{+/+} mice likely restricted T-cell (re-) activation and differentiation and thereby

potentially led to a less severe disease progression compared to Devic B7-H1^{-/-} mice.

Since CD4⁺ Foxp3⁺ regulatory T cells have been attributed strong immune-inhibitory properties, we sought to elucidate whether altered Treg induction and infiltration into the CNS could play a role in the disease induction. According to the flow-cytometric analysis of Treg cells within CNS-infiltrating mononuclear cells, we concluded that the Treg compartment was not affected by the B7-H1 deficiency and did not contribute to the lower activation levels of encephalitogenic CD4⁺ T cells in the CNS of Devic B7-H1^{-/-} mice. Moreover, antibody-secretion by IgH^{MOG}-transgenic B cells seemed not to be influenced by B7-H1 deficiency. Therefore, we concluded that Devic B7-H1^{-/-} mice have no major alterations in their humoral immunity compared to Devic B7-H1^{+/+} mice that could have contributed to the differences in the clinical course of the EAE-like disease.

It is highly likely that the subtle role of B7-H1 is masked by the full-blown autoimmune inflammatory processes within the CNS parenchyma at disease. If this was the case, the role of B7-H1 is likely more pronounced during the initiation of the disease when T cell priming, early inflammatory processes and BBB collapse take place. This assumption is further supported by the fact that peripheral CD4⁺ T cells of young, symptom-free Devic B7-H1^{-/-} mice, indeed, exhibited high LFA-1 expression levels and thereby differed significantly from CD4⁺ T cells of non-diseased Devic B7-H1^{+/+} mice. The engagement of the β 2-intergrin LFA-1 expressed on the surface of encephalitogenic T cells with its ligands ICAM-1 and/or ICAM-2 expressed on endothelial cells of CNS microvessels was proven to be crucial for transendothelial migration (Laschinger et al., 2002). Based on this, we hypothesized that the enhanced LFA-1 expression in young Devic B7-H1^{-/-} mice could at least partly contribute to earlier disease onset via a mechanism mediated by B7-H1 deficiency that, however, still has to be elucidated. This effect, however, might become less pronounced when full blown inflammation takes place. This view was supported by the fact that we observed similarly high LFA-1 expression of encephalitogenic CD4⁺ T cells in Devic B7-H1^{+/+} and Devic B7-H1^{-/-} mice at disease maximum. Therefore, we concluded that the mere absence of B7-H1 on encephalitogenic CD4⁺ T cells did likely not take major effect on the varying extents of CNS-infiltration in between Devic B7-H1^{+/+} and Devic B7-H1^{-/-} mice. However, temporal differences in the induction of LFA-1 could have facilitated migration of V α 3.2⁺ V β 11⁺ CD4⁺ T cells at an earlier time point during the preclinical phase in

Devic B7-H1^{-/-} mice.

In analogy to induced EAE models, MOG-specific Th1 and Th17 CD4⁺ effector T cells are regarded as major players in the progression of murine Devic-like disease. Noteworthy, however, MOG-specific B cells have been shown to significantly contribute to the pathogenesis of the EAE-like disease in Devic mice, too (Bettelli et al., 2006; Krishnamoorthy et al., 2006). More severe EAE courses observed in B7-H1^{-/-} mice have commonly been attributed to a consistently - in the preclinical and/or the clinical phase - enhanced proinflammatory T-cell responses (Carter et al., 2007; Latchman et al., 2004). Kinetics studies by Ortler et al. revealed that lack of B7-H1 accelerated the differentiation of peripheral autoreactive T cells into Th1 and Th17 effector T-cell subsets in B7-H1^{-/-} compared to B7-H1^{+/+} mice exclusively during the early phase of EAE (Ortler et al., 2008). In contrast, though, others showed that the interruption of the PD-1/B7-H1 pathway by PD-1-blocking monoclonal antibodies significantly raised the peripheral proinflammatory Th1 T-cell responses in C57BL/6 mice undergoing MOG₃₅₋₅₅-induced EAE especially at disease maximum (Salama et al., 2003). In the present study, the Th1 and Th17 effector function of peripheral T cells were comparable in Devic B7-H1^{+/+} and Devic B7-H1^{-/-} mice at peak of the EAE-like disease. However, higher Th1 immune responses were detected in young, symptom-free Devic B7-H1^{-/-} mice as compared to Devic B7-H1^{+/+} mice. As this finding correlates with the accelerated disease onset observed in Devic B7-H1^{-/-} mice, we assumed that lack of B7-H1 might have facilitated the differentiation of peripheral antigen-specific CD4⁺ T cells into Th1 effector T cells during the early (initiation) phase of the disease. Although needed to be further evaluated, similar Th1 and Th17 T-cell responses in diseased mice suggested that the lack of B7-H1 did obviously not affect T-cell differentiation to the same degree during the clinical phase. This effect might be conditioned by higher amounts of autoantigen sequestered in the CNS due to abundantly ongoing inflammatory processes elicited by activated immune cells. As shown by Latchmann et al., B7-H1 on APCs exerted its inhibitory functions on T-cell activation most effectively at low doses of available antigen (Latchman et al., 2004). Therefore, we assumed that Th1 CD4⁺ T cells took fully effect and contributed to disease induction in Devic B7-H1^{+/+} mice as soon as the inhibitory effect of B7-H1 was overcome by high presence of antigen. Conversely, attenuation of disease-governing Th1 immune responses by B7-H1 would then have caused the delayed onset in Devic

B7-H1^{+/+} compared to Devic B7-H1^{-/-} mice.

Although many questions still miss definite answers, the present study provided evidence that B7-H1 exerted an immune-regulatory and disease modifying function in the transgenic model for spontaneous autoimmune neuroinflammation - the Devic mouse model. Our observations indicated that B7-H1 likely plays role at multiple levels, i.e. milder phenotypes, and that many of its effects might be important in modulating the initiation as well as the clinical phase of the disease. As a model for spontaneous immunity featuring a nearly 100 % incidence rate, the Devic B7-H1^{-/-} mouse may prove instrumental in clarifying disease-limiting factors and in validating novel therapeutic approaches for CNS autoimmunity, in particular the human NMO.

8 Abbreviation Directory

A. dest.	aqua destillata
APC	antigen-presenting cell
APC	allophycocyanin
B7-H1	B7 homologue 1
B7-DC	B7 family member whose expression was allocated to DCs
BBB	blood-brain-barrier
BCR	B-cell receptor
bp	base pairs
BSA	bovine serum albumin
CBA	cytokine bead array
CCL	chemokine receptor ligand
CCR	chemokine receptor
CD	cluster of differentiation
CFA	complete Freund's adjuvant
CNS	central nervous system
cpm	counts per minute
CTL	cytotoxic T lymphocytes
DAB	diaminobenzidine
DC	dendritic cell
DMSO	dimethyl sulfoxide
DN	double-negative
DNA	desoxyribonucleic acid
DP	double-positive
d.p.i.	days post-injection
EAE	experimental autoimmune encephalomyelitis
ELISA	enzyme-linked immunoabsorbent assay
FACS	fluorescence-activated cell sorting
FasL	Fas ligand
FCS	fetal calf serum
Fig.	figure
FITC	fluorescein isothiocyanate
FoxP3	forkhead box P3
GM-CSF	granulocyte-macrophage colony-stimulating factor
h	hour
HRP	horseradish peroxidase
ICCS	intracellular cytokine staining
ICOS	inducible co-stimulator
IFN	interferon
Ig	immunoglobulin
IgH ^{MOG}	transgenic MOG-specific Ig heavy chain knock-in

ITIM	immunoreceptor tyrosine-based inhibitory motif
ITSM	immunoreceptor tyrosine-based switch motif
ko	knock-out
IL	interleukin
i.p.	intraperitoneal
i.v.	intravenous
LN	lymph node
LPS	lipopolysaccharide
MBP	myelin basic protein
MHC	major histocompatibility complex
min	minutes
MOG	myelin oligodendrocyte glycoprotein
MS	multiple sclerosis
NK cells	natural killer cells
NMO	neuromyelitis optica
NOD	non-obese diabetic
OD	optical density
OSE	opticospinal EAE
OSMS	opticospinal MS
OT-I	transgenic ovalbumin-specific TCR
PBS	phosphate buffered saline
PCR	polymerase chain reaction
PD-1	programmed death-1
PD-L	programmed death-1 ligand
PE	phycoerythrocin
PerCP	peridinin chlorophyll protein
PLC	phospholipase C
PLP	proteolipid protein
PS	phosphatidylserine
RAG	recombination-activating gene
RA	rheumatoid arthritis
R-EAE	relapsing EAE
RNA	ribonucleic acid
rpm	rounds per minute
RT	room temperature
SCID	severe combined immunodeficiency
SD	standard deviation
SLE	systemic lupus erythematosus
SN	single-negative
SNP	single nucleotide polymorphism
SPF	specific pathogen-free
Tab.	table
TCR	T-cell receptor

TCR ^{MOG}	transgenic MOG-specific TCR
Th	T helper (cell)
TGF	transforming growth factor
TLR	toll-like receptor
TMB	tetramethylbenzidine
TNF- α	tumor necrosis factor α
Treg	regulatory T cell
U	units
vs.	versus
wt	wild type

9 References

- Abbas, A.K., K.M. Murphy, and A. Sher. 1996. Functional diversity of helper T lymphocytes. *Nature* 383:787-793.
- Agata, Y., A. Kawasaki, H. Nishimura, Y. Ishida, T. Tsubata, H. Yagita, and T. Honjo. 1996. Expression of the PD-1 antigen on the surface of stimulated mouse T and B lymphocytes. *International immunology* 8:765-772.
- Albert, L.J., and R.D. Inman. 1999. Molecular mimicry and autoimmunity. *The New England journal of medicine* 341:2068-2074.
- Amiry-Moghaddam, M., D.S. Frydenlund, and O.P. Ottersen. 2004. Anchoring of aquaporin-4 in brain: molecular mechanisms and implications for the physiology and pathophysiology of water transport. *Neuroscience* 129:999-1010.
- Anderton, S.M., and D.C. Wraith. 2002. Selection and fine-tuning of the autoimmune T-cell repertoire. *Nature reviews. Immunology* 2:487-498.
- Ansari, M.J., A.D. Salama, T. Chitnis, R.N. Smith, H. Yagita, H. Akiba, T. Yamazaki, M. Azuma, H. Iwai, S.J. Khoury, H. Auchincloss, Jr., and M.H. Sayegh. 2003. The programmed death-1 (PD-1) pathway regulates autoimmune diabetes in nonobese diabetic (NOD) mice. *The Journal of experimental medicine* 198:63-69.
- Asgari, N., T. Owens, J. Frokiaer, E. Stenager, S.T. Lillevang, and K.O. Kyvik. 2011. Neuromyelitis optica (NMO)--an autoimmune disease of the central nervous system (CNS). *Acta neurologica Scandinavica* 123:369-384.
- Babbe, H., A. Roers, A. Waisman, H. Lassmann, N. Goebels, R. Hohlfeld, M. Friese, R. Schroder, M. Deckert, S. Schmidt, R. Ravid, and K. Rajewsky. 2000. Clonal expansions of CD8(+) T cells dominate the T cell infiltrate in active multiple sclerosis lesions as shown by micromanipulation and single cell polymerase chain reaction. *The Journal of experimental medicine* 192:393-404.
- Baecher-Allan, C., J.A. Brown, G.J. Freeman, and D.A. Hafler. 2003. CD4+CD25+ regulatory cells from human peripheral blood express very high levels of CD25 ex vivo. *Novartis Foundation symposium* 252:67-88; discussion 88-91, 106-114.
- Balashov, K.E., J.B. Rottman, H.L. Weiner, and W.W. Hancock. 1999. CCR5(+) and CXCR3(+) T cells are increased in multiple sclerosis and their ligands MIP-

- 1alpha and IP-10 are expressed in demyelinating brain lesions. *Proceedings of the National Academy of Sciences of the United States of America* 96:6873-6878.
- Baron, J.L., J.A. Madri, N.H. Ruddle, G. Hashim, and C.A. Janeway, Jr. 1993. Surface expression of alpha 4 integrin by CD4 T cells is required for their entry into brain parenchyma. *The Journal of experimental medicine* 177:57-68.
- Becher, B., I. Bechmann, and M. Greter. 2006. Antigen presentation in autoimmunity and CNS inflammation: how T lymphocytes recognize the brain. *J Mol Med (Berl)* 84:532-543.
- Becher, B., M. Blain, and J.P. Antel. 2000. CD40 engagement stimulates IL-12 p70 production by human microglial cells: basis for Th1 polarization in the CNS. *Journal of neuroimmunology* 102:44-50.
- Ben-Nun, A., H. Wekerle, and I.R. Cohen. 1981. The rapid isolation of clonable antigen-specific T lymphocyte lines capable of mediating autoimmune encephalomyelitis. *European journal of immunology* 11:195-199.
- Bennett, F., D. Luxenberg, V. Ling, I.M. Wang, K. Marquette, D. Lowe, N. Khan, G. Veldman, K.A. Jacobs, V.E. Valge-Archer, M. Collins, and B.M. Carreno. 2003. Program death-1 engagement upon TCR activation has distinct effects on costimulation and cytokine-driven proliferation: attenuation of ICOS, IL-4, and IL-21, but not CD28, IL-7, and IL-15 responses. *J Immunol* 170:711-718.
- Berer, K., M. Mues, M. Koutrolos, Z.A. Rasbi, M. Boziki, C. Johner, H. Wekerle, and G. Krishnamoorthy. 2011. Commensal microbiota and myelin autoantigen cooperate to trigger autoimmune demyelination. *Nature* 479:538-541.
- Bettelli, E., D. Baeten, A. Jager, R.A. Sobel, and V.K. Kuchroo. 2006. Myelin oligodendrocyte glycoprotein-specific T and B cells cooperate to induce a Devic-like disease in mice. *The Journal of clinical investigation* 116:2393-2402.
- Bettelli, E., M. Pagany, H.L. Weiner, C. Lington, R.A. Sobel, and V.K. Kuchroo. 2003. Myelin oligodendrocyte glycoprotein-specific T cell receptor transgenic mice develop spontaneous autoimmune optic neuritis. *The Journal of experimental medicine* 197:1073-1081.
- Bluestone, J.A. 1995. New perspectives of CD28-B7-mediated T cell costimulation. *Immunity* 2:555-559.
- Bretscher, P.A. 1999. A two-step, two-signal model for the primary activation of

- precursor helper T cells. *Proceedings of the National Academy of Sciences of the United States of America* 96:185-190.
- Bromley, S.K., W.R. Burack, K.G. Johnson, K. Somersalo, T.N. Sims, C. Sumen, M.M. Davis, A.S. Shaw, P.M. Allen, and M.L. Dustin. 2001. The immunological synapse. *Annual review of immunology* 19:375-396.
- Butte, M.J., M.E. Keir, T.B. Phamduy, A.H. Sharpe, and G.J. Freeman. 2007. Programmed death-1 ligand 1 interacts specifically with the B7-1 costimulatory molecule to inhibit T cell responses. *Immunity* 27:111-122.
- Cannella, B., and C.S. Raine. 1995. The adhesion molecule and cytokine profile of multiple sclerosis lesions. *Annals of neurology* 37:424-435.
- Carter, L., L.A. Fouser, J. Jussif, L. Fitz, B. Deng, C.R. Wood, M. Collins, T. Honjo, G.J. Freeman, and B.M. Carreno. 2002. PD-1:PD-L inhibitory pathway affects both CD4(+) and CD8(+) T cells and is overcome by IL-2. *European journal of immunology* 32:634-643.
- Carter, L.L., M.W. Leach, M.L. Azoitei, J. Cui, J.W. Pelker, J. Jussif, S. Benoit, G. Ireland, D. Luxenberg, G.R. Askew, K.L. Milarski, C. Groves, T. Brown, B.A. Carito, K. Percival, B.M. Carreno, M. Collins, and S. Marusic. 2007. PD-1/PD-L1, but not PD-1/PD-L2, interactions regulate the severity of experimental autoimmune encephalomyelitis. *Journal of neuroimmunology* 182:124-134.
- Chambers, C.A. 2001. The expanding world of co-stimulation: the two-signal model revisited. *Trends in immunology* 22:217-223.
- Chemnitz, J.M., R.V. Parry, K.E. Nichols, C.H. June, and J.L. Riley. 2004. SHP-1 and SHP-2 associate with immunoreceptor tyrosine-based switch motif of programmed death 1 upon primary human T cell stimulation, but only receptor ligation prevents T cell activation. *J Immunol* 173:945-954.
- Chen, L. 2004. Co-inhibitory molecules of the B7-CD28 family in the control of T-cell immunity. *Nature reviews. Immunology* 4:336-347.
- Chen, W., W. Jin, N. Hardegen, K.J. Lei, L. Li, N. Marinos, G. McGrady, and S.M. Wahl. 2003. Conversion of peripheral CD4+CD25- naive T cells to CD4+CD25+ regulatory T cells by TGF-beta induction of transcription factor Foxp3. *The Journal of experimental medicine* 198:1875-1886.
- Compston, A. 1999. The genetic epidemiology of multiple sclerosis. *Philos Trans R Soc Lond B Biol Sci* 354:1623-1634.

- Compston, A., and A. Coles. 2002. Multiple sclerosis. *Lancet* 359:1221-1231.
- Confavreux, C., S. Vukusic, T. Moreau, and P. Adeleine. 2000. Relapses and Progression of Disability in Multiple Sclerosis. *New England Journal of Medicine* 343:1430-1438.
- Constant, S., C. Pfeiffer, A. Woodard, T. Pasqualini, and K. Bottomly. 1995. Extent of T cell receptor ligation can determine the functional differentiation of naive CD4+ T cells. *The Journal of experimental medicine* 182:1591-1596.
- Correale, J., and M. de los Milagros Bassani Molinas. 2002. Oligoclonal bands and antibody responses in multiple sclerosis. *J Neurol* 249:375-389.
- Cruz-Orengo, L., D.W. Holman, D. Dorsey, L. Zhou, P. Zhang, M. Wright, E.E. McCandless, J.R. Patel, G.D. Luker, D.R. Littman, J.H. Russell, and R.S. Klein. 2011. CXCR7 influences leukocyte entry into the CNS parenchyma by controlling abluminal CXCL12 abundance during autoimmunity. *The Journal of experimental medicine* 208:327-339.
- Curotto de Lafaille, M.A., and J.J. Lafaille. 2009. Natural and adaptive foxp3+ regulatory T cells: more of the same or a division of labor? *Immunity* 30:626-635.
- Das Sarma, J. 2010. A mechanism of virus-induced demyelination. *Interdisciplinary perspectives on infectious diseases* 2010:109239.
- de la Rosa, M., S. Rutz, H. Dorninger, and A. Scheffold. 2004. Interleukin-2 is essential for CD4+CD25+ regulatory T cell function. *European journal of immunology* 34:2480-2488.
- Dempsey, P.W., S.A. Vaidya, and G. Cheng. 2003. The art of war: Innate and adaptive immune responses. *Cellular and molecular life sciences : CMLS* 60:2604-2621.
- Devic, M.E. 1895. Mye'lite subaigue complique'e de ne'vrite optique. *Bull. Méd.* 8:1033-1034.
- Dittel, B.N. 2008. CD4 T cells: Balancing the coming and going of autoimmune-mediated inflammation in the CNS. *Brain, behavior, and immunity* 22:421-430.
- Dong, C. 2008. TH17 cells in development: an updated view of their molecular identity and genetic programming. *Nature reviews. Immunology* 8:337-348.
- Dong, H., S.E. Strome, E.L. Matteson, K.G. Moder, D.B. Flies, G. Zhu, H. Tamura, C.L. Driscoll, and L. Chen. 2003. Costimulating aberrant T cell responses by B7-H1 autoantibodies in rheumatoid arthritis. *The Journal of clinical*

- investigation* 111:363-370.
- Dong, H., S.E. Strome, D.R. Salomao, H. Tamura, F. Hirano, D.B. Flies, P.C. Roche, J. Lu, G. Zhu, K. Tamada, V.A. Lennon, E. Celis, and L. Chen. 2002. Tumor-associated B7-H1 promotes T-cell apoptosis: a potential mechanism of immune evasion. *Nature medicine* 8:793-800.
- Dong, H., G. Zhu, K. Tamada, and L. Chen. 1999. B7-H1, a third member of the B7 family, co-stimulates T-cell proliferation and interleukin-10 secretion. *Nature medicine* 5:1365-1369.
- Dopp, J.M., S.M. Breneman, and J.A. Olschowka. 1994. Expression of ICAM-1, VCAM-1, L-selectin, and leukosialin in the mouse central nervous system during the induction and remission stages of experimental allergic encephalomyelitis. *Journal of neuroimmunology* 54:129-144.
- Engelhardt, B. 2006. Molecular mechanisms involved in T cell migration across the blood-brain barrier. *J Neural Transm* 113:477-485.
- Fearon, D.T., and R.M. Locksley. 1996. The instructive role of innate immunity in the acquired immune response. *Science* 272:50-53.
- Fife, B.T., M.C. Paniagua, N.W. Lukacs, S.L. Kunkel, and W.J. Karpus. 2001. Selective CC chemokine receptor expression by central nervous system-infiltrating encephalitogenic T cells during experimental autoimmune encephalomyelitis. *Journal of neuroscience research* 66:705-714.
- Fontenot, J.D., M.A. Gavin, and A.Y. Rudensky. 2003. Foxp3 programs the development and function of CD4⁺CD25⁺ regulatory T cells. *Nature immunology* 4:330-336.
- Francisco, L.M., P.T. Sage, and A.H. Sharpe. 2010. The PD-1 pathway in tolerance and autoimmunity. *Immunological reviews* 236:219-242.
- Francisco, L.M., V.H. Salinas, K.E. Brown, V.K. Vanguri, G.J. Freeman, V.K. Kuchroo, and A.H. Sharpe. 2009. PD-L1 regulates the development, maintenance, and function of induced regulatory T cells. *The Journal of experimental medicine* 206:3015-3029.
- Freeman, G.J., A.J. Long, Y. Iwai, K. Bourque, T. Chernova, H. Nishimura, L.J. Fitz, N. Malenkovich, T. Okazaki, M.C. Byrne, H.F. Horton, L. Fouser, L. Carter, V. Ling, M.R. Bowman, B.M. Carreno, M. Collins, C.R. Wood, and T. Honjo. 2000. Engagement of the PD-1 immunoinhibitory receptor by a novel B7 family

- member leads to negative regulation of lymphocyte activation. *The Journal of experimental medicine* 192:1027-1034.
- Fu, S.M., U.S. Deshmukh, and F. Gaskin. 2011. Pathogenesis of systemic lupus erythematosus revisited 2011: end organ resistance to damage, autoantibody initiation and diversification, and HLA-DR. *Journal of autoimmunity* 37:104-112.
- Garcia-Vicuna, R., M.V. Gomez-Gavira, M.J. Dominguez-Luis, M.K. Pec, I. Gonzalez-Alvaro, J.M. Alvaro-Gracia, and F. Diaz-Gonzalez. 2004. CC and CXC chemokine receptors mediate migration, proliferation, and matrix metalloproteinase production by fibroblast-like synoviocytes from rheumatoid arthritis patients. *Arthritis and rheumatism* 50:3866-3877.
- Ghoreschi, K., A. Laurence, X.P. Yang, K. Hirahara, and J.J. O'Shea. 2011. T helper 17 cell heterogeneity and pathogenicity in autoimmune disease. *Trends in immunology* 32:395-401.
- Gold, R., C. Linington, and H. Lassmann. 2006. Understanding pathogenesis and therapy of multiple sclerosis via animal models: 70 years of merits and culprits in experimental autoimmune encephalomyelitis research. *Brain : a journal of neurology* 129:1953-1971.
- Goverman, J. 2009. Autoimmune T cell responses in the central nervous system. *Nature reviews. Immunology* 9:393-407.
- Goverman, J., A. Woods, L. Larson, L.P. Weiner, L. Hood, and D.M. Zaller. 1993. Transgenic mice that express a myelin basic protein-specific T cell receptor develop spontaneous autoimmunity. *Cell* 72:551-560.
- Goverman, J.M. 2011. Immune tolerance in multiple sclerosis. *Immunological reviews* 241:228-240.
- Guo, F., C. Iclozan, W.K. Suh, C. Anasetti, and X.Z. Yu. 2008. CD28 controls differentiation of regulatory T cells from naive CD4 T cells. *J Immunol* 181:2285-2291.
- Gutcher, I., and B. Becher. 2007. APC-derived cytokines and T cell polarization in autoimmune inflammation. *The Journal of clinical investigation* 117:1119-1127.
- Hori, S., T. Nomura, and S. Sakaguchi. 2003. Control of regulatory T cell development by the transcription factor Foxp3. *Science* 299:1057-1061.
- Iezzi, G., K. Karjalainen, and A. Lanzavecchia. 1998. The duration of antigenic

- stimulation determines the fate of naive and effector T cells. *Immunity* 8:89-95.
- Ishida, M., Y. Iwai, Y. Tanaka, T. Okazaki, G.J. Freeman, N. Minato, and T. Honjo. 2002. Differential expression of PD-L1 and PD-L2, ligands for an inhibitory receptor PD-1, in the cells of lymphohematopoietic tissues. *Immunology letters* 84:57-62.
- Ishida, Y., Y. Agata, K. Shibahara, and T. Honjo. 1992. Induced expression of PD-1, a novel member of the immunoglobulin gene superfamily, upon programmed cell death. *The EMBO journal* 11:3887-3895.
- Iwai, Y., M. Ishida, Y. Tanaka, T. Okazaki, T. Honjo, and N. Minato. 2002. Involvement of PD-L1 on tumor cells in the escape from host immune system and tumor immunotherapy by PD-L1 blockade. *Proceedings of the National Academy of Sciences of the United States of America* 99:12293-12297.
- Izikson, L., R.S. Klein, I.F. Charo, H.L. Weiner, and A.D. Luster. 2000. Resistance to experimental autoimmune encephalomyelitis in mice lacking the CC chemokine receptor (CCR)2. *The Journal of experimental medicine* 192:1075-1080.
- Jäger, A., V. Dardalhon, R.A. Sobel, E. Bettelli, and V.K. Kuchroo. 2009. Th1, Th17, and Th9 Effector Cells Induce Experimental Autoimmune Encephalomyelitis with Different Pathological Phenotypes. *The Journal of Immunology* 183:7169-7177.
- Jager, A., and V.K. Kuchroo. 2010. Effector and regulatory T-cell subsets in autoimmunity and tissue inflammation. *Scandinavian journal of immunology* 72:173-184.
- Janeway, C.A., Jr., and R. Medzhitov. 2002. Innate immune recognition. *Annual review of immunology* 20:197-216.
- Jordan, M.S., A. Boesteanu, A.J. Reed, A.L. Petrone, A.E. Hosenbeck, M.A. Lerman, A. Naji, and A.J. Caton. 2001. Thymic selection of CD4+CD25+ regulatory T cells induced by an agonist self-peptide. *Nature immunology* 2:301-306.
- Kanai, T., T. Totsuka, K. Uraushihara, S. Makita, T. Nakamura, K. Koganei, T. Fukushima, H. Akiba, H. Yagita, K. Okumura, U. Machida, H. Iwai, M. Azuma, L. Chen, and M. Watanabe. 2003. Blockade of B7-H1 suppresses the development of chronic intestinal inflammation. *J Immunol* 171:4156-4163.
- Karpus, W.J., N.W. Lukacs, B.L. McRae, R.M. Strieter, S.L. Kunkel, and S.D. Miller. 1995. An important role for the chemokine macrophage inflammatory protein-1

- alpha in the pathogenesis of the T cell-mediated autoimmune disease, experimental autoimmune encephalomyelitis. *J Immunol* 155:5003-5010.
- Keir, M.E., M.J. Butte, G.J. Freeman, and A.H. Sharpe. 2008. PD-1 and its ligands in tolerance and immunity. *Annual review of immunology* 26:677-704.
- Keir, M.E., G.J. Freeman, and A.H. Sharpe. 2007. PD-1 regulates self-reactive CD8+ T cell responses to antigen in lymph nodes and tissues. *J Immunol* 179:5064-5070.
- Keir, M.E., Y.E. Latchman, G.J. Freeman, and A.H. Sharpe. 2005. Programmed death-1 (PD-1):PD-ligand 1 interactions inhibit TCR-mediated positive selection of thymocytes. *J Immunol* 175:7372-7379.
- Keir, M.E., S.C. Liang, I. Guleria, Y.E. Latchman, A. Qipo, L.A. Albacker, M. Koulmanda, G.J. Freeman, M.H. Sayegh, and A.H. Sharpe. 2006. Tissue expression of PD-L1 mediates peripheral T cell tolerance. *The Journal of experimental medicine* 203:883-895.
- Knip, M., and H. Siljander. 2008. Autoimmune mechanisms in type 1 diabetes. *Autoimmunity reviews* 7:550-557.
- Komiyama, Y., S. Nakae, T. Matsuki, A. Nambu, H. Ishigame, S. Kakuta, K. Sudo, and Y. Iwakura. 2006. IL-17 plays an important role in the development of experimental autoimmune encephalomyelitis. *J Immunol* 177:566-573.
- Koritschoner R. S., S.F. 1925. Induktion von Paralyse und Rückenmarksentzündung durch Immunisierung von Kaninchen mit menschlichem Rückenmarksgewebe. *Z Immunitätsf Exp Therapie* 42:217-283.
- Krishnamoorthy, G., H. Lassmann, H. Wekerle, and A. Holz. 2006. Spontaneous opticospinal encephalomyelitis in a double-transgenic mouse model of autoimmune T cell/B cell cooperation. *The Journal of clinical investigation* 116:2385-2392.
- Kroner, A., M. Mehling, B. Hemmer, P. Rieckmann, K.V. Toyka, M. Maurer, and H. Wiendl. 2005. A PD-1 polymorphism is associated with disease progression in multiple sclerosis. *Annals of neurology* 58:50-57.
- Krupnick, A.S., A.E. Gelman, W. Barchet, S. Richardson, F.H. Kreisel, L.A. Turka, M. Colonna, G.A. Patterson, and D. Kreisel. 2005. Murine vascular endothelium activates and induces the generation of allogeneic CD4+25+Foxp3+ regulatory T cells. *J Immunol* 175:6265-6270.
- Lafaille, J.J., K. Nagashima, M. Katsuki, and S. Tonegawa. 1994. High incidence of

- spontaneous autoimmune encephalomyelitis in immunodeficient anti-myelin basic protein T cell receptor transgenic mice. *Cell* 78:399-408.
- Lafferty, K.J., and R.G. Gill. 1993. The maintenance of self-tolerance. *Immunol Cell Biol* 71:209-214.
- Langrish, C.L., Y. Chen, W.M. Blumenschein, J. Mattson, B. Basham, J.D. Sedgwick, T. McClanahan, R.A. Kastelein, and D.J. Cua. 2005. IL-23 drives a pathogenic T cell population that induces autoimmune inflammation. *The Journal of experimental medicine* 201:233-240.
- Laschinger, M., P. Vajkoczy, and B. Engelhardt. 2002. Encephalitogenic T cells use LFA-1 for transendothelial migration but not during capture and initial adhesion strengthening in healthy spinal cord microvessels in vivo. *European journal of immunology* 32:3598-3606.
- Lassmann, H., W. Bruck, and C.F. Lucchinetti. 2007. The immunopathology of multiple sclerosis: an overview. *Brain Pathol* 17:210-218.
- Latchman, Y., C.R. Wood, T. Chernova, D. Chaudhary, M. Borde, I. Chernova, Y. Iwai, A.J. Long, J.A. Brown, R. Nunes, E.A. Greenfield, K. Bourque, V.A. Boussiotis, L.L. Carter, B.M. Carreno, N. Malenkovich, H. Nishimura, T. Okazaki, T. Honjo, A.H. Sharpe, and G.J. Freeman. 2001. PD-L2 is a second ligand for PD-1 and inhibits T cell activation. *Nature immunology* 2:261-268.
- Latchman, Y.E., S.C. Liang, Y. Wu, T. Chernova, R.A. Sobel, M. Klemm, V.K. Kuchroo, G.J. Freeman, and A.H. Sharpe. 2004. PD-L1-deficient mice show that PD-L1 on T cells, antigen-presenting cells, and host tissues negatively regulates T cells. *Proceedings of the National Academy of Sciences of the United States of America* 101:10691-10696.
- Lennon, V.A., T.J. Kryzer, S.J. Pittock, A.S. Verkman, and S.R. Hinson. 2005. IgG marker of optic-spinal multiple sclerosis binds to the aquaporin-4 water channel. *The Journal of experimental medicine* 202:473-477.
- Levin, L.I., K.L. Munger, E.J. O'Reilly, K.I. Falk, and A. Ascherio. 2010. Primary infection with the Epstein-Barr virus and risk of multiple sclerosis. *Annals of neurology* 67:824-830.
- Liang, S.C., Y.E. Latchman, J.E. Buhlmann, M.F. Tomczak, B.H. Horwitz, G.J. Freeman, and A.H. Sharpe. 2003. Regulation of PD-1, PD-L1, and PD-L2 expression during normal and autoimmune responses. *European journal of*

- immunology* 33:2706-2716.
- Liblau, R., E. Tournier-Lasserre, J. Maciazek, G. Dumas, O. Siffert, G. Hashim, and M.A. Bach. 1991. T cell response to myelin basic protein epitopes in multiple sclerosis patients and healthy subjects. *European journal of immunology* 21:1391-1395.
- Litzenburger, T., R. Fassler, J. Bauer, H. Lassmann, C. Linington, H. Wekerle, and A. Iglesias. 1998. B lymphocytes producing demyelinating autoantibodies: development and function in gene-targeted transgenic mice. *The Journal of experimental medicine* 188:169-180.
- Lukacs, N.W., A. Berlin, D. Schols, R.T. Skerlj, and G.J. Bridger. 2002. AMD3100, a CXCR4 antagonist, attenuates allergic lung inflammation and airway hyperreactivity. *The American journal of pathology* 160:1353-1360.
- Magnus, T., B. Schreiner, T. Korn, C. Jack, H. Guo, J. Antel, I. Ifergan, L. Chen, F. Bischof, A. Bar-Or, and H. Wiendl. 2005. Microglial expression of the B7 family member B7 homolog 1 confers strong immune inhibition: implications for immune responses and autoimmunity in the CNS. *The Journal of neuroscience : the official journal of the Society for Neuroscience* 25:2537-2546.
- Manley, G.T., M. Fujimura, T. Ma, N. Noshita, F. Filiz, A.W. Bollen, P. Chan, and A.S. Verkman. 2000. Aquaporin-4 deletion in mice reduces brain edema after acute water intoxication and ischemic stroke. *Nature medicine* 6:159-163.
- Matejuk, A., A.A. Vandenbark, G.G. Burrows, B.F. Bebo, Jr., and H. Offner. 2000. Reduced chemokine and chemokine receptor expression in spinal cords of TCR BV8S2 transgenic mice protected against experimental autoimmune encephalomyelitis with BV8S2 protein. *J Immunol* 164:3924-3931.
- Matusevicius, D., P. Kivisakk, B. He, N. Kostulas, V. Ozenci, S. Fredrikson, and H. Link. 1999. Interleukin-17 mRNA expression in blood and CSF mononuclear cells is augmented in multiple sclerosis. *Mult Scler* 5:101-104.
- McMahon, E.J., S.L. Bailey, C.V. Castenada, H. Waldner, and S.D. Miller. 2005. Epitope spreading initiates in the CNS in two mouse models of multiple sclerosis. *Nature medicine* 11:335-339.
- Miller, S.D., and W.J. Karpus. 2007. Experimental autoimmune encephalomyelitis in the mouse. *Current protocols in immunology / edited by John E. Coligan ... [et*

- al.] Chapter 15:Unit 15 11.*
- Misu, T., K. Fujihara, I. Nakashima, I. Miyazawa, N. Okita, S. Takase, and Y. Itoyama. 2002. Pure optic-spinal form of multiple sclerosis in Japan. *Brain : a journal of neurology* 125:2460-2468.
- Nikolich-Zugich, J., M.K. Slifka, and I. Messaoudi. 2004. The many important facets of T-cell repertoire diversity. *Nature reviews. Immunology* 4:123-132.
- Nishimura, H., Y. Agata, A. Kawasaki, M. Sato, S. Imamura, N. Minato, H. Yagita, T. Nakano, and T. Honjo. 1996. Developmentally regulated expression of the PD-1 protein on the surface of double-negative (CD4-CD8-) thymocytes. *International immunology* 8:773-780.
- Nishimura, H., T. Honjo, and N. Minato. 2000. Facilitation of beta selection and modification of positive selection in the thymus of PD-1-deficient mice. *The Journal of experimental medicine* 191:891-898.
- Nishimura, H., N. Minato, T. Nakano, and T. Honjo. 1998. Immunological studies on PD-1 deficient mice: implication of PD-1 as a negative regulator for B cell responses. *International immunology* 10:1563-1572.
- Nishimura, H., M. Nose, H. Hiai, N. Minato, and T. Honjo. 1999. Development of lupus-like autoimmune diseases by disruption of the PD-1 gene encoding an ITIM motif-carrying immunoreceptor. *Immunity* 11:141-151.
- Okazaki, T., and T. Honjo. 2007. PD-1 and PD-1 ligands: from discovery to clinical application. *International immunology* 19:813-824.
- Olerup, O., and J. Hillert. 1991. HLA class II-associated genetic susceptibility in multiple sclerosis: a critical evaluation. *Tissue Antigens* 38:1-15.
- Ortler, S., C. Leder, M. Mittelbronn, A.L. Zozulya, P.A. Knolle, L. Chen, A. Kroner, and H. Wiendl. 2008. B7-H1 restricts neuroantigen-specific T cell responses and confines inflammatory CNS damage: implications for the lesion pathogenesis of multiple sclerosis. *European journal of immunology* 38:1734-1744.
- Petermann, F., and T. Korn. 2011. Cytokines and effector T cell subsets causing autoimmune CNS disease. *FEBS letters* 585:3747-3757.
- Petroff, M.G., L. Chen, T.A. Phillips, D. Azzola, P. Sedlmayr, and J.S. Hunt. 2003. B7 family molecules are favorably positioned at the human maternal-fetal interface. *Biology of reproduction* 68:1496-1504.
- Polman, C.H., P.W. O'Connor, E. Havrdova, M. Hutchinson, L. Kappos, D.H. Miller,

- J.T. Phillips, F.D. Lublin, G. Giovannoni, A. Wajgt, M. Toal, F. Lynn, M.A. Panzara, and A.W. Sandrock. 2006. A randomized, placebo-controlled trial of natalizumab for relapsing multiple sclerosis. *The New England journal of medicine* 354:899-910.
- Prokunina, L., C. Castillejo-Lopez, F. Oberg, I. Gunnarsson, L. Berg, V. Magnusson, A.J. Brookes, D. Tentler, H. Kristjansdottir, G. Grondal, A.I. Bolstad, E. Svenungsson, I. Lundberg, G. Sturfelt, A. Jonssen, L. Truedsson, G. Lima, J. Alcocer-Varela, R. Jonsson, U.B. Gyllensten, J.B. Harley, D. Alarcon-Segovia, K. Steinsson, and M.E. Alarcon-Riquelme. 2002. A regulatory polymorphism in PDCD1 is associated with susceptibility to systemic lupus erythematosus in humans. *Nature genetics* 32:666-669.
- Prokunina, L., I. Gunnarsson, G. Sturfelt, L. Truedsson, V.A. Seligman, J.L. Olson, M.F. Seldin, L.A. Criswell, and M.E. Alarcon-Riquelme. 2004. The systemic lupus erythematosus-associated PDCD1 polymorphism PD1.3A in lupus nephritis. *Arthritis and rheumatism* 50:327-328.
- Riley, J.L. 2009. PD-1 signaling in primary T cells. *Immunological reviews* 229:114-125.
- Robb, R.J. 1984. Interleukin 2: the molecule and its function. *Immunology today* 5:203-209.
- Rodig, N., T. Ryan, J.A. Allen, H. Pang, N. Grabie, T. Chernova, E.A. Greenfield, S.C. Liang, A.H. Sharpe, A.H. Lichtman, and G.J. Freeman. 2003. Endothelial expression of PD-L1 and PD-L2 down-regulates CD8+ T cell activation and cytotoxicity. *European journal of immunology* 33:3117-3126.
- Sakaguchi, S., T. Yamaguchi, T. Nomura, and M. Ono. 2008. Regulatory T cells and immune tolerance. *Cell* 133:775-787.
- Salama, A.D., T. Chitnis, J. Imitola, M.J. Ansari, H. Akiba, F. Tushima, M. Azuma, H. Yagita, M.H. Sayegh, and S.J. Khoury. 2003. Critical role of the programmed death-1 (PD-1) pathway in regulation of experimental autoimmune encephalomyelitis. *The Journal of experimental medicine* 198:71-78.
- Scheffold, A., J. Hühn, and T. Höfer. 2005. Regulation of CD4+CD25+ regulatory T cell activity: it takes (IL-)two to tango. *European journal of immunology* 35:1336-1341.
- Schreiner, B., S.L. Bailey, T. Shin, L. Chen, and S.D. Miller. 2008. PD-1 ligands

- expressed on myeloid-derived APC in the CNS regulate T-cell responses in EAE. *European journal of immunology* 38:2706-2717.
- Schreiner, B., M. Mitsdoerffer, B.C. Kieseier, L. Chen, H.P. Hartung, M. Weller, and H. Wiendl. 2004. Interferon-beta enhances monocyte and dendritic cell expression of B7-H1 (PD-L1), a strong inhibitor of autologous T-cell activation: relevance for the immune modulatory effect in multiple sclerosis. *Journal of neuroimmunology* 155:172-182.
- Shinohara, T., M. Taniwaki, Y. Ishida, M. Kawaichi, and T. Honjo. 1994. Structure and chromosomal localization of the human PD-1 gene (PDCD1). *Genomics* 23:704-706.
- Smith-Garvin, J.E., G.A. Koretzky, and M.S. Jordan. 2009. T cell activation. *Annual review of immunology* 27:591-619.
- Sospedra, M., and R. Martin. 2005. Immunology of multiple sclerosis. *Annual review of immunology* 23:683-747.
- Stromnes, I.M., and J.M. Goverman. 2006. Passive induction of experimental allergic encephalomyelitis. *Nature protocols* 1:1952-1960.
- Subudhi, S.K., M.L. Alegre, and Y.X. Fu. 2005. The balance of immune responses: costimulation verse coinhibition. *J Mol Med (Berl)* 83:193-202.
- Subudhi, S.K., P. Zhou, L.M. Yerian, R.K. Chin, J.C. Lo, R.A. Anders, Y. Sun, L. Chen, Y. Wang, M.L. Alegre, and Y.X. Fu. 2004. Local expression of B7-H1 promotes organ-specific autoimmunity and transplant rejection. *The Journal of clinical investigation* 113:694-700.
- Sun, J.B., T. Olsson, W.Z. Wang, B.G. Xiao, V. Kostulas, S. Fredrikson, H.P. Ekre, and H. Link. 1991. Autoreactive T and B cells responding to myelin proteolipid protein in multiple sclerosis and controls. *European journal of immunology* 21:1461-1468.
- Tsuji, S., M. Matsumoto, O. Takeuchi, S. Akira, I. Azuma, A. Hayashi, K. Toyoshima, and T. Seya. 2000. Maturation of human dendritic cells by cell wall skeleton of *Mycobacterium bovis* bacillus Calmette-Guerin: involvement of toll-like receptors. *Infect Immun* 68:6883-6890.
- Vajda, Z., M. Pedersen, E.M. Fuchtbauer, K. Wertz, H. Stodkilde-Jorgensen, E. Sulyok, T. Doczi, J.D. Neely, P. Agre, J. Frokiaer, and S. Nielsen. 2002. Delayed onset of brain edema and mislocalization of aquaporin-4 in dystrophin-null transgenic

- mice. *Proceedings of the National Academy of Sciences of the United States of America* 99:13131-13136.
- Vanderlugt, C.J., and S.D. Miller. 1996. Epitope spreading. *Current opinion in immunology* 8:831-836.
- Vermes, I., C. Haanen, H. Steffens-Nakken, and C. Reutelingsperger. 1995. A novel assay for apoptosis. Flow cytometric detection of phosphatidylserine expression on early apoptotic cells using fluorescein labelled Annexin V. *J Immunol Methods* 184:39-51.
- Wallstrom, E., M. Khademi, M. Andersson, and T. Olsson. 2000. Increased numbers of mononuclear cells from blood and CSF expressing interferon-gamma mRNA in multiple sclerosis are from both the CD4+ and the CD8+ subsets. *Eur J Neurol* 7:71-76.
- Wang, J., T. Yoshida, F. Nakaki, H. Hiai, T. Okazaki, and T. Honjo. 2005. Establishment of NOD-Pdcd1^{-/-} mice as an efficient animal model of type I diabetes. *Proceedings of the National Academy of Sciences of the United States of America* 102:11823-11828.
- Webb, L.M., and M. Feldmann. 1995. Critical role of CD28/B7 costimulation in the development of human Th2 cytokine-producing cells. *Blood* 86:3479-3486.
- Weinshenker, B.G., B. Bass, G.P. Rice, J. Noseworthy, W. Carriere, J. Baskerville, and G.C. Ebers. 1989. The natural history of multiple sclerosis: a geographically based study. I. Clinical course and disability. *Brain : a journal of neurology* 112:133-146.
- Wells, A.D., M.C. Walsh, J.A. Bluestone, and L.A. Turka. 2001. Signaling through CD28 and CTLA-4 controls two distinct forms of T cell anergy. *The Journal of clinical investigation* 108:895-903.
- Wensky, A.K., G.C. Furtado, M.C. Marcondes, S. Chen, D. Manfra, S.A. Lira, D. Zagzag, and J.J. Lafaille. 2005. IFN-gamma determines distinct clinical outcomes in autoimmune encephalomyelitis. *J Immunol* 174:1416-1423.
- Wingerchuk, D.M., W.F. Hogancamp, P.C. O'Brien, and B.G. Weinshenker. 1999. The clinical course of neuromyelitis optica (Devic's syndrome). *Neurology* 53:1107-1114.
- Yamazaki, T., H. Akiba, H. Iwai, H. Matsuda, M. Aoki, Y. Tanno, T. Shin, H. Tsuchiya, D.M. Pardoll, K. Okumura, M. Azuma, and H. Yagita. 2002.

- Expression of programmed death 1 ligands by murine T cells and APC. *J Immunol* 169:5538-5545.
- Yao, S., S. Wang, Y. Zhu, L. Luo, G. Zhu, S. Flies, H. Xu, W. Ruff, M. Broadwater, I.H. Choi, K. Tamada, and L. Chen. 2009. PD-1 on dendritic cells impedes innate immunity against bacterial infection. *Blood* 113:5811-5818.
- Zhang, X., J.C. Schwartz, X. Guo, S. Bhatia, E. Cao, M. Lorenz, M. Cammer, L. Chen, Z.Y. Zhang, M.A. Edidin, S.G. Nathenson, and S.C. Almo. 2004. Structural and functional analysis of the costimulatory receptor programmed death-1. *Immunity* 20:337-347.
- Zhou, L., M.M. Chong, and D.R. Littman. 2009. Plasticity of CD4+ T cell lineage differentiation. *Immunity* 30:646-655.
- Ziegler, S.F., F. Ramsdell, and M.R. Alderson. 1994. The activation antigen CD69. *Stem Cells* 12:456-465.
- Zozulya, A.L., B.D. Clarkson, S. Ortler, Z. Fabry, and H. Wiendl. 2010. The role of dendritic cells in CNS autoimmunity. *J Mol Med (Berl)* 88:535-544.

10 Declaration

Hiermit erkläre ich, die vorliegende Arbeit selbständig angefertigt – die immunhistologische Analyse in Kooperation mit Dr. Chi Wang Ip – und keine anderen als die angegebenen Quellen und Hilfsmittel verwendet zu haben.

Diese Arbeit hat weder in gleicher noch in ähnlicher Form in einem anderen Prüfungsverfahren vorgelegen.

Ich habe in keinem früheren Verfahren einen akademischen Titel erworben oder zu erwerben versucht.

.....

Würzburg, 2013

11 Acknowledgments

While working on my PhD degree, I experienced great support from many people: family, friends and colleagues. I owe a lot of thanks to them as they helped me through hard times, kept motivating and pushing me and thereby contributed to the realisation of this work.

First, I would like to thank Prof. Dr. Heinz Wiendl for the opportunity to do my PhD thesis at the Department of Neurology in Würzburg and to work in his team with highly motivated scientists in this interesting area of science. Despite the group moving to Münster, Prof. Wiendl made it possible for me to finish the practical work in Würzburg which I'm especially grateful about.

I would like to thank Prof. Dr. Erich Buchner, senior professor at the Institut für Klinische Neurobiologie, Universitätsklinikums Würzburg, for being the second corrector of this thesis and for his encouraging words.

I would like to thank Prof. Dr. Guido Stoll and Prof. Dr. Christoph Kleinschnitz for their support and the opportunity to participate in a very interesting project. Many thanks to Dr. Peter Kraft for his commitment and the pleasant cooperation in our common project.

I owe many thanks to my supervisor Dr. Vilmos Posevitz for his commitment, endurance and patience, helpful suggestions and discussions during our common time at the AG Wiendl. I am especially grateful for his comments and reviews of my thesis and his motivating words during good and bad times.

I would like to thank Dr. Chi Wang Ip for the helpful and pleasant cooperation in the performance of the immunohistochemical analyses.

I would like to thank Prof. Dr. Rudolf Martini for his support concerning "animal housing" issues.

Regarding animal housing, breeding and coordination and performance of challenging tasks beyond, for example embryo transfers etc., Helga Brünner and Jacqueline Schreiber did an excellent job. Many thanks to them!

I am very grateful to my “Flachbau” colleagues who created a lovely, encouraging and sometimes challenging atmosphere. “Thank you very much!” for all the support I received from the team.

“Thank you very much!”, Dr. Hakim Bouterfa, for giving me the chance to make my first steps in clinical research and development at OPS and for being so supportive and patient regarding this thesis.

And finally, I need to thank my loved family, especially my auntie Ulrike, and my friends, especially Dr. Christiane Albert-Weißberger, for their enormous support over the last years.

12 Curriculum Vitae

Angela Dreykluft
 Martin-Luther-Str. 5
 97072 Würzburg
 Deutschland
 Angela.Dreykluft@web.de

Geburtsdatum: 25.11.1980
 Geburtsort: Würzburg

Ausbildung

06/2000 Abitur am Kaiser-Heinrich-Gymnasium, Bamberg
 03/2001 Studium der Humanmedizin, Westfälische-Wilhelms-Universität
 - 9/2003 Münster
 03/2003 Physikum an der Westfälischen-Wilhelms-Universität Münster
 10/2003 Bachelorstudium der Biomedizin an der Bayerischen
 -06/2005 Julius-Maximilian-Universität Würzburg
 Bachelor-Thesis: „Molekulare Analyse Antikörper-induzierter
 Lipotoxizität“, Prof. Dr. P. Vollmers, Pathologie der Universität
 Würzburg
 10/2005 Masterstudium der Biomedizin an der Bayerischen Julius- Maximilian-
 -08/2007 Universität Würzburg
 Master-Thesis: “Characterisation of immunomodulatory effects of
 monocyte-derived cells: Relevance for suppressing unwanted immune
 responses?”, Prof. Dr. Ch. Otto, Experimentelle Transplantations-
 Immunologie, Zentrum für Operative Medizin Würzburg

Beschäftigungsverhältnisse

10/2007 wissenschaftliche Mitarbeiterin, Neurologische Klinik und Poliklinik,
 -10/2011 Universitätsklinik Würzburg
 11/2011 Projektassistentin Klinische Forschung, OctreoPharm Sciences
 -heute GmbH, Würzburg

.....
 Würzburg, 2013

13 Publications

Articles

Kleinschnitz C, Kraft P, Dreykluft A, Hagedorn I, Göbel K, Schuhmann MK, Langhauser F, Helluy X, Schwarz T, Bittner S, Mayer CT, Brede M, Varallyay C, Pham M, Bendszus M, Jakob P, Magnus T, Meuth SG, Iwakura Y, Zerneck A, Sparwasser T, Nieswandt B, Stoll G, Wiendl H. 2012. Regulatory T cells are strong promoters of acute ischemic stroke in mice by inducing dysfunction of the cerebral microvasculature. *Blood* 15:15.

Gobel, K., S. Bittner, N. Melzer, S. Pankratz, A. Dreykluft, M.K. Schuhmann, S.G. Meuth, and H. Wiendl. 2012. CD4(+) CD25(+) FoxP3(+) regulatory T cells suppress cytotoxicity of CD8(+) effector T cells: implications for their capacity to limit inflammatory central nervous system damage at the parenchymal level. *Journal of neuroinflammation* 9:41

Kleinschnitz, C., N. Schwab, P. Kraft, I. Hagedorn, A. Dreykluft, T. Schwarz, M. Austinat, B. Nieswandt, H. Wiendl, and G. Stoll. 2010. Early detrimental T-cell effects in experimental cerebral ischemia are neither related to adaptive immunity nor thrombus formation. *Blood* 115:3835-3842.

Brandlein, S., N. Rauschert, L. Rasche, A. Dreykluft, F. Hensel, E. Conzelmann, H.K. Muller-Hermelink, and H.P. Vollmers. 2007. The human IgM antibody SAM-6 induces tumor-specific apoptosis with oxidized low-density lipoprotein. *Molecular cancer therapeutics* 6:326-333.

Muller, M., S.L. Carter, M.J. Hofer, P. Manders, D.R. Getts, M.T. Getts, A. Dreykluft, B. Lu, C. Gerard, N.J. King, and I.L. Campbell. 2007. CXCR3 signaling reduces the severity of experimental autoimmune encephalomyelitis by controlling the parenchymal distribution of effector and regulatory T cells in the central nervous system. *J Immunol* 179:2774-2786.

Abstracts/Poster

Annual Congress of the EANM, 2012, Milan, Italy: "Development and preclinical evaluation of the new pan-somatostatin PET imaging probe 68Ga-DOTA-SOM230 (SOMscan®)". Fani M., Gourni E., Mann A., Kliewer A., Dreykluft A., Weber W. A., Bouterfa H., Schulz S., Maecke H. R.

5th Annual NET Conference, NANETS, 2012, San Diego, California: "Development and preclinical evaluation of the new pan-somatostatin PET imaging probe 68Ga-DOTA-SOM230 (SOMscan®)". Fani M., Gourni E., Braun F., Mann A., Kliewer A., Kaufmann J., Dreykluft A., Weber W. A., Bouterfa H., Schulz S., Maecke H. R.

ECTRIMS, 2011, Amsterdam, Netherlands: "Susceptibility and severity of spontaneous autoimmune neuroinflammation is critically determined by the co-inhibitory B7-homologue 1 at the level of T cell activation, migration and CNS accumulation". Dreykluft A., Posevitz V., Ip C. W., Wiendl H

1st Münster Immunology Meeting, 2010, Münster, Germany: "Susceptibility and severity of spontaneous autoimmune neuroinflammation is critically determined by the co-inhibitory B7-homologue 1 at the level of T cell activation, migration and CNS accumulation". Dreykluft A., Posevitz V., Ip C. W., Wiendl H.

97th AACR Meeting, 2006, Washington, USA: "The "intrinsic" pathway of antibody SAM-6 induced lipoptosis" Vollmers H.P., Dreykluft A., Rauschert N., Rasche L., Müller K., Wozniak E., Hensel F. et Brändlein S.

DGN - Symposium, 2006, Mannheim, Germany: "More severe chronic phase experimental autoimmune encephalomyelitis with altered T-lymphocyte distribution and increased demyelinating lesions in CXCR3-deficient mice" Müller M., Carter S., Manders P., Hofer M., Dreykluft A., Ringelstein E.B., Campbell I.L.

9th International Symposium of Molecular Medicine, 2006, Hersonissos, Crete, Greece: "The "intrinsic" pathway of antibody SAM-6 induced lipoptosis" Vollmers H.P., Dreykluft A., Rauschert N., Rasche L. et Brändlein S.